

A comparison of results from 2D and 3D approaches for spiral mandrel die flow simulation

Bc. Pavel Kubík

Master Thesis
2008



Tomas Bata University in Zlín
Faculty of Technology

Univerzita Tomáše Bati ve Zlíně

Fakulta technologická

Ústav výrobního inženýrství

akademický rok: 2007/2008

ZADÁNÍ DIPLOMOVÉ PRÁCE

(PROJEKTU, UMĚLECKÉHO DÍLA, UMĚLECKÉHO VÝKONU)

Jméno a příjmení: **Bc. Pavel KUBÍK**
Studijní program: **N 3909 Procesní inženýrství**
Studijní obor: **Konstrukce technologických zařízení**

Téma práce: **Porovnání výsledků 2D a 3D modelování simulace toku spirálovou hlavou**

Zásady pro vypracování:

- a) Provést literární rešerši k danému tématu
- b) Seznámit se s programy 3D Fem a Spiral Die program, které budou využívány v diplomové práci.
- c) Pro vybrané typy spirálových hlav (průměr 100 mm, 350 mm a 1000 mm) provést řešení pomocí programu 3D Fem a porovnat je s výsledky řešení programu Spiral Die, který obsahuje zjednodušující předpoklady. Soustředit se zejména na rozdělení materiálu na konci spirálového trnu a na tok materiálu spirálou a výtok ze spirály.
- d) Porovnat výsledky obou výpočtů pro všechny geometrie hlav a zjistit souhlas či nesouhlas daných řešení.
- e) Pokud se zjistí nesouhlas řešení, navrhnout možné modifikace zjednodušeného programu Spiral Die, tak aby lépe popisoval chování hlav, jak je popsáno přesným řešením ve 3D.

Rozsah práce:

Rozsah příloh:

Forma zpracování diplomové práce: **tištěná/elektronická**

Seznam odborné literatury:

Kanai T, Campbell G.A.: Film Processing, Carl Hanser Verlag 1999, ISBN 1-56990-252-6

O'Brien K.T.: Computer Modeling for Extrusion and Other Continuous Polymer Processes, Carl Hanser Verlag, Munich, Vienna, New York, Barcelona, 1992 ISBN 3-446-15845-6

Compuplast Tutorial for 3DFem program, Compuplast International, a.s., Zlín, 2007

Compuplast Tutorial for Spiral Die program, Compuplast International, a.s., Zlín, 2007

Perdikoulis J., Vlček J., Vlachopoulos J.: Adv.Polym.Technol.(1987) 7, p. 333-341

Perdikoulis J., Vlček J., Vlachopoulos J.: Adv.Polym.Technol.(1987) 10, p. 111-123

Perdikoulis J., Tzoganakis C., Vlachopoulos J., Plast.Rubber Process.Appl.(1989) 11

Vedoucí diplomové práce: **doc. RNDr. Jiří Vlček, CSc.**
Compuplast Int.

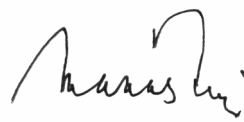
Datum zadání diplomové práce: **19. února 2008**

Termín odevzdání diplomové práce: **23. května 2008**

Ve Zlíně dne 29. ledna 2008



doc. Ing. Petr Hlaváček, CSc.
děkan



doc. Ing. Miroslav Maňas, CSc.
ředitel ústavu

ABSTRAKT

Jednou z nejdůležitějších částí procesu vyfukování je správný design a rozměry vyfukovací hlavy. Nejčastěji používaným typem vyfukovacích hlav je hlava spirálová. Simulace toku materiálu spirálovou hlavou je ale velmi složitá. Pro účely simulace se velmi často využívají specializované simulační softwary, jako je celosvětově využívaný simulační software Virtual Extrusion Laboratory, který obsahuje zjednodušený 2D modul, ale i 3D-FEM modul, jenž simuluje tokové chování taveniny s maximální přesností. Zatím, ale není znám algoritmus pro odečítání výsledků z 3D-FEM modulu a jejich následné srovnání z 2D modulem. Pro odečítání výsledků výtoku materiálu na výstupu z hlavy lze použít předdefinovanou funkci v panelu nástrojů. Je také nutné správně nastavit hodnoty výpočetního zařízení, protože 3D řešení neuvažuje automaticky výpočet teploty. Pro odečítání hodnot toku materiálu spirálou je nutné rozdělit hlavu pomocí funkce 2D řez a z těchto jednotlivých řezů pomocí funkce integrál pro každou spirálu stanovit hodnoty průtoku materiálu spirálou.

Výsledkem testování uvedených softwarů je poznatek, že zjednodušený 2D modul je dostatečně přesný, aby mohl být použit pro návrh spirálové hlavy, kde se výstupní štěrbinu otevírá pozvolna a stejně tak se i mění hloubka kanálu. Zároveň je nutné brát na vědomí, že průtok materiálu spirálou předpovídá o něco rychlejší, než ve skutečnosti je. U geometrií, u kterých se výstupní štěrbinu otevírá náhle, 2D modul selhává při předpovědi průtoku materiálu na výstupu z hlavy.

Klíčová slova: Vyfukování, 3D-FEM, polymer, spirálová hlava, Virtual Extrusion Laboratory software

ABSTRACT

The most important thing of spiral die flow simulation in VEL software is to find difference, if there will be someone, between the 2D Spiral Die module and 3D-FEM module modeling results and try to make an algorithm for better reading of 3D-FEM module modeling results. The Spiral die program has been used for designing a lot of dies around the world and most of them were successful. Spiral die program can be used for the die design, when the gap opens gradually and also the channel depth is changed gradually, with keeping in mind that the leakage is a little bit faster than the program predicts and the geometry should be gradually changing. The calculation of the last example confirms also this experience because this die is some kind of geometry extreme when the gap opens suddenly. It can be seen that in this case the Spiral die program fails to predict reasonably the distribution.

Keywords: Blown film, 3D-FEM, polymer, spiral mandrel die, Virtual Extrusion Laboratory software

ACKNOWLEDGEMENT

I would like to express my thanks to all people who contributed to my Master thesis.

First of all, I am especially thankful and grateful to my supervisor, doc. Ing. Jiří Vlček, CSc. for his valuable advice that helped me create the below-presented results and for his cooperation on the research.

Then I must express my gratitude to Ing. Jiří Švábík for his time reasons, very important consultation on Virtual Extrusion Laboratory software, especially 3D-FEM module.

The support of the project by Compuplast International is gratefully acknowledged.

Last but not the least, I would like to extend my gratitude to my family for their support and interest in my work.

I agree that the results of my Master thesis can be used by my supervisor's decision. I will be mentioned as a co-author in case of any publication.

I declare I worked on this Master thesis by myself and I have mentioned all the used literature.

Zlín, May 23, 2008

.....

Pavel Kubík

CONTENTS

INTRODUCTION	9
I THEORETICAL BACKGROUND.....	10
1 PLASTICS	11
1.1 POLYSTYRENE - PS.....	12
1.2 POLYCARBONATE – PC	12
1.3 POLYETHYLENE – PE	13
2 FILM BLOWING PROCESS	14
2.1 PROCESS DESCRIPTION	14
2.2 COEXTRUSION	15
2.3 FILM BLOWING LINES	17
3 SPIRAL DIE ANALYSIS	18
3.1 ANNULAR FLOW GEOMETRY.....	18
3.2 BASIC DESIGN CONSIDERATION	22
3.3 MATHEMATICAL MODELING	24
4 3D MODELING METHOD – FEM IMPLEMENTATION.....	31
5 AIMS OF THE WORK	35
II EXPERIMENTAL	36
6 PROJECT DATA PREPARATION – SPIRAL DIE MODULE.....	37
6.1 MATERIAL DEFINITION	37
6.2 DIE GEOMETRY DIMENSIONS	37
6.3 DIE GEOMETRY DEFINITION.....	40
6.3.1 Basic Die Characteristics Definition.....	41
6.3.2 Body Definition.....	41
6.3.3 Mandrel Definition.....	42
6.3.4 Channel Definition	43
6.3.5 Annuli Definition	45
6.3.6 Pipes Definition.....	48
6.4 PROJECT DEFINITION	49
7 PROJECT DATA PREPARATION – 3D FEM MODULE.....	51
7.1 SOLVER SETTINGS.....	51
8 RESULTS AND DISCUSSION.....	53

8.1	CONICAL DIE – SPIRAL DIE MODULE RESULTS.....	53
8.2	CONICAL DIE – 3D FEM MODULE RESULTS	54
8.3	DIE WITH STRONG LEAKAGE – SPIRAL DIE MODULE RESULTS	66
8.4	DIE WITH STRONG LEAKAGE – 3D FEM MODULE RESULTS	67
8.5	DIE WITH STRONG FLOW IN SPIRALS – SPIRAL DIE MODULE RESULTS	78
8.6	DIE WITH STRONG FLOW IN SPIRALS – 3D FEM MODULE RESULTS.....	79
8.7	RESULTS COMPARISON	90
	RESUME	96
	REFERENCES.....	97
	LIST OF SYMBOLS	100
	LIST OF FIGURES	102
	LIST OF TABLES	105
	LIST OF APPENDICES	106

INTRODUCTION

Polymers – synthetic macromolecular materials get through the everyday life of people of all industrial countries all over the world. They became the basic parts of huge amount of materials like thermoplastics, thermosets or elastomers. Plastics are absolutely irreplaceable in many types of the world`s industry. If become a miracle and all types of plastics were lost or destroyed, it will be end of humans civilization. Plastics are so popular because they have many useful applications and properties like cheap prize, good thermo or electro insulating properties and easy manufacturing.

We have many types of technologies to manufacturing polymers. The most important and the most common technologies are injection molding, extrusion, coextrusion, thermoforming and film blowing process, as well. One of the most important part of the film blowing process is the die which gives the final value and shape of blowing material. It also controls the flow of the polymer melt. The best type and the most common in film blowing process is the spiral die. We need to know as many pieces of information about the melt behaviour whitin the die as it is possible. That is the reason why we use softwares for flow simulation. It gives us many useful pieces of information about geometry, design and flow conditions necessary for the best process setting parameters and it saves our money.

I. THEORETICAL BACKGROUND

1 PLASTICS

Plastics are materials that contain polymer as a main part. They contain many other types of additives, too.

Main divisions of plastics are:

- Thermoplastics
- Thermosets
- Elastomers

Thermoplastics - Thermoplastics are polymers that are softened by heat. They are transformed to a viscoelastic melt. They can be processed and fabricated with suitable technology, they are transformed to the shape of a real product by cooling. This process can be repeatable many times.

The most common thermoplastics are:

Polyethylene PE, Polypropylene PP, Polystyrene PS, Polycarbonate PC, polyvinylchloride PVC...

Thermosets – Thermosets are polymers, that are solidified by heat because the higher temperature faster the transformation of their inside structure to a three dimensional polymer net. Those sorts of plastics are insoluble and unmeltable.

Thermosets are many types of synthetic resins like polyester resins, epoxy resins and phenolic resins.

Elastomers - Elastomers are polymers, which have viscoelastic behavior in high temperature range. They are very elastic with very big elastic deformation that can be from 100 to 1000 percent. They have big resistivity against abrasive wear and their properties can be improved by chemical reaction - vulcanization process.

Elastomers are for example rubbers like natural rubber, butadiene-styrene rubber, isoprene rubber, polybutadiene rubber and chloroprene rubber. [1]

1.1 Polystyrene - PS

Polystyrene is one of the fully synthetic and the most explore kind of plastics. It is create by linear and unbranched chains that are solid and unflexible, with basic monomer period:

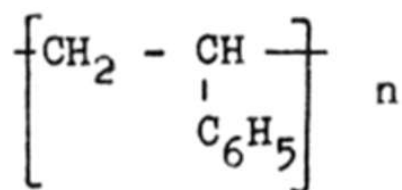


Fig. 1. Polystyrene structure

Polystyrene is an amorphous polymer. It was showed by the roentgen test. It has relatively good mechanical properties. Products of polystyrene are good for electrostatic charging which signalize its excellent electric properties. It is easy to burn. It looses a lot of soot when it is in fire. It has small water absorption and it is soluble in many types of semi-polar solvent. It has very good chemical properties, too. It has small resistivity against wind. It gets yellow. This absence is easy dispatched by addition of suitable stabilizers. Manufacturing of polystyrene is easy for its good flow properties. It makes it good for thermoforming of really complicated products, extrusion or injection molding. It can be paint and metal plate. If it doesn't contain free styren it doesn't toxic and it can be use in food processing industry for yoghurt pots. It is also use for cover of casual kitchen consumer. [1]

1.2 Polycarbonate – PC

Polycarbonate is achromatic and transparent material. It has excellent mechanical properties like its measure stability, small water absorption, and constant electric properties in high temperature activity. It receives from 0.1 to 0.3 percent of water. It is soluble in hydrocarbons, esters and ketons. It has resistivity against aqueous solutions of organic acids. It has good resistivity against light and wind, too. It strongly decreases its Young modulus when it is fills by glass fibers. Its less crystallinity in comparison with polyethylenthereftalate make using of polycarbonate not only for fibers and foils but especially as plastic raw materials. It can be processed by all kind of know plastic work technologies. Its granulate have to be dried in vacuum before manufacturing. The most important methods of its manufacturing are injection molding, extrusion and thermoforming.

Polycarbonate is mainly use in electrochemical industry, car industry, and for the gears, bearings or technical applications. [1]

1.3 Polyethylene – PE

Polyethylene is one of the most useful and the most common commodity polymers. Its chain is created only by CH₂ groups.

It can be in form with linear chain structure or branched form. It deforms by temperature and time dependence in cases of permanent stress. This is called cool flow. It has very big linear thermal expansion and its sequential shrinkage can be more than 6 percent. It absorbs infra-red and it is transparent for ultraviolet and roentgen rays. It also has good adhesion to surface of another material. That is why it is used for surface coating. It is not good for bearings because its friction coefficient is too high. It has good electro-isolation properties, too. It has resistivity to acids and hydroxides. It is transparent for gasses and vapours. It can be processed by all kind of know plastic work technologies.

It is using like wrapping material and for foils or bag production. It is used for discharging tubes, isolation foil and watering system in agriculture, too. It can be use for sheathing in cabling industry. [1]

2 FILM BLOWING PROCESS

Film blowing is one of the most common processes for manufacturing of plastics.

2.1 Process description

The first step of the process is melt preparation. It always starts inside the extruder where solid material is transported, compressed and melted to the compact melt. The melt is extruded through an annular die which is shown in fig.2.



Fig. 2. Melt extrusion

After extrusion it is extensionally stretched and cooled by air. It takes some time to freeze. That means the material is in the molten state in some area after it leaves the die. It needs the help of inner cooling rings for quicker and better freezing to solid film. The film can be oriented biaxially, too. We can do this by using small die gaps and low draw-down ratios. If the gap is too big the film can undergo pure planar orientation next to the freeze line. The most used plastics for film blowing process are polyolefins such as low-density

polyethylene LDPE, linear low-density polyethylene LLDPE, and high-density polyethylene HDPE, because they have very fast crystallization and freezing time from 1.5 to 5 seconds. Manufacturers in the North America are installing more than 80 new film lines every year with production over 140 million kilograms of plastics. The cost of a single layer line is from 350 to 700 thousands dollars and coextrusion lines are over 3 millions. [2, 3]

The film blowing process has important process parameters, as well. One of them is the blow-up ratio. It is the ratio of the bubble radius at the freeze line to the bubble radius at the die exit.

$$BUR = \frac{R_1}{R_0} \quad (1)$$

The second is the draw-down ratio. It is the ratio between the film velocity at the freeze line to the velocity at the die exit.

$$DDR = \frac{v_F}{v_D} \quad (2)$$

These two parameters are responsible for the final bubble shape and film stretching during the process. [4]

2.2 Coextrusion

Coextrusion is the process of feeding die with two or more different polymer types. Polymer flows are joining together within the die to create one compact film. The individual layers are not mixed but they have their position in the flow, because they have different viscosities. Every type of polymer use for the coextrusion process has to have its own extruder connected with the die. It is shown in fig.3. We use coextrusion process in cases when we need a set of properties that cannot be obtained from a single film blowing process. The different layers can bring high strength, low permeability to oxygen, dual colors, low cost, printability etc. [5]



Fig. 3. Coextrusion feeding process

The best application for coextruded film is food packaging, including meat, cheeses or cereals. It is also used for agricultural supplies, medical products, and electronic components. Coextrusion rises the cost and complexity of a film blowing line, too.

2.3 Film Blowing Lines

Manufacturers are using three main types of film blowing lines today. It depends where the nip roll is. It can be situated horizontal with the floor, at the bottom of the line, but the most commonly used situation is that the nip rolls is on the top of the line. The most common use film blowing line is in figure 4. [3]



Fig. 4. Film blowing line

3 SPIRAL DIE ANALYSIS

A spiral mandrel die is an apparatus for production of annular flow of a polymer melt, mainly in the blowing film process. The prime geometries of spiral mandrel dies are all the same, but their design is different. Flow simulation is hard to study, but we have models that describe this behaviour very well. [6]

3.1 Annular Flow Geometry

The most common effect of spiral mandrel die is to transform polymer melt into the annulus. An annular flow is rising between two concentric circles of steel. External circle is outside body and internal circle is known as mandrel, which keeps concentricity to the body. There are more possibilities to do this. The most commonly used solutions are on fig. 5.

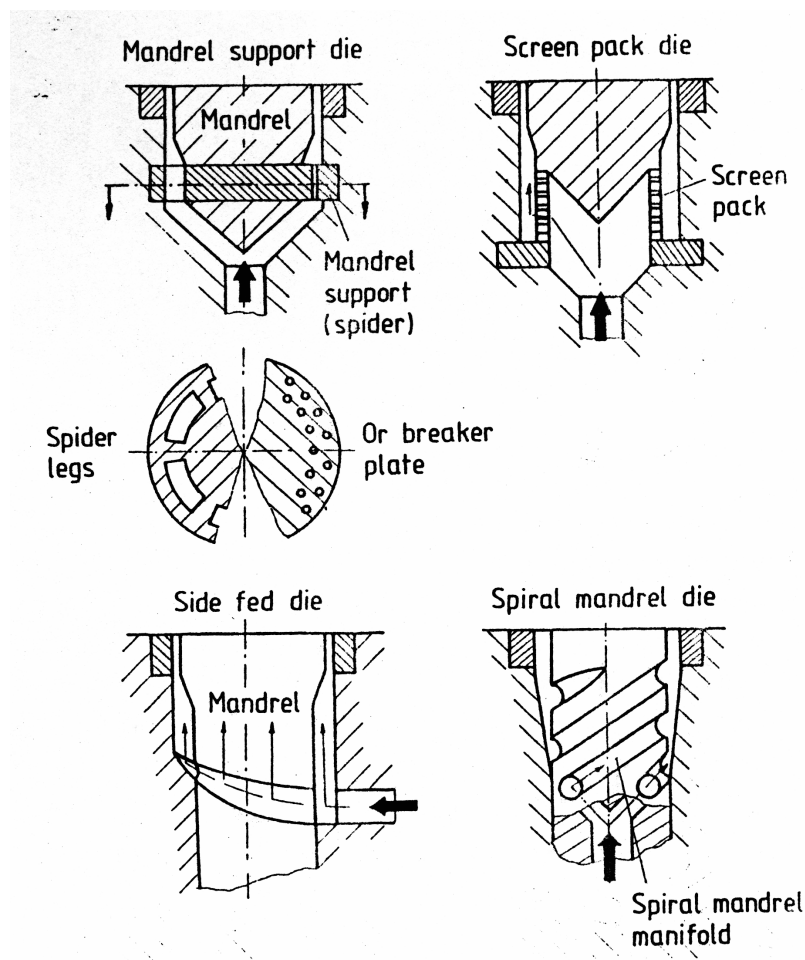


Fig. 5. Types of die constructions

These solutions are not good because the flow have to brake and join again. It is the reason of weld lines problem. Weld lines are bad for mechanical properties of the blown

film. They are visible with an eye. Good mandrel construction can dramatically decrease the weld lines problem. Some of good construction solutions are on fig 6.

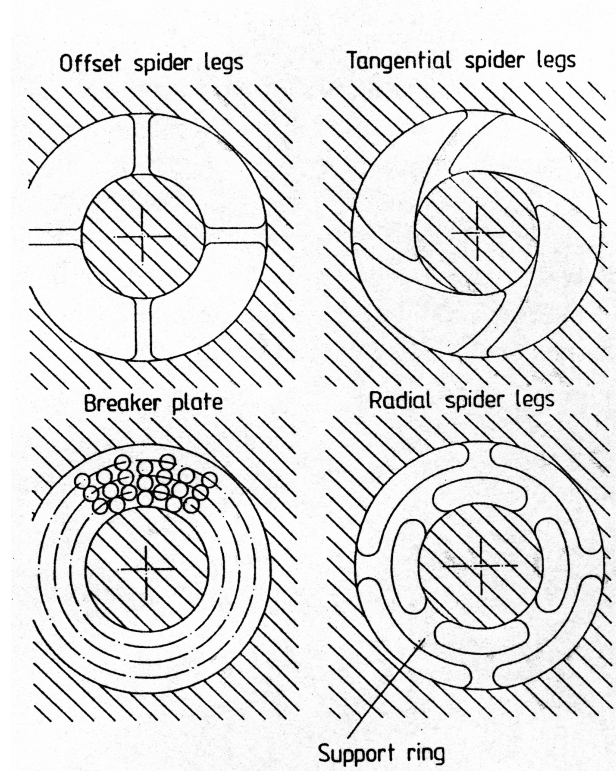


Fig. 6. Basic mandrel support systems

Let`s have a look on fig 8. It shows classic system of spiral die melt distribution. As you can see on the picture, polymer melt distribution goes through the spirals and in the same time it goes through the space between the body and the mandrel. It is positive for weld lines problem, as shown in fig. 7. [6-35]

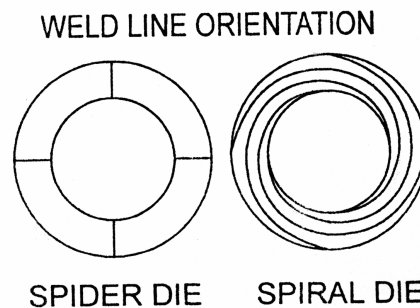


Fig. 7. Weld lines orientation

Weld lines are still there but they have much better orientation than at non-spiral die constructions. Non-spiral die constructions have weld lines in radial direction through the die axis. Spiral die construction is the best solution and it becomes the most favorite in

the world's plastic industry for the film blowing process, because weld lines are created in round paths and they join together from all different spirals to one compact complex.

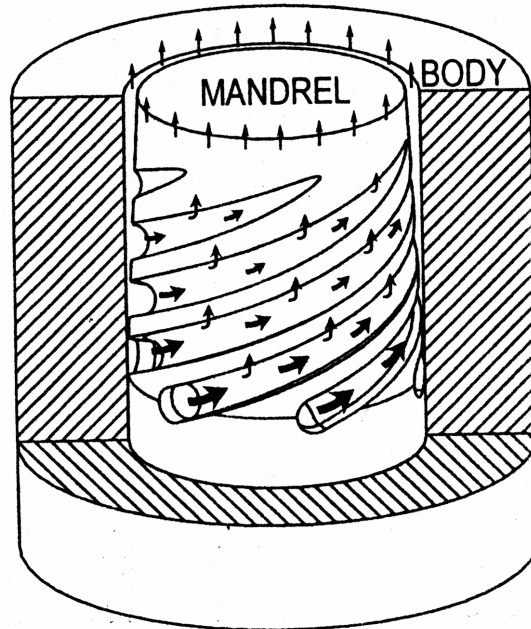


Fig. 8. Spiral mandrel die flow distribution

Spirals have strict rules for their numbers. They go out from size of mandrel, size of spirals, and helix angle of the spirals. Today's standard is from 0.2 to 0.5 spirals per centimeter of mandrel diameter. Spiral depth goes linearly with its length, but new CNC milling machines can do the non-linear dependence. There is an area for detach spirals or channels in axial direction. It is called the spiral land. Every spiral is going 360° angle in this area.

Typical design for film blowing spiral die construction is on fig. 9. The melt travels from the inner part to the edge of the die, where is immediately distributed by the spirals. Then it travels to the relaxation chamber after the distribution. Before the exit from the die, the melt has to travel through small size interspace.

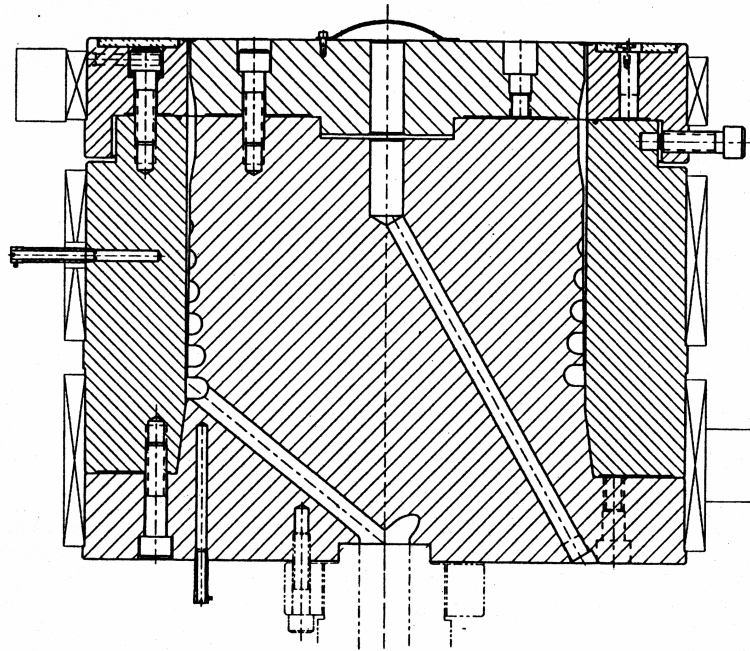


Fig. 9. Typical spider mandrel die construction

Die size is responsible for the diameter of final film proportion at the end of the die. It can be from 20 mm to more than 2000 mm. spiral mandrel dies can be used for coextrusion technology, too. All materials used in coextrusion must have their own spiral die until they join together. A three-layer spiral mandrel die is in fig. 10. [6-35]

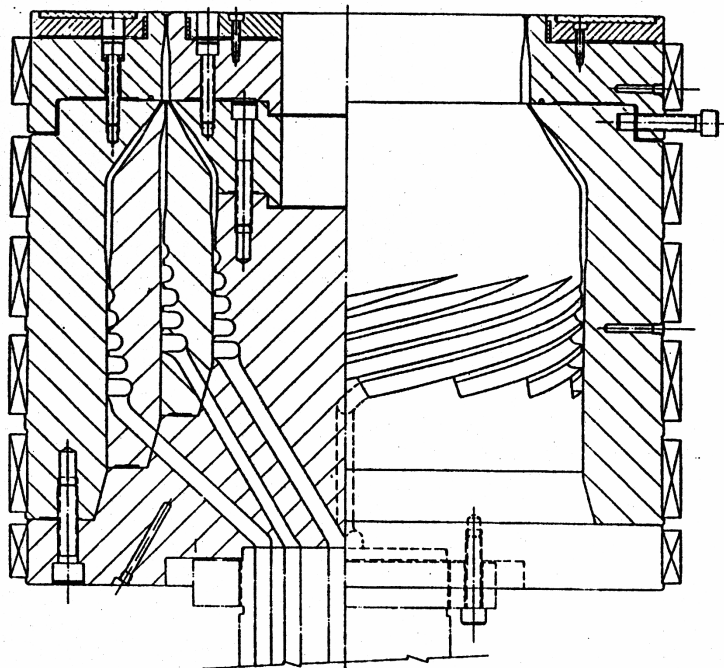


Fig. 10. Three-layer spider mandrel die

3.2 Basic Design Consideration

Before designing a spiral mandrel die we must know some important things. First of all it is the right polymer type that we use for film blowing process. It is important for its good manufacturing. Every type of polymer is different from others. It is very difficult to create a spiral mandrel die for a new type of polymer which is not known well so far, because many design considerations are only from practical experience. We have to know as much piece of information about the polymer type used for process as it is possible. One of the basic information we have to know is information about the shear viscosity and the temperature for manufacturing. It gives us information about thinning, thermal stability and elasticity that are important for design, too.

There are other standards that are very important for process like flow rate and the output. The cooling rate of the polymer melt is important, too. The average standard output is about 0.5 kg/h/mm of the die diameter, but it is possible to have output over 1 kg/h/mm of the die diameter but it needs knowledge about the newest cooling systems. There can be other parameters to limit the output, for example extruder, bag making machine and winders. We need pieces of information about the shear rate, velocities, residence times or system operating pressure as well.

The pressure usage during the process is from one fourth to one half of spiral system. It depends on other different criteria. First of all it is the value of wall shear rate of the material. Some of the polymers like polyolefines can have less wall shear rates than polymers like polyvinylchloride PVC, polyvinylidenechloride PVDC or ethylvinylalcohol EVOH that can have wall shear rate much higher. The smallest wall shear rate among the process temperature sets the pressure conditions for the blowing film process. It is very important to know everything about the pressure conditions for a good spiral mandrel die design.

Biggest pressure that can be used for blowing film process is given by extruder or the screen changer. The extruder can generate maximum pressure about 50 MPa or 70 MPa. For extruders with vented zone is the highest pressure the pressure when polymer used for the process is flowing out of the vent. The melt temperature rises during the time that polymer spends in the screw because of the high head pressure, also the output decreases. That's the reason why the lower pressure is better. [6-35]

There are many things to consider for lower pressure limit. First of all it is the used polymer and its stability at the extrusion temperature. A non-stable polymer like PVDC have to have as small residence time in the die as is possible. Decreasing of the residence time increases the velocity and shear rate in the die, too. The pressure change during the process depends on the length of the flow channel.

There are two important sectors in spiral mandrel die distribution system. They are in fig. 11. The first sector where polymer melt leaves spirals is called the relaxation chamber. It is necessary for relaxation of internal stresses in the polymer melt. The second sector is called as the final sizing gap, final land gap, or lip gap that is different for every tape of polymer and final product of the blowing film process. The final gap can be from 1 to 4 mm.

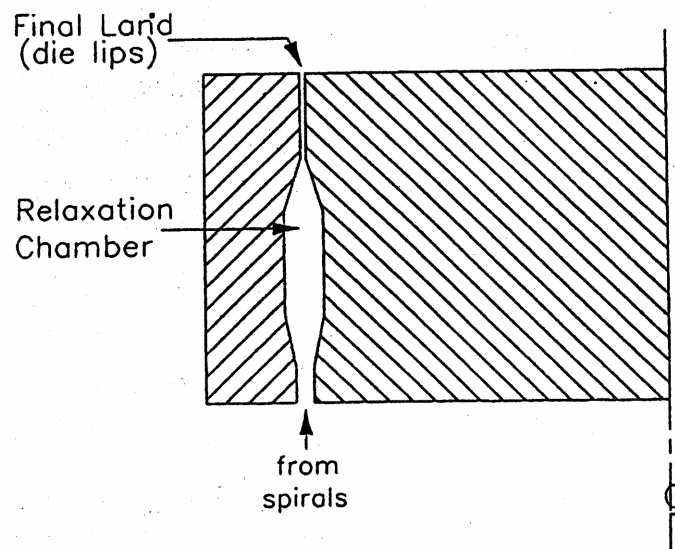


Fig. 11. Relaxation chambers and final gap

Manufacturers try to minimize the flow variation in the final gap. Figure 12 shows that there are some basic corrections like wide chambers, long final land, and neck-in / neck-out systems. They have to reduce flow variations which were created by spiral distribution or die sensitivity to machining tolerances which needs long spirals in the die. That is the reason why the residence time and pressure of material in the die goes up. They have to minimize, because it is one of the most important design criterias.

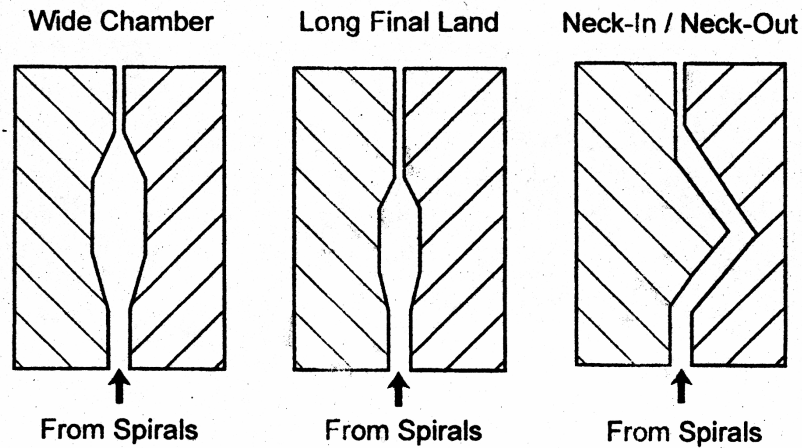


Fig. 12. Basic correction of flow variation

Many of dies are protected before the damage by hardening, chrome or nickel plating. It is also important for its cleaning. Every surface in contact with the flow polymer have to be polished to decrease residence time and possible degradation effect of polymer. [6-35]

3.3 Mathematical Modeling

Mathematical modeling of spiral mandrel dies is very important. It brings pieces of knowledge about the real physics of the process. For spiral mandrel die design is very good to make simulation of the polymer melt flow process. It gives us information about hard measure process characteristics. We use mathematical modeling for virtual simulation of the process without using the die to increase the process efficiency. It can prevent some mistakes in the spiral mandrel die design. We can test possible polymer types that we use for blowing film process, too. [6-35]

The first published and used model of spiral mandrel die process was presented by Proctor [6-35]. He tried to make the easy flow distribution prediction. The flow space in cross section view shows fig. 13.

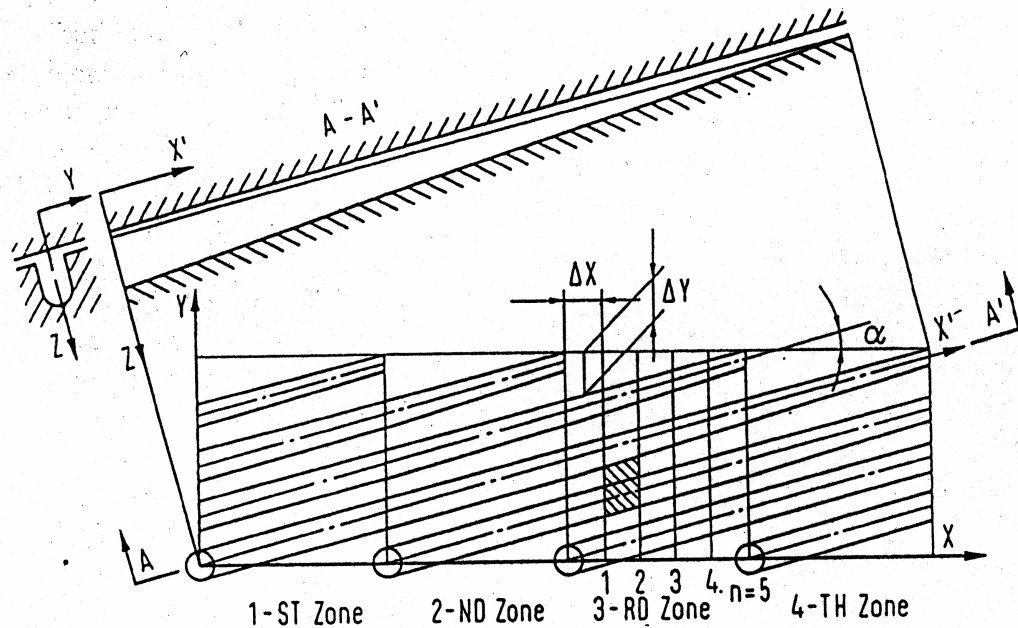


Fig. 13. Cross-section view of the spiral mandrel die

The first assumption is neglect the effect of curvature. We have the width of the gap between the mandrel and the die smaller than the mandrel diameter. We can see the mandrel like a flat system with its own coordinates. It shows fig.13. On this figure we can see four spirals system. Every spiral has all 360° and has the same proportions. There is a cross-section view of channel proportions, as well. The similar areas on the figure are called zones. We need to study only one of them for the best understanding of the problem, because the modeling of the one spiral or one zone is the same thing. We choose zone three this shown in fig. 13, because the amount of material flowing out from the first section of zone three into the second section of zone four is the same as from the second section of zone three to the first section of zone two. This is important for the volumetric flow balances.

The space is cut into the elements. In x direction, there are five or more elements for a better accuracy. In y direction, there are four elements. That means we usually have twenty elements for calculation. Number of elements rises the time which is necessary for the making of good results.

On figure 14 you can see the difference between the typical spiral mandrel die design and Proctor approximative model geometry. As it shows, the flow rate entering the second element in channel A is marked as Q_{1A} and when it leaves the second element to

enter the third is marked as Q_{3A} . The material that flows axial of channel A to the second element of channel B is marked as Q_{2A} . The depth of the spiral is going up, Proctor's assumptions were that the pressure drop in the channel rises linearly. The flow is similar to the flow through a rectangular channel of the same cross-section area. The flow in the annular gap is also similar to the flow through the groove of element size $h_2 \times L_2$. The flows are not influence on each other. The assumption about the pressure linearity is very good for easy calculation of the problem and it is also good for volumetric flow variations. There are many books to make this problem easier or make another model for this problem.

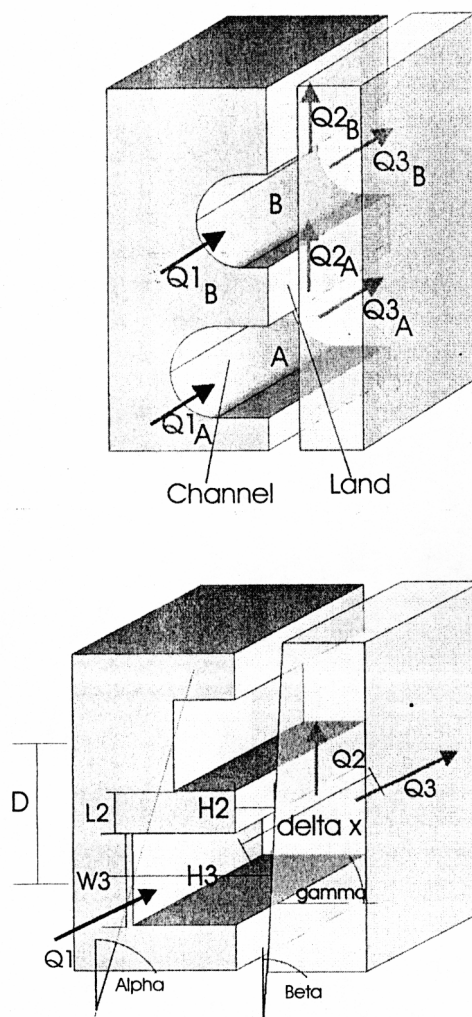


fig. 14. Geometry comparison

All of these models usually use a “lumped parameter” or “control volume” method when the flow space is cut on many sectors with totally controlled volume and flow profile. They became the most popular models for spiral mandrel die analyzing and design considerations. There is a lot of computer software methods based on the “lumped parame-

ter” method, too. One of these shows figure 13. The spiral distribution system is cut on 20 control volumes. The control volumes are subdivided to smaller control volumes that are shown in figures 15 and 16. Figure 14 shows a perspective view of flow space. [6-35]

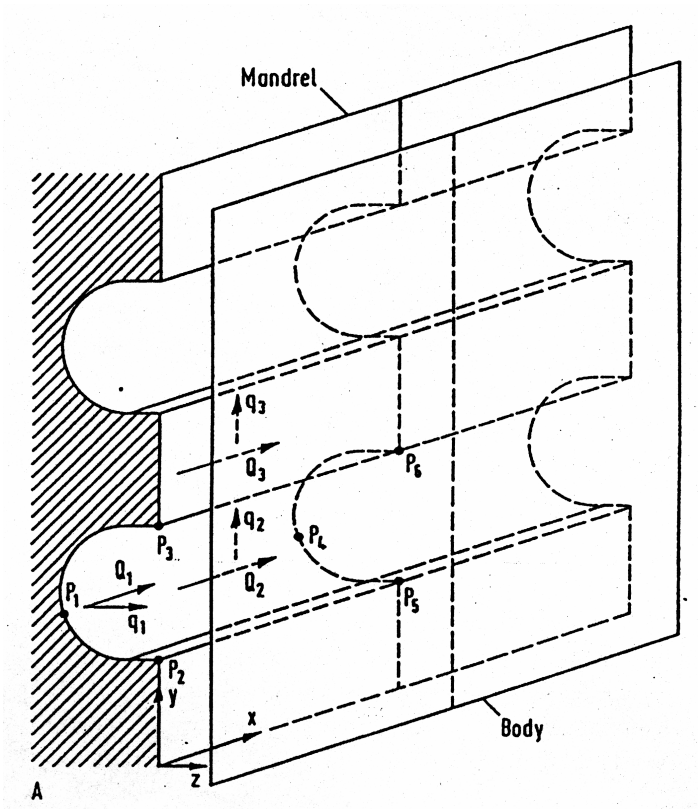


Fig. 15. Perspective view of flow space

Figure 15 shows one element subdivided into smaller control volume elements.

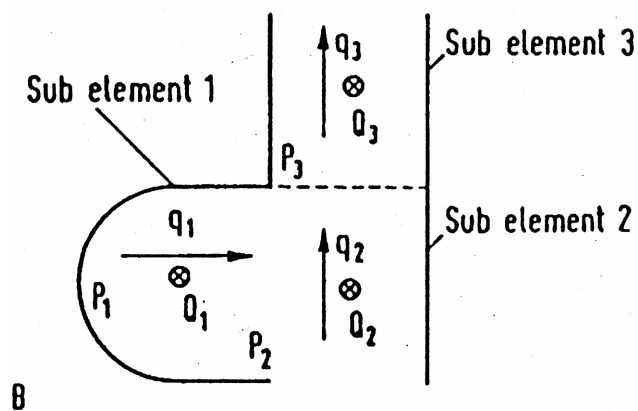


Fig. 16. Subdivision of control volume

There are three main types of element for subdivision.

- In the channel (subelement 1)
- Over the channel (subelement 2)
- Over the land (subelement 3)

All dimensions are known, but they can change through the element's length. The lumped parameter method needs a fully developed flow. It needs to be substituted by constant mean dimensions that are similar to the values at the center of each element. It gives us a possibility to use the Poiseuille flow calculation. Like shown in figures 15 and 16 there are subelements with position of pressure node. The model shows that flows in element 1 are in the x and z direction and in elements 2 and 3 are flows in x and y direction. It can be described by fig. 16 that shows a typical subelement used for the model.

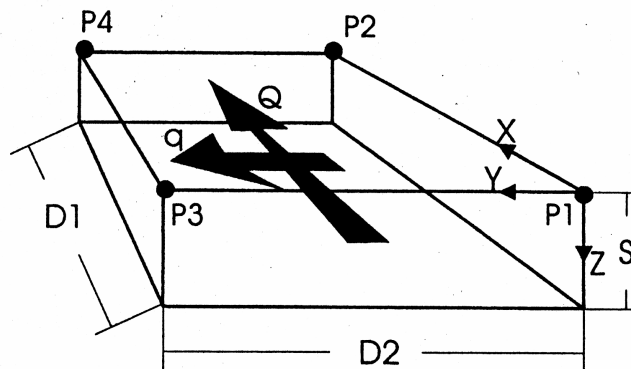


Fig. 17. Typical subelement for the model

There is the Poiseuille flow between plates. The quantities of interest for any of the subelement are the pressure and volumetric flows Q or q as show fig. 16.. When we use The Poiseullie flow equations we can combine the flow to the pressure. The momentum equations are of the following form:

$$\frac{(p_1 + p_2)}{2} - \frac{(p_3 + p_4)}{2} - f(Q, q)q = 0 \quad (3)$$

$$\frac{(p_1 + p_3)}{2} - \frac{(p_2 + p_4)}{2} - g(Q, q)Q = 0 \quad (4)$$

The function f and g indicate the flow resistance in x and y directions. Using a generalized Newtonian model (Power law) and assuming a fully developed Poiseuille flow the resistance can be given by the following equation:

$$f(Q, q) = \frac{2m(\dot{\gamma})^{n-1} \dot{\gamma}_1 D_1}{S q} \quad (5)$$

$$g(Q, q) = \frac{2m(\dot{\gamma})^{n-1} \dot{\gamma}_2 D_2}{S Q} \quad (6)$$

The total shear rate is determined from the individual shear rates in each direction by:

$$\dot{\gamma} = \sqrt{\dot{\gamma}_1^2 + \dot{\gamma}_2^2} \quad (7)$$

where

$$\dot{\gamma}_1 = \frac{q \left(2 + \frac{1}{n} \right)}{2 D_1 S^2} \quad (8)$$

and

$$\dot{\gamma}_2 = \frac{Q \left(2 + \frac{1}{n} \right)}{2 D_2 S^2} \quad (9)$$

These two equations are not enough to solve the three unknowns of the problem. We need one more equation to solve the problem.

$$Q + q = Q_1 + q_2 \quad (10)$$

The last important information for the solution of equation system is to specifies the total flow rate at the inlet of the spiral.

Figure 17 compares the predicted flow variation to the measured data. As also shown in fig. 17, the model prediction is similar to the experiment. We can use the software pack for the prediction of results, too.

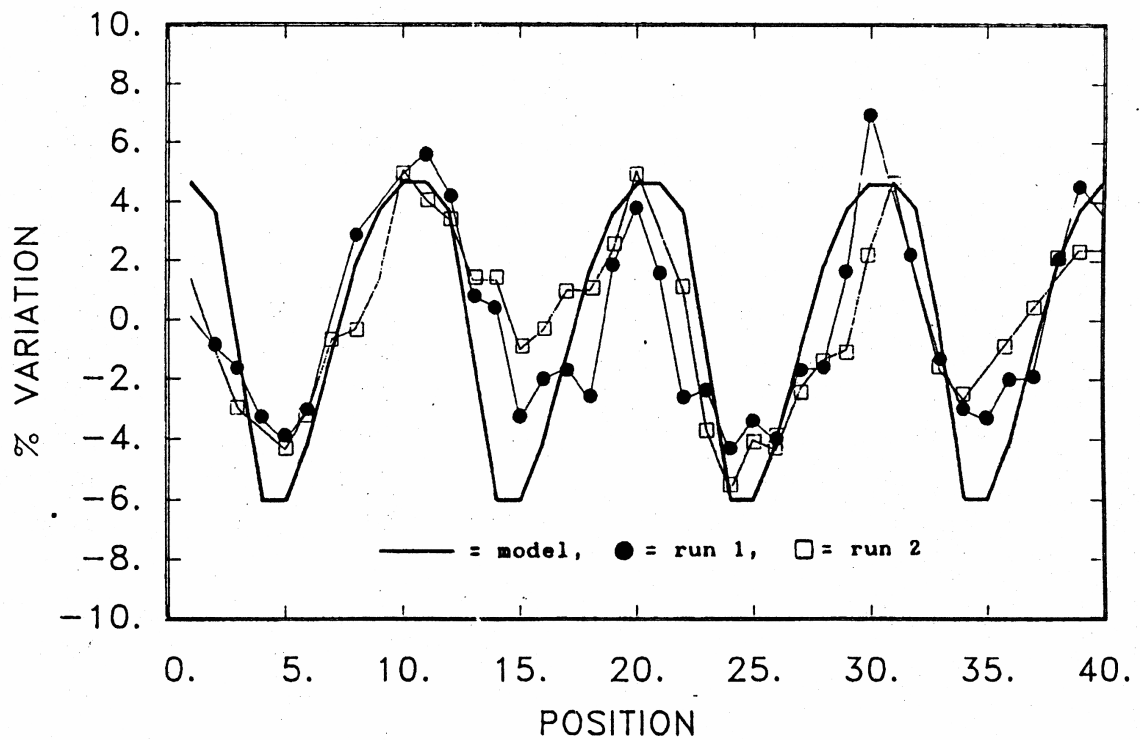


Fig. 18. Model prediction versus experimentally measured data

We need to equate the flow characteristics in other parts of the spiral mandrel die. It is possible to use simplification for flow through tube or annulus in these cases. We need an advanced mathematical modeling and software applications for coextrusion dies, too. The coextrusion dies have to be calculated as a set of simple spiral mandrel dies until the point where the stream lines are joined together. [6-35]

4 3D MODELING METHOD – FEM IMPLEMENTATION

The set of partial differential equations can be solved by analytical methods. We are using modern systems of solution like a FEM analysis, now.

The solved geometry is broken into elements. Elements are small interconnected regions. They can be called subdomain, too. The variables solved are approximated by local approximating functions (piecewise continuous Legendre or Hermite polynomials) that are nonzero only in that element. The residual arising from approximation are weighted by shape function and minimized. [36]

The standard Galerkin FEM set of equations

$$\begin{aligned}\nabla \tau - \nabla P &= 0 \\ \nabla v &= 0 \\ \rho \cdot c_p (v \cdot \nabla T) &= k(\nabla^2 T) + \tau : \nabla v\end{aligned}\quad (11)$$

can be rewritten to

$$\begin{aligned}\int_{\Omega} (\nabla \bar{\tau} - \nabla \bar{P}) N^i &= 0 \\ \int_{\Omega} (\nabla \bar{v}) M^i &= 0 \\ \int_{\Omega} [\rho \cdot c_p (\bar{v} \cdot \nabla \bar{\tau}) - k(\nabla^2 \bar{T}) + \bar{\tau} : \nabla \bar{v}] N^i &= 0\end{aligned}\quad (12)$$

The residuals which have to be minimized are:

$$\begin{aligned}R^i &= \int_{\Omega} (\nabla \bar{\tau} - \nabla \bar{P}) N^i \\ R^i &= \int_{\Omega} (\nabla \bar{v}) M^i \\ R^i &= \int_{\Omega} [\rho \cdot c_p (\bar{v} \cdot \nabla \bar{\tau}) - k(\nabla^2 \bar{T}) + \bar{\tau} : \nabla \bar{v}] N^i\end{aligned}\quad (13)$$

The set of equations for unknowns u (variables v, P, T) is solved by Pickard or Newton-Raphson procedure.

We can write the following equations

$$\begin{aligned}\bar{v}_1 &= \bar{u}_1 = \sum_j N^j u_1^j \\ \bar{v}_2 &= \bar{u}_2 = \sum_j N^j u_2^j \\ \bar{v}_3 &= \bar{u}_3 = \sum_j N^j u_3^j \\ \bar{P} &= \bar{u}_4 = \sum_j M^j u_4^j \\ \bar{T} &= \bar{u}_5 = \sum_j N^j u_5^j\end{aligned}\tag{14}$$

$$\bar{u}_{i,k} = \sum_j N_{,k}^j u_i^j\tag{15}$$

where u_i^j are the nodal values of the variable u_i . When declaring:

$$\begin{aligned}B_j^i &= 2\bar{u}_{j,j} N_{,j}^i + (\bar{u}_{j+1,j} + \bar{u}_{j,j+1}) N_{,j+1}^i + (\bar{u}_{j+2,j} + \bar{u}_{j,j+2}) N_{,j+2}^i \\ j &= 1,2,3,1,2\end{aligned}\tag{16}$$

The residual and their derivatives can be rewritten as

$$R_k^i = \int_{\Omega} -\bar{u}_4 N^i_{,k} + \bar{\eta} B_k^i \quad k = 1,2,3$$

$$R_k^i = \int_{\Omega} \sum_{m=0}^3 \bar{u}_{m,m} M^i \quad k = 4$$

$$R_k^i = \int_{\Omega} N^i \left(\rho \cdot c_p \sum_{m=0}^3 \bar{u}_m \bar{u}_{k,m} - \bar{\eta} \bar{T}_2 \right) + k \sum_{m=0}^3 u_{k,m} N^i_{,m} \quad k = 5$$

$$R_{k,\bar{u}_l}^{ij} = \int_{\Omega} \bar{\eta} \left(\sum_0^3 N^i_{,0} N^j_{,0} + N^i_{,k} N^j_{,k} \right) + \bar{\eta}_{,\bar{u}_l} B_k^i \quad k = l = 1,2,3$$

$$R_{k,\bar{u}_l}^{ij} = \int_{\Omega} \bar{\eta} N^j_{,k} N^i_{,k} + \bar{\eta}_{,\bar{u}_l} B_k^i \quad k \neq l \quad k = 1,2,3 \quad l = 1,2,3$$

$$R_{k,\bar{u}_l}^{ij} = \int_{\Omega} -M^j N^i_{,k} ; k = 1,2,3 \quad l = 4$$

$$R_{k, \bar{u}_l}^{ij} = \int_{\Omega} \bar{\eta}_{, \bar{u}_l} B_k^i; k = 1, 2, 3 \quad l = 5$$

$$R_{k, \bar{u}_l}^{ij} = \int_{\Omega} N^i \left(\rho \cdot c_p N^j \bar{u}_{k, l} - 2\bar{\eta} B_l^j - \bar{\eta}_{, \bar{u}_l} \bar{I}_2 \right) \quad k = 5 \quad l = 1, 2, 3$$

$$R_{k, \bar{u}_l}^{ij} = \int_{\Omega} N^i \left(\rho \cdot c_p \sum_{m=0}^3 \bar{u}_m N^j_{, m} - \bar{\eta}_{, \bar{u}_l} \bar{I}_2 \right) + k \sum_{m=0}^3 N^i_{, m} N^j_{, m} \quad k = l = 5$$

$$R_{k, \bar{u}_l}^{ij} = \int_{\Omega} N^j_{, l} M^i \quad k = 4 \quad l = 1, 2, 3 \quad (17)$$

The viscosity is calculated from the Power Law or Carreau model

$$\bar{\eta} = f(\bar{I}_2)$$

$$\bar{\eta}_{, \bar{u}_l} = \bar{\eta}_{, \bar{I}_2} \bar{I}_{2, \bar{u}_l} \quad (18)$$

the second invariant of the strain tensor I_2 and its derivatives are

$$\bar{I}_2 = 4 \sum_{m=0}^3 \bar{u}_{m, m}^2 + 2(\bar{u}_{1, 2} + \bar{u}_{2, 1})^2 + 2(\bar{u}_{1, 3} + \bar{u}_{3, 1})^2 + 2(\bar{u}_{2, 3} + \bar{u}_{3, 2})^2$$

$$\bar{I}_{2, \bar{u}_l} = \frac{B_l^i}{\bar{I}_2} \quad (19)$$

The transformation to local coordinates can be describe as

$$\bar{u}_{j, k} = \sum_j N^i_{, k} u_j^i$$

$$\bar{x}_{j, k} = \sum_j N^i_{, k} x_j^i \quad (20)$$

$$\begin{bmatrix} N^i_{, 1} \\ N^i_{, 2} \\ N^i_{, 2} \end{bmatrix} = J^{-1} \begin{bmatrix} N^i_{, 1} \\ N^i_{, 2} \\ N^i_{, 3} \end{bmatrix}$$

$$J = \begin{Bmatrix} \bar{x}_{1,1} & \bar{x}_{2,1} & \bar{x}_{3,1} \\ \bar{x}_{1,2} & \bar{x}_{2,2} & \bar{x}_{3,2} \\ \bar{x}_{1,3} & \bar{x}_{2,3} & \bar{x}_{3,3} \end{Bmatrix} \quad J_{ij} = \bar{x}_{j,i} \quad (21)$$

$$d\Omega = |J| d\xi \cdot d\eta \cdot d\zeta \quad (22)$$

The appropriate shape functions necessary for numerical integration and their derivatives can be found in Zienkiewicz [36].

The integrals are calculated using Gauss quadrature rule [37]

$$\int_{\Omega} f(x, y, z) = \sum_i w_i f(a_i, b_i, c_i)$$

5 AIMS OF THE WORK

The main aim of this Master Thesis is to compare results of the 2D and 3D modeling of the spiral mandrel dies flow simulation. It will be compared in Compulast International by The Virtual Extrusion Laboratory software. The most important thing is to find difference, if there will be someone, between the 2D Spiral Die module and 3D-FEM module modeling results and try to make an algorithm for better reading of 3D-FEM module modeling results.

II. EXPERIMENTAL

6 PROJECT DATA PREPARATION – SPIRAL DIE MODULE

The first of all we have to start a new *project* that is the main part of the Spiral Die module necessary for a good solution. This project is joined with material and geometry of the spiral die. So we have to define geometry and material, too. We have three different spiral dies called Conical die, Die with strong leakage and Die with strong flow in spirals for this master thesis so we choose the Conical die as an example.

6.1 Material definition

We can use a material if all its properties are completely defined. The most important properties of used material Typical 1 MI Film (Cross) (HDPE) are:

Rheology		Thermal Properties			
		Melt Properties		Solid Properties	
η [Pa.s]	8000	ρ [kg/m ³]	790	T_m [°C]	110
n	0,1710			T_f [°C]	90
r [s]	0,2320	C_p [J/kgC]	2300	Rho [kg/m ³]	920
b [1/°C]	0,0155			C_p [J/kgC]	2300
λ_1	0	λ [W/mK]	0,24	λ [W/mK]	0,28
λ_2	105,90			H_f [J/kg]	130000

Tab. 1. Material properties

Used material is completely predefined in Compuplast's Virtual Extrusion Laboratory software. This software will be used for the solution of the dies.

6.2 Die geometry dimensions

We also have to have the die geometry at the start of the project. In these sketches you can see dimensions of the Conical die and their coincidence with geometry editor. There are body dimensions, mandrel dimensions, channel dimension, section above the spiral part and pipe system (anulli) dimensions on the following figures.

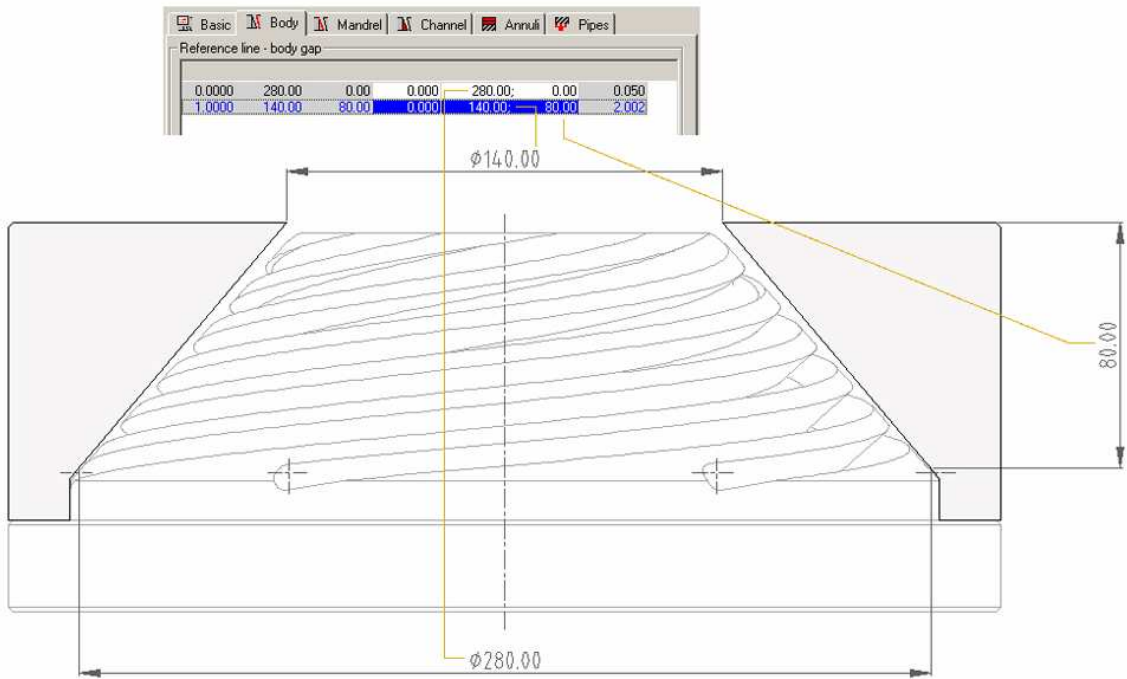


Fig. 19. Body dimensions

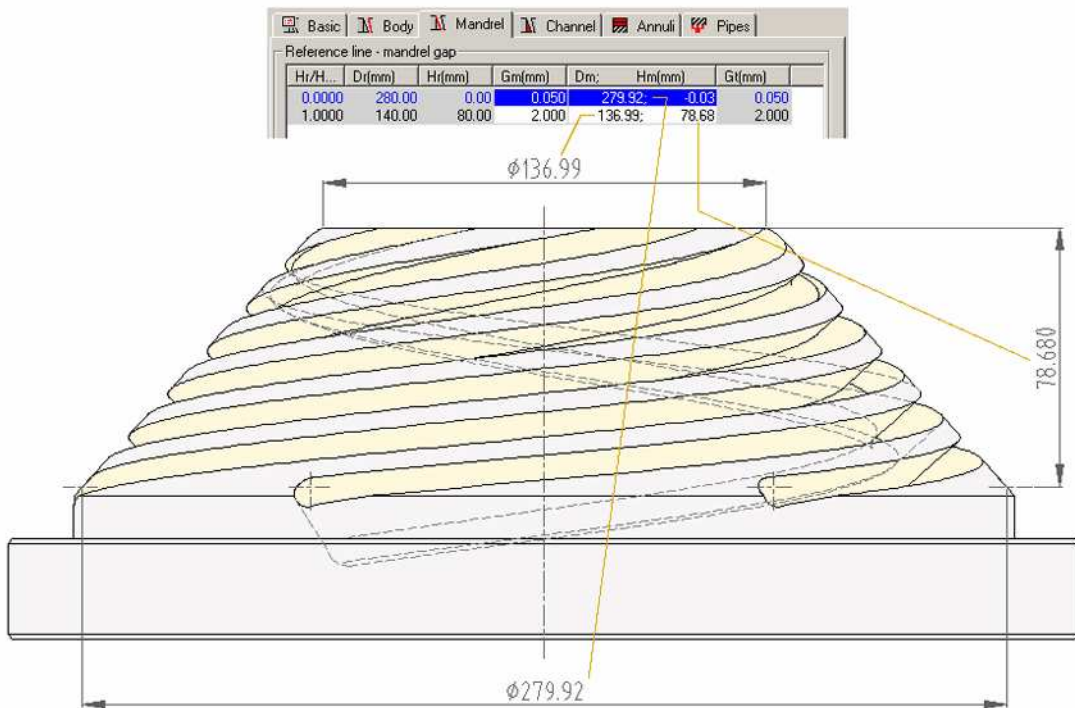


Fig. 20. Mandrel dimensions

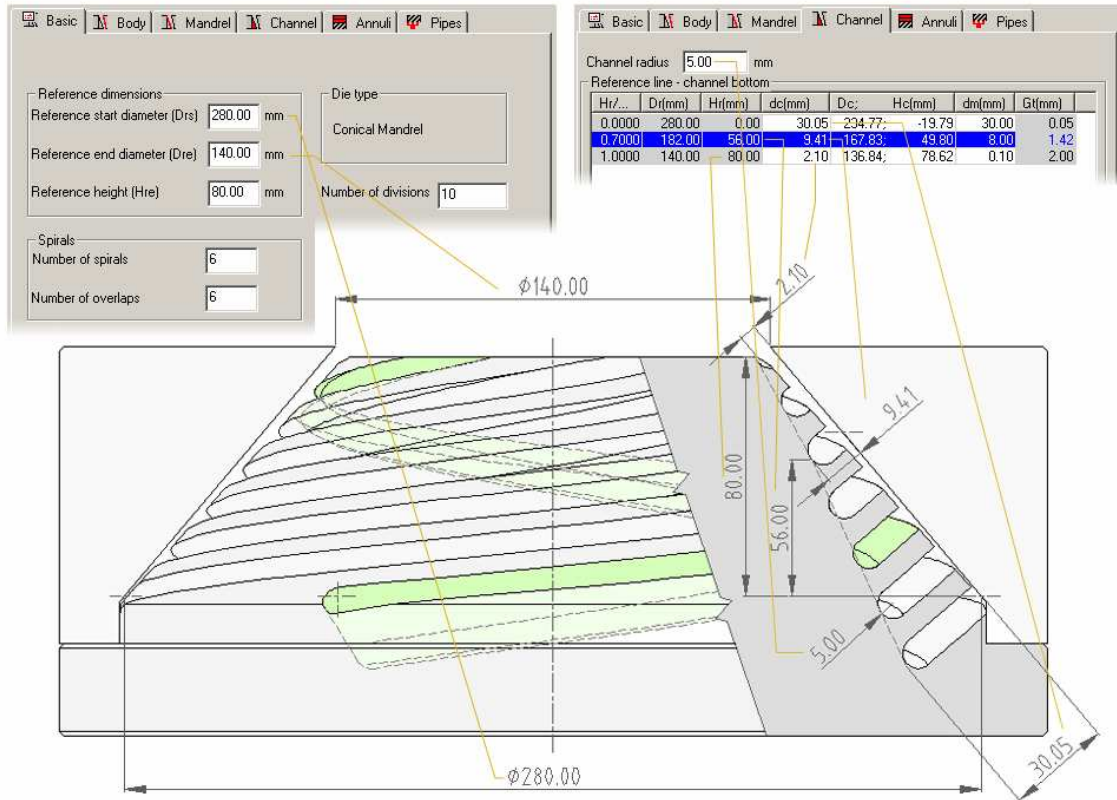


Fig. 21. Channel dimensions

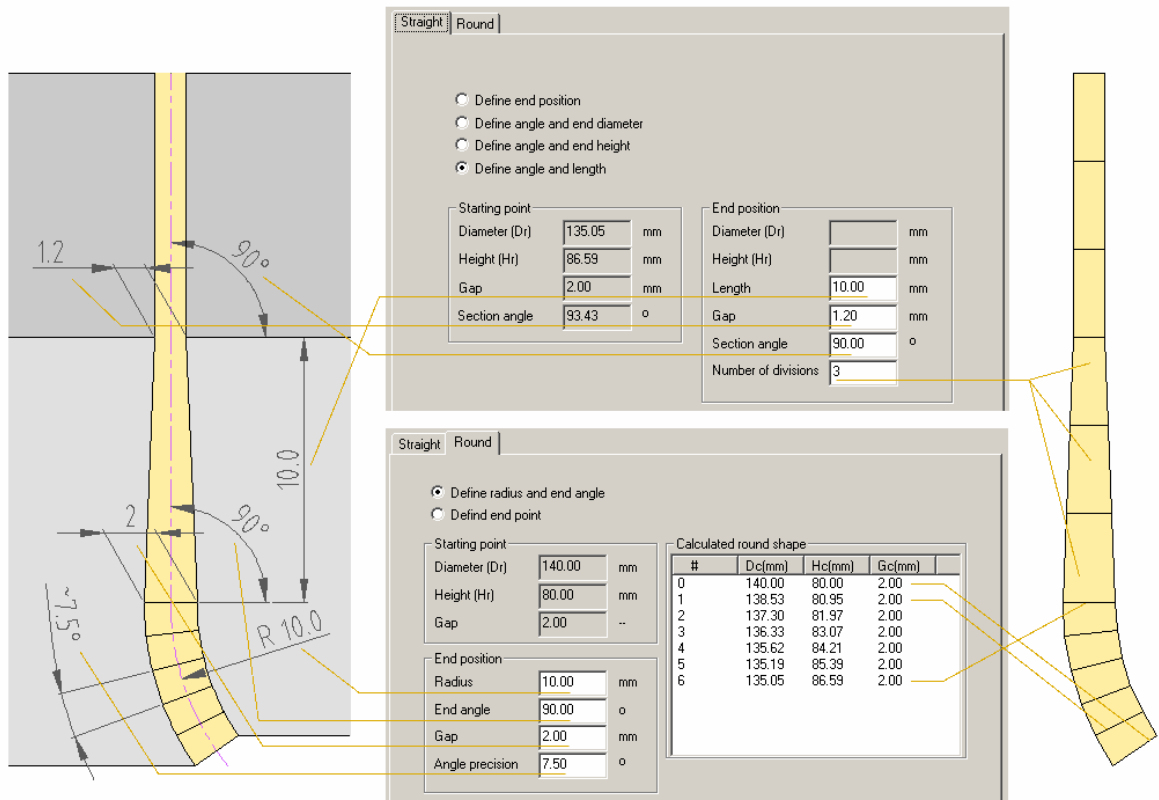


Fig. 22. Section above the spiral part

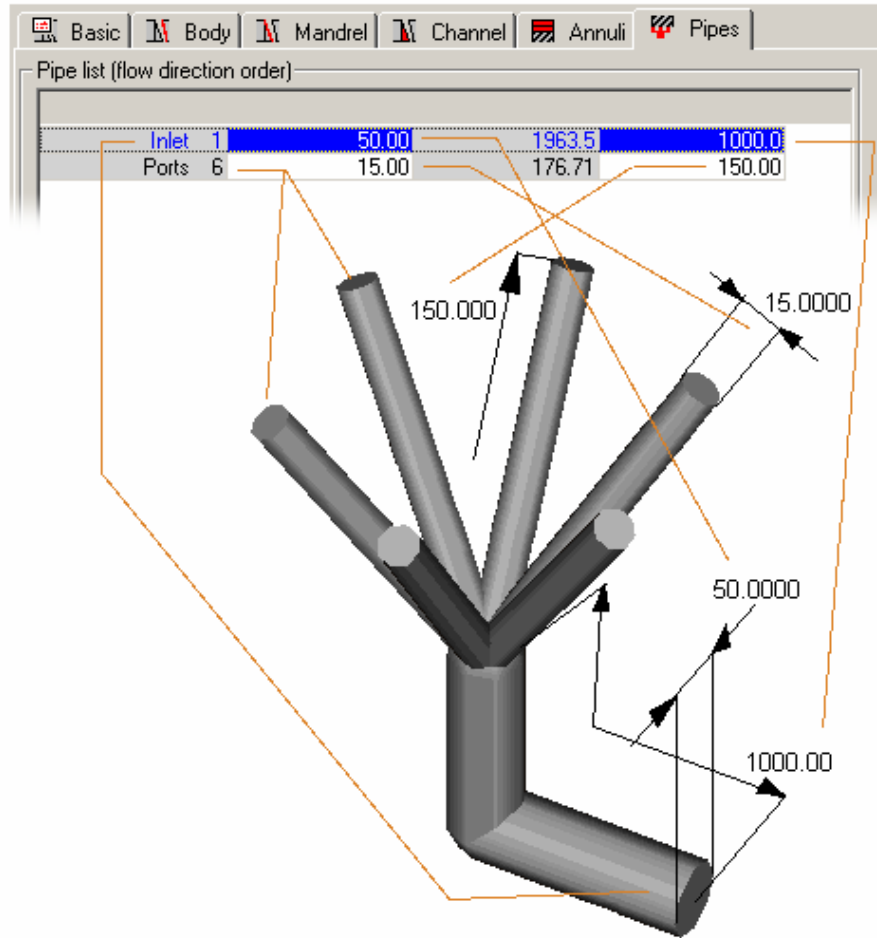


Fig. 23. Pipe system dimensions

6.3 Die Geometry Definition

Following figures show a mandrel of the die we are going to solve.

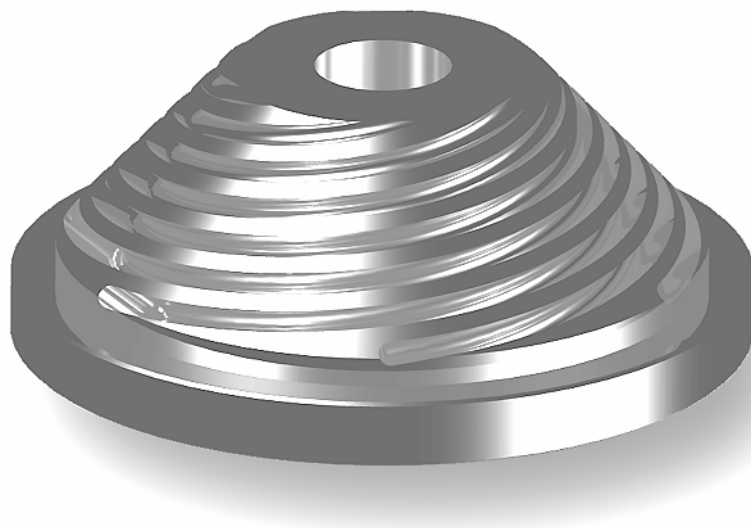


Fig. 24. Mandrel design

6.3.1 Basic Die Characteristics Definition

First of all, we have to enter the die name. Then we can start the geometry editing by the **Edit** button in the main toolbar. The Spiral Die Geometry editor starts. It contains *Basic* die characteristics and detail pieces of information of other die parts.

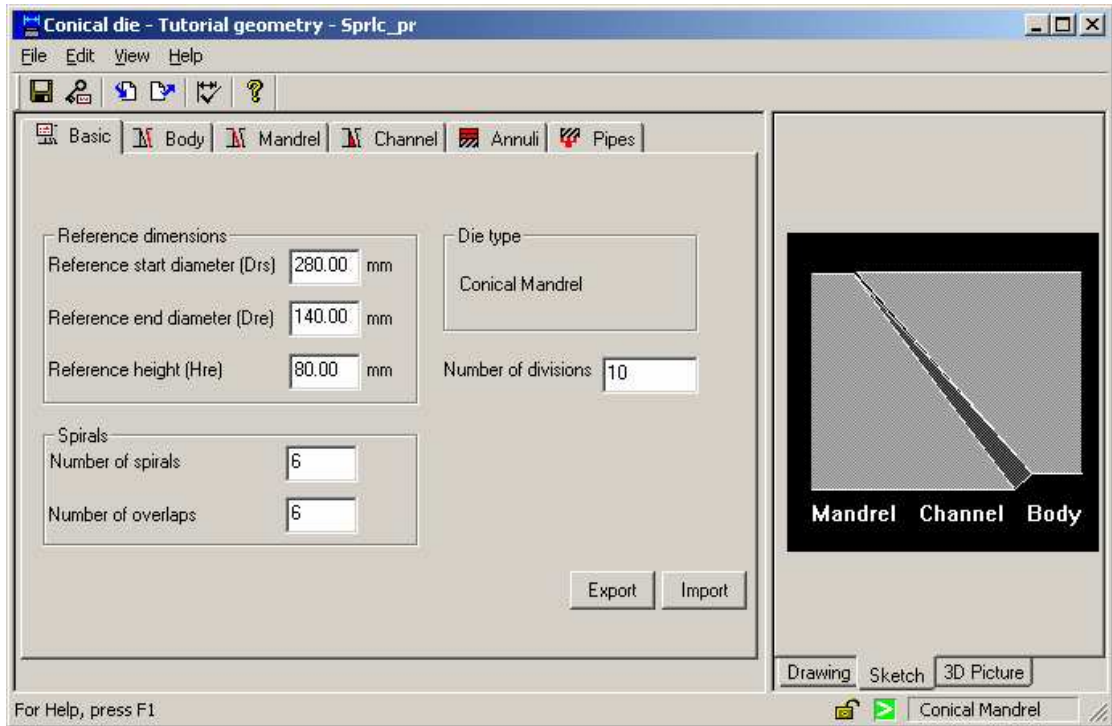


Fig. 25. Reference diameters editation

Now, we are setting the *Reference start diameter* value to 280 mm. Next set the *Reference end diameter* value to 140 mm. Further, the *Reference height* 80 mm must be set, as well. Both reference diameters and reference height define a *reference cone*. The Die type is now set as the *Conical Mandrel Die*.

Let's go to set *Number of spirals* and *Number of overlaps*, which are on the first tab sheet of the project data editor. The *Number of spirals* will be 6 and the *Number of overlaps* will be 6, too. It means that each spiral groove "makes" just one turn.

The *Number of division* parameter influences the precision of the numerical solution. The value is equal to 10. Switch to the *Body* sheet. [38]

6.3.2 Body Definition

Body sheet can set dimensions for the body part of the die. It contains some predefined parameters, too. The inner surface shaping (machining) is more expensive than the

shaping of outer ones. In the most cases the inner body surface is used to be identical with the shape of *the reference cone*. Than we continue to *Mandrel* sheet.

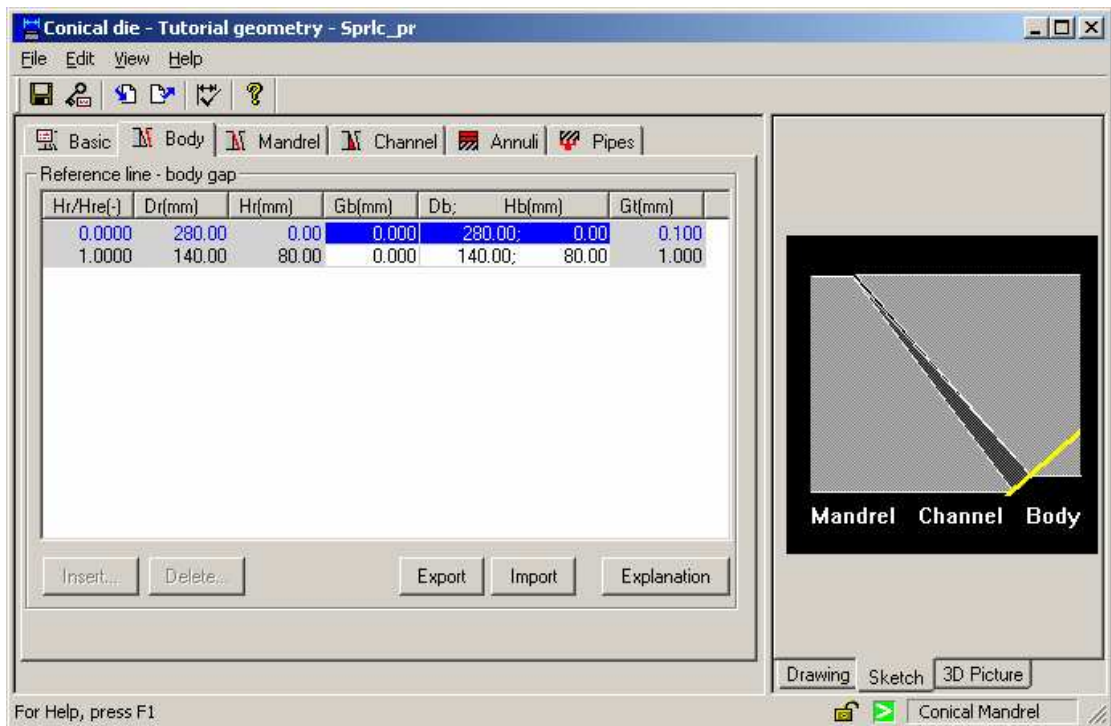


Fig. 26. Body dimensions editation

6.3.3 Mandrel Definition

We are setting the die *reference diameters*, *reference height* and the *gap* values in this sheet. The *gap Gm* start diameter (bottom) is setting to 0.1 mm and at the top is equal to 2.00 mm (at the end of spirals).

We do this if we click on the *Gm* value in the second row of the table, which is the same as the top of mandrel and set the value 2.00 in. It represents the gap from the reference cone to the mandrel.

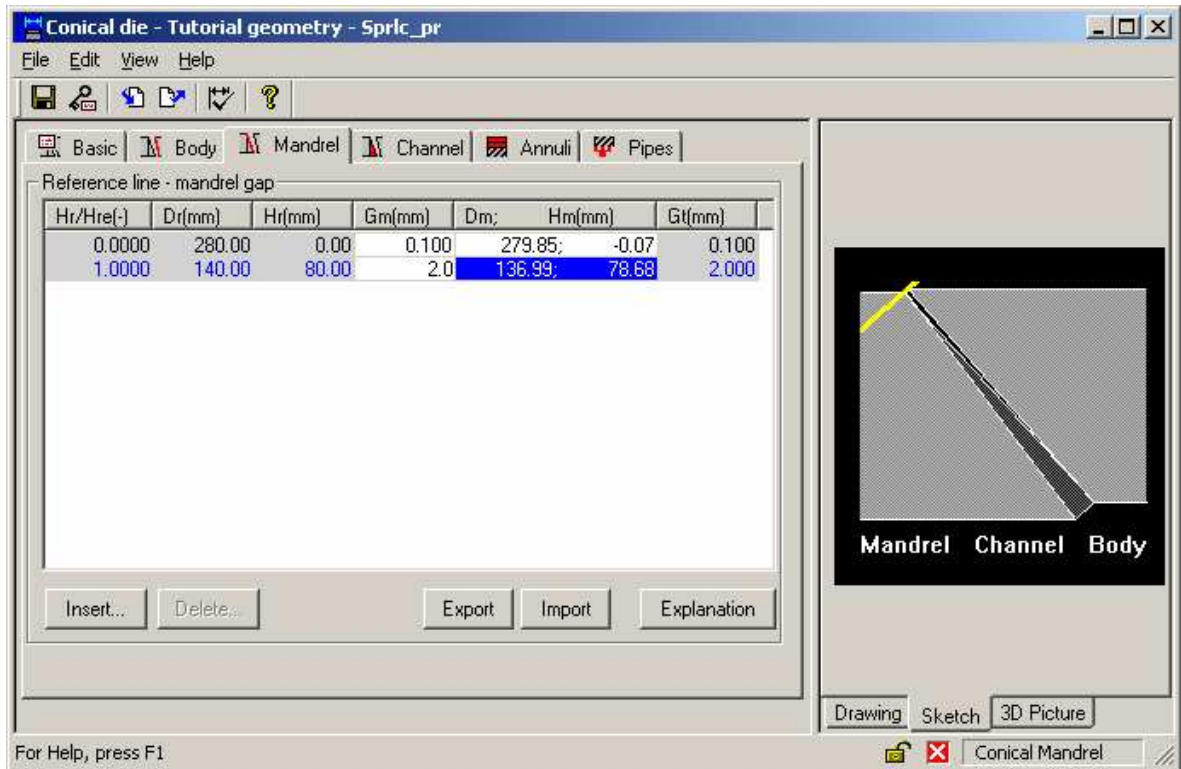


Fig. 27. Mandrel dimensions editation

The fourth sheet is **Channel**.

6.3.4 Channel Definition

This sheet is very similar to the mandrel sheet. There is only *Channel radius* added. Enter its value to 5.00 mm.

The channel depth changes over the mandrel height. We have to add positions between the beginning and the end positions. We have to create a channel profile change. We use the *real channel depth* measured from the mandrel surface and make the change. [38]

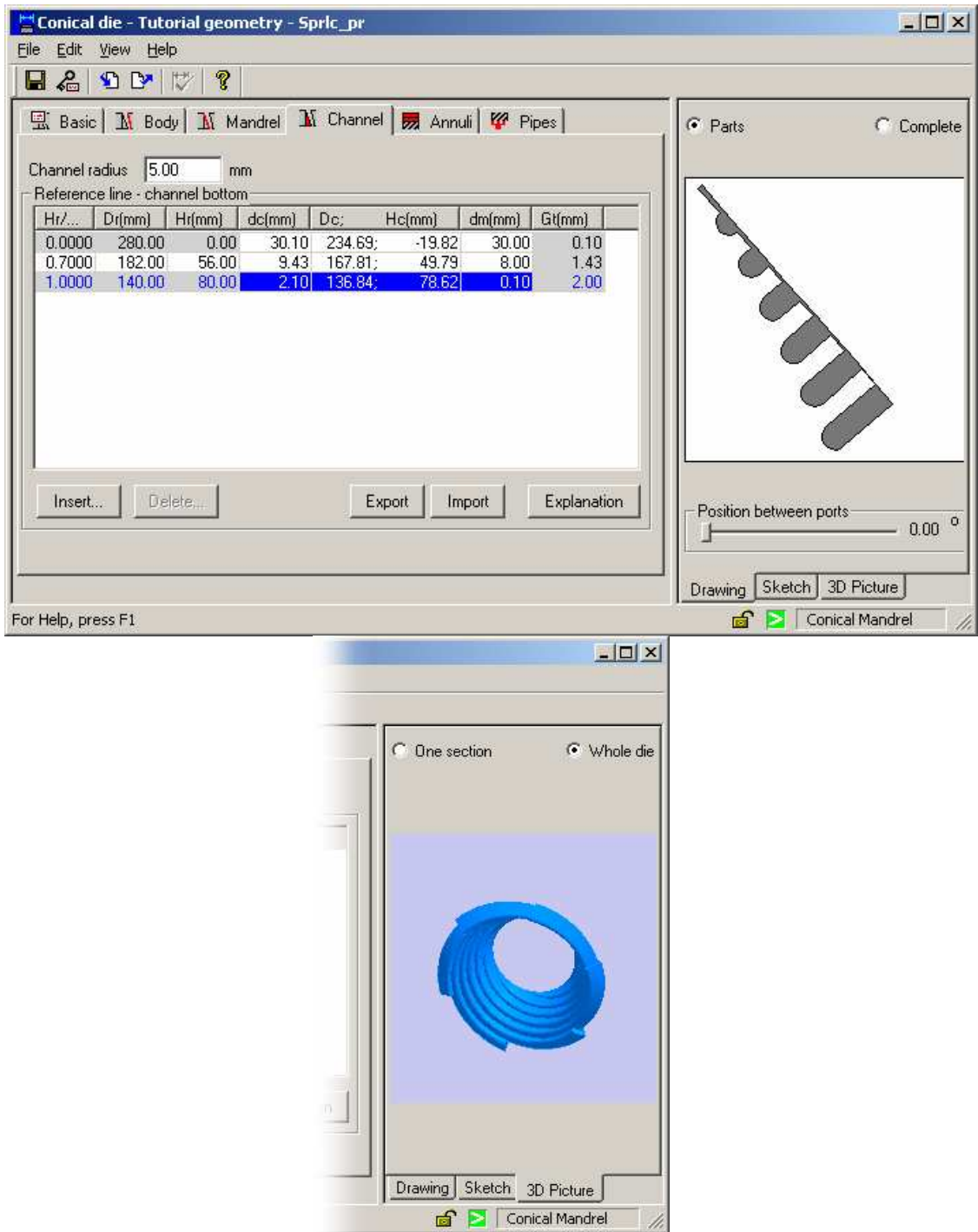


Fig. 28. Channel dimensions editation

Switch to the *Annuli* sheet.

6.3.5 Annuli Definition

Dimensions of the mandrel and die body were entered in the previous sheets. Now, we can enter dimensions of the parts "above" the body and spiral mandrel. To do this, select the *Annuli* sheet.

There is only a yellow line in the beginning. The line shows the *spiral part outlet*. There is no channel change in the sheet so far. We have to make a mouse click to the **add button**. Definition table opens.

We select **Define radius and end angle option**. It will make round sections between the end of the flow channel and a created flow channel outlet. We are set the values of the *end angle* and channel *radius*. The height is calculated by click on the **Calculate** button.

The screenshot shows a dialog box titled "Section above definition" with two tabs: "Straight" and "Round". The "Round" tab is active. Under "Starting point", there are fields for Diameter (Dr) = 140.00 mm, Height (Hr) = 80.00 mm, and Gap = 2.00 mm. Under "End position", there are fields for Radius = 10.00 mm, End angle = 90.00°, Gap = 2.00 mm, and Angle precision = 7.50°. A "Calculated round shape" table is empty. At the bottom are "Accept", "Calculate", and "Cancel" buttons. To the right of the dialog box is a summary table:

Method Define radius and end angle	
Radius [mm]	10.0
End angle	90°
Gap [mm]	2.00
Angle precision	7.50°

Fig. 29. Channel radius and end angle

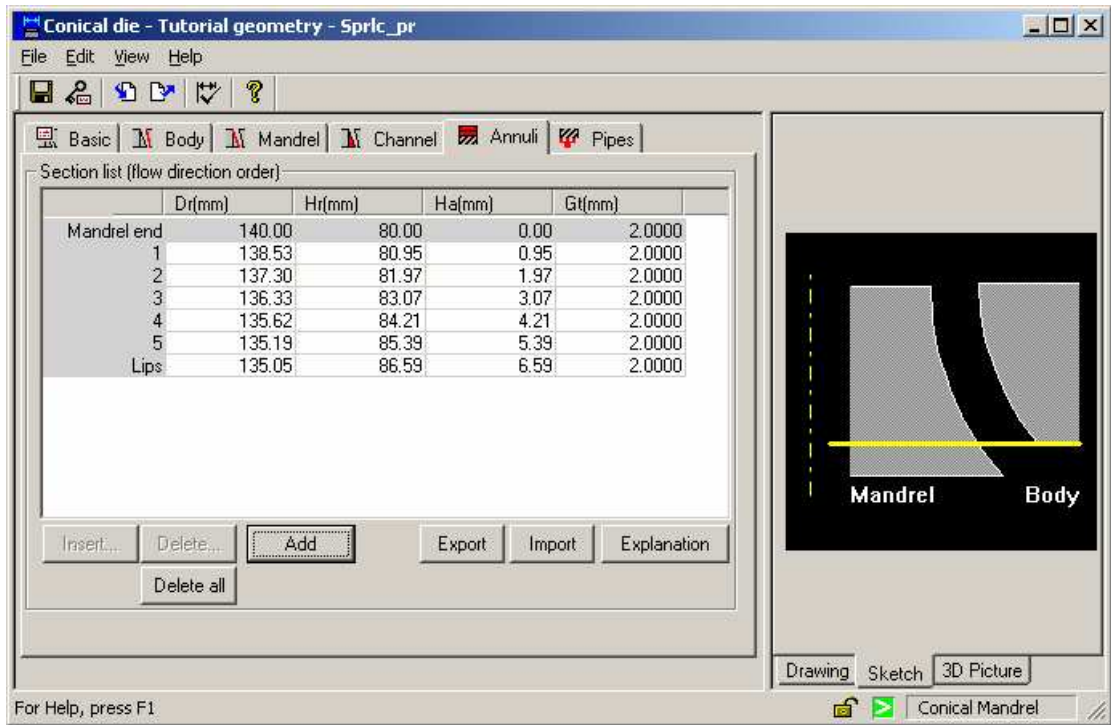


Fig. 30. Round section calculated values

We have to add *tapered transition channel* and *parallel channel* to the *finish die output lips* geometry. Click the **Add** button again to add a straight tapered transition channel. Choose the **Define angle and length** method for the channel definition. Enter the values and press the **Calculate** button again. [38]

Method	Define angle and length
Length	10.0 [mm]
Gap	1.20 [mm]
Section angle	90.0°
Number of divisions	3

Tab. 2. Transition channel values

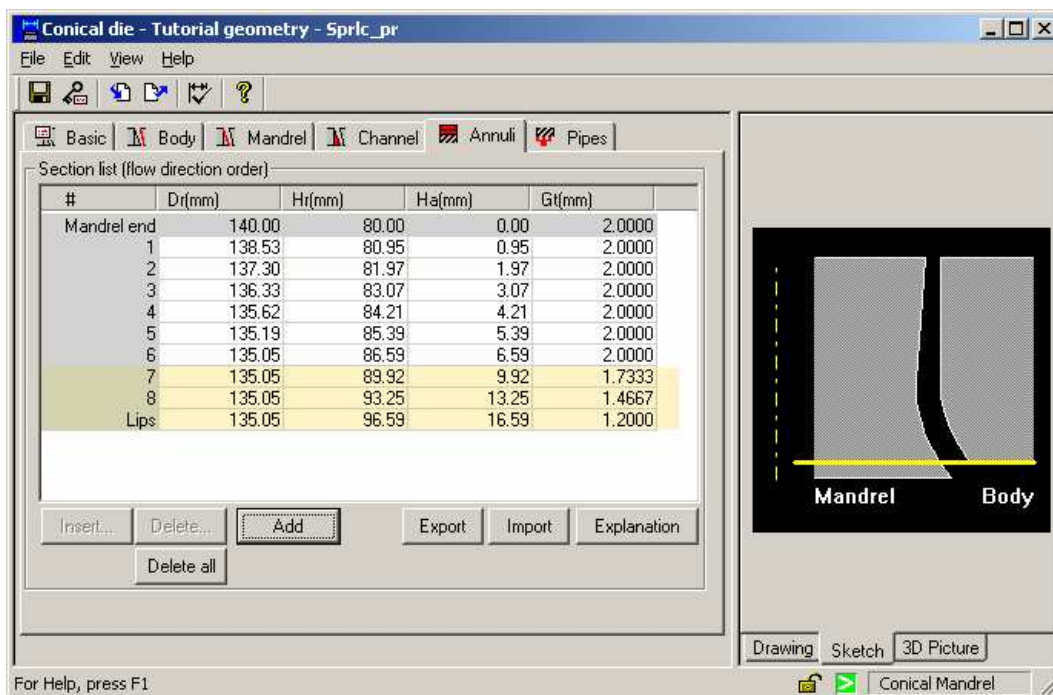


Fig. 31. Transition channel calculated values

There are three new sections in the **Anulli** sheet. Let`s do the same procedure for *output lips*. Press the **Add** button and enter the following parameters.

Method	Define angle and length
Length	10.0 [mm]
Gap	1.20 [mm]
Section angle	90.0°
Number of divisions	3

Tab. 3. Output lips values

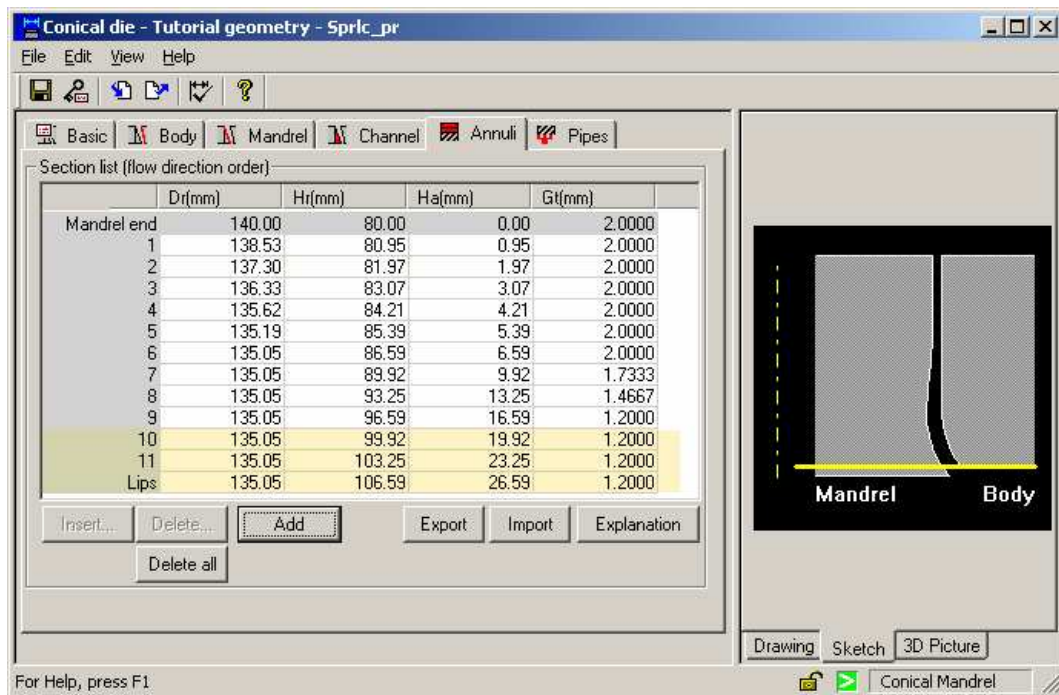


Fig. 32. Output lips caculated values

Click the **Calculate** button and the **Accept** button to enter parameters. The part of the die named *annuli* or *sections above* is completed. The last one is the *Pipes* sheet.

6.3.6 Pipes Definition

The last sheet contains entering dimensions of substitutional geometry of the pipe system, which distributes the melt from extruder to single spiral *ports*. There is only one item called **Die inlet**. So we have to create feeding pipe system prior the spiral part. Click **Add** button to insert the pipe feeding system. We have 6 *ports* of the spiral mandrel die. That means we need 6 *pipes* of feeding system.

Pipes diameter is set to $D = 15$ mm. The pipe length is exactly $L = 150$ mm. The calculated pipe cross-section area is $S = 176.71 \text{ mm}^2$. Click the **Add** button again to create another pipe section. The number of *Splits* is initially equal to 1. Let`s go to set the pipe length to $L = 1000$ mm and the pipe diameter $D = 50$ mm. The pipes feeding system is defined completely.

The flow order is given by the pipe order. That means the material will flow from the bottom upwards. [38]

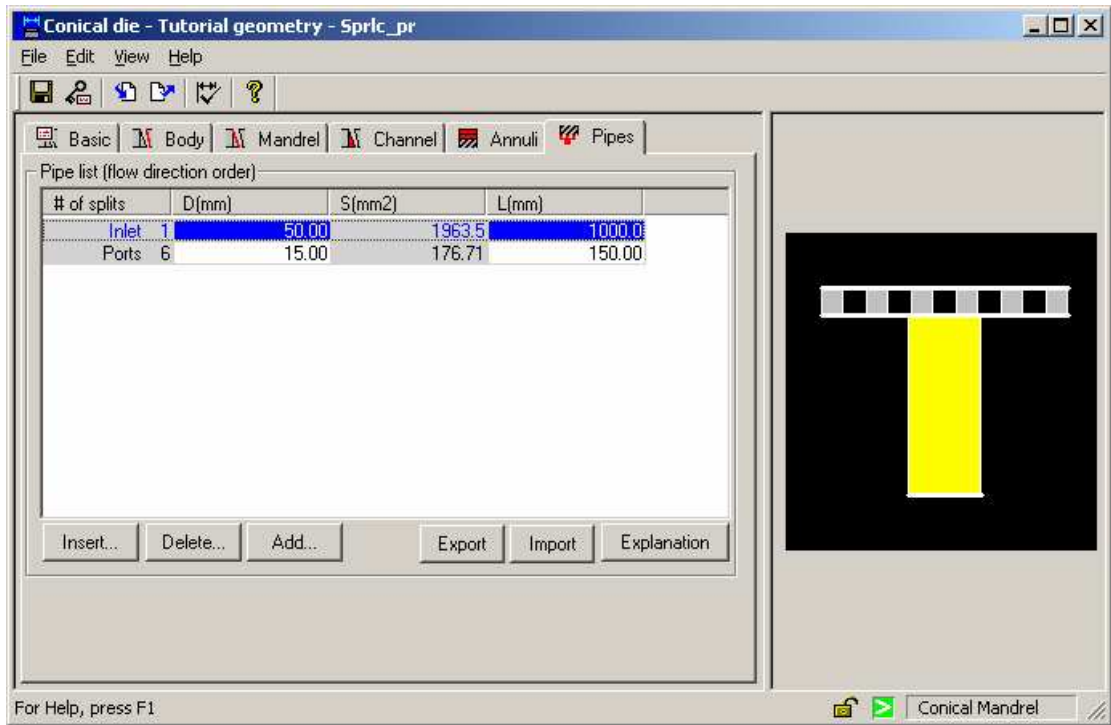


Fig. 33. Pipes feeding system

6.4 Project definition

We specified dimensions of the flow domain by entering the die dimensions. We also have to set the process conditions. The basic process conditions are the *mass flow rate*, the material *input temperature*, the *die temperature* and *material* from material database of the VEL software. It is necessary specify the conditions for the solution like number of divisions and conditions for numerical iterations, too.

Project Name	Conical die
Used die	Conical die
Body temperature	240 °C
Material	HDPE, Typical 1MI Film
Mass flow rate	220 kg/h
Material temperature	190 °C
Number of iterations	300

Tolerance level	0.01
Number of divisions	20
Type of solution	Solver 2D

Tab. 4. Project definition data

We can start a solution by using the Vel internal solver. Than we have to transform data to the VEL`'s 3D-Fem module and start a new 3D solution. [38]

7 PROJECT DATA PREPARATION – 3D FEM MODULE

3D-FEM module is much easier than Spiral die module. We use Spiral Die 3D Templates for all project data transformation. Than open the Conical Die template. There is only one important thing to do in the 3D-FEM module. We have to convert grid from 2D grid to 3D grid. We do this by click on the *Grids/convert* in the main toolbar.

7.1 Solver Settings

The 3D-FEM Solver is more complicated than 2D solver. We have to present much time to its setting because it is necessary for a better and correct solution. First of all we set the number of interations and other usefull parameters. When the number of interations is bigger the solution time become longer but for a better solution we need about 300 interations. We can set the update of results, save datas or graf update during the calculation, too.

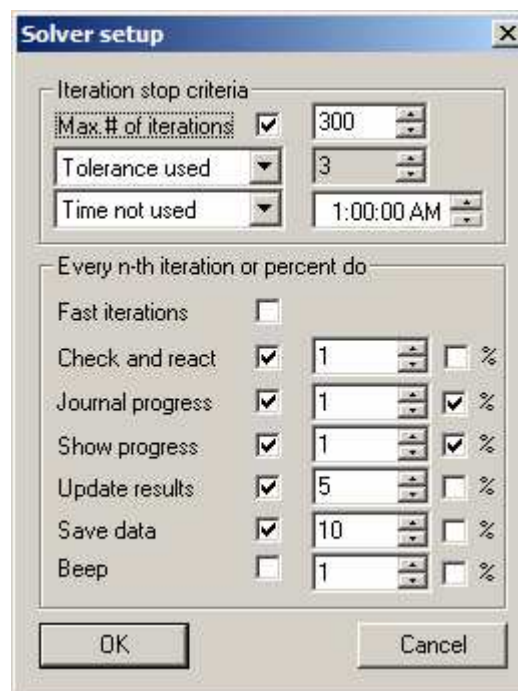


Fig. 34. Iteration setup

The most important settings are the relaxation values. The relaxation values are tolerances between the last two interations calculations. The calculation ends only when all tolerances are correct. We also have to set temperature interations, because the temperature is not calculated without setting. All relaxation values are on following figures. [39]

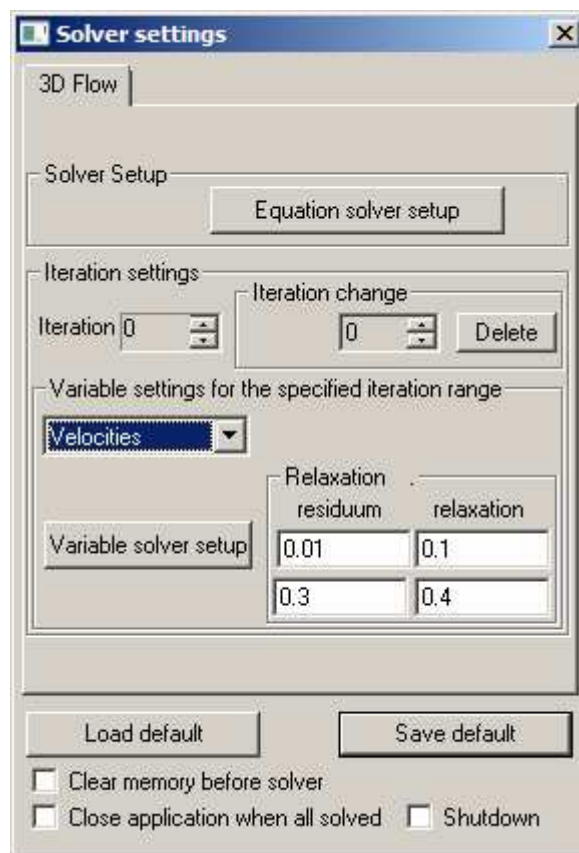
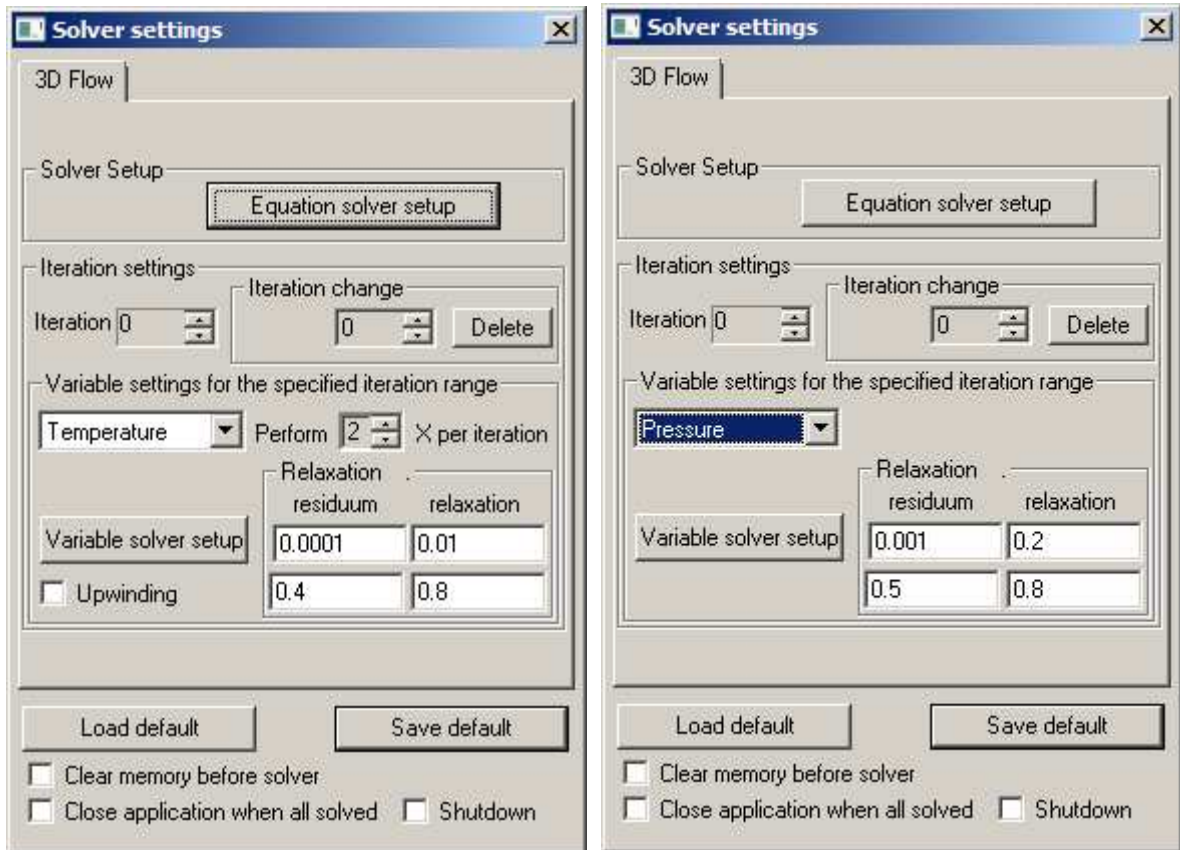


Fig. 35. Relaxation values

8 RESULTS AND DISCUSSION

When is the calculation finished we can look at results by clicking the **results** button. The most important results are flow rate throughgt spiral system, flow rate at the outlet and pressure drop.

8.1 Conical Die – Spiral die module results

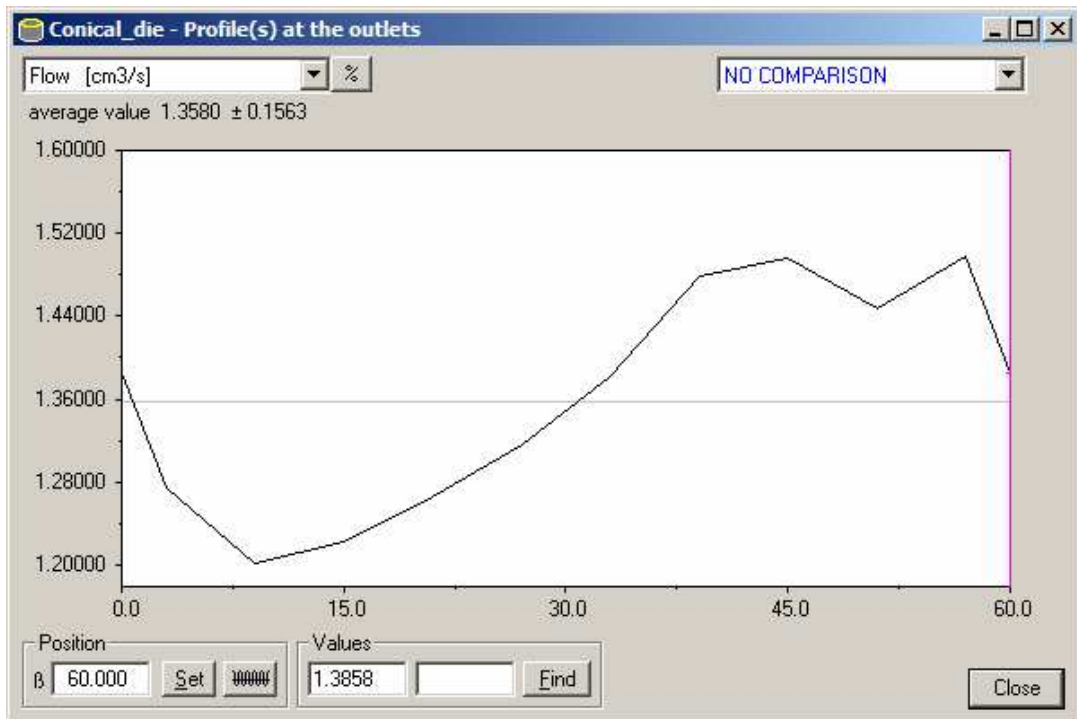


Fig. 36. Conical die - Outlet flow rate

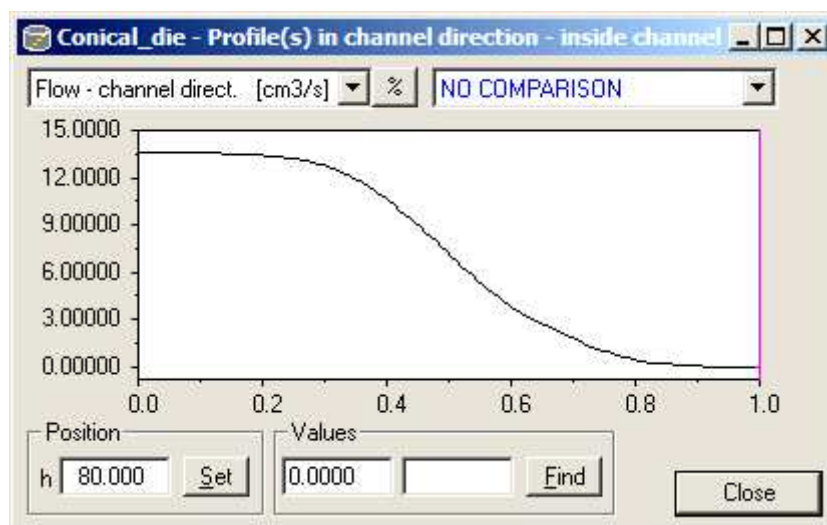


Fig. 37. Conical die – Channel flow rate

8.2 Conical Die – 3D FEM module results

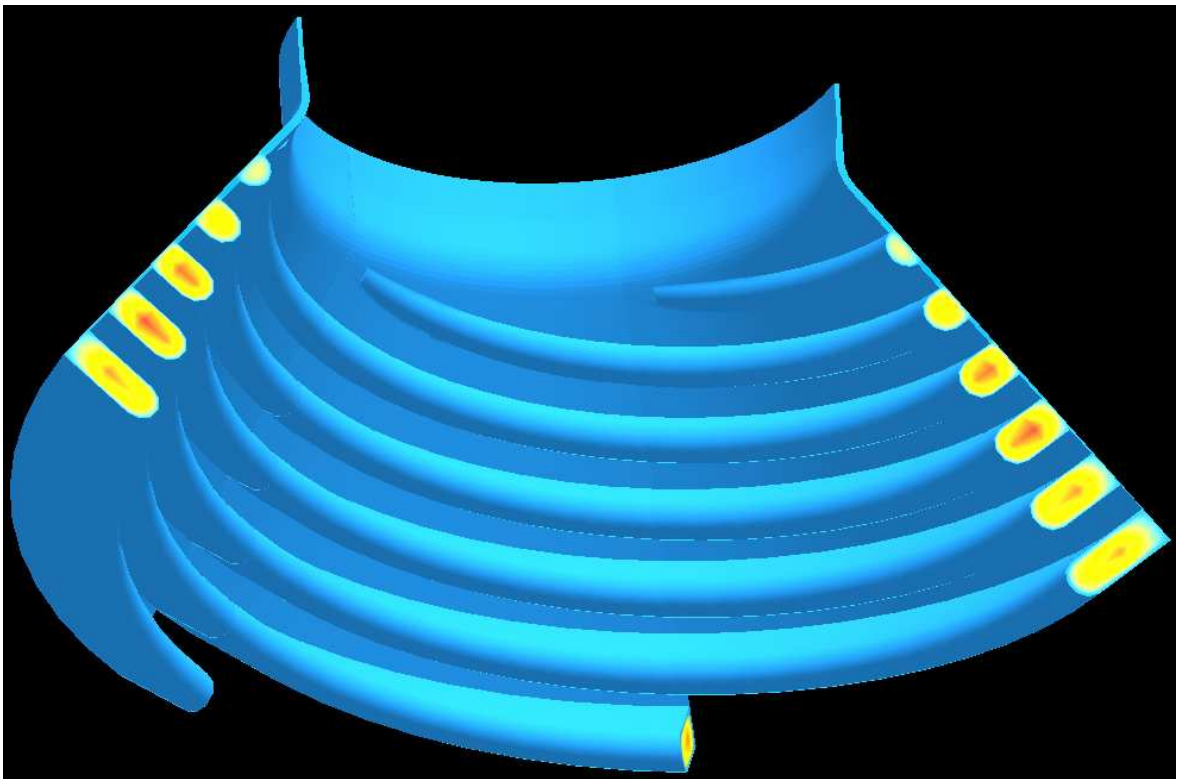
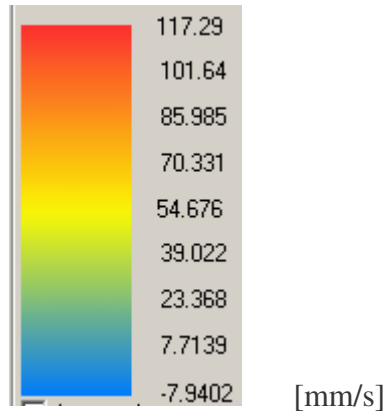
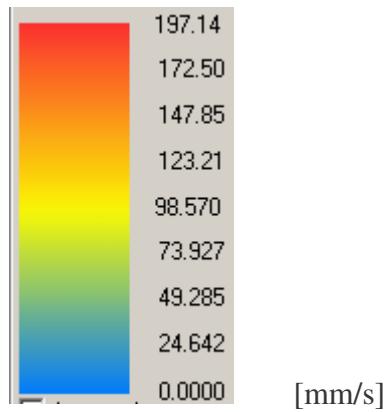


Fig. 38. Conical Die - Angle velocity profile



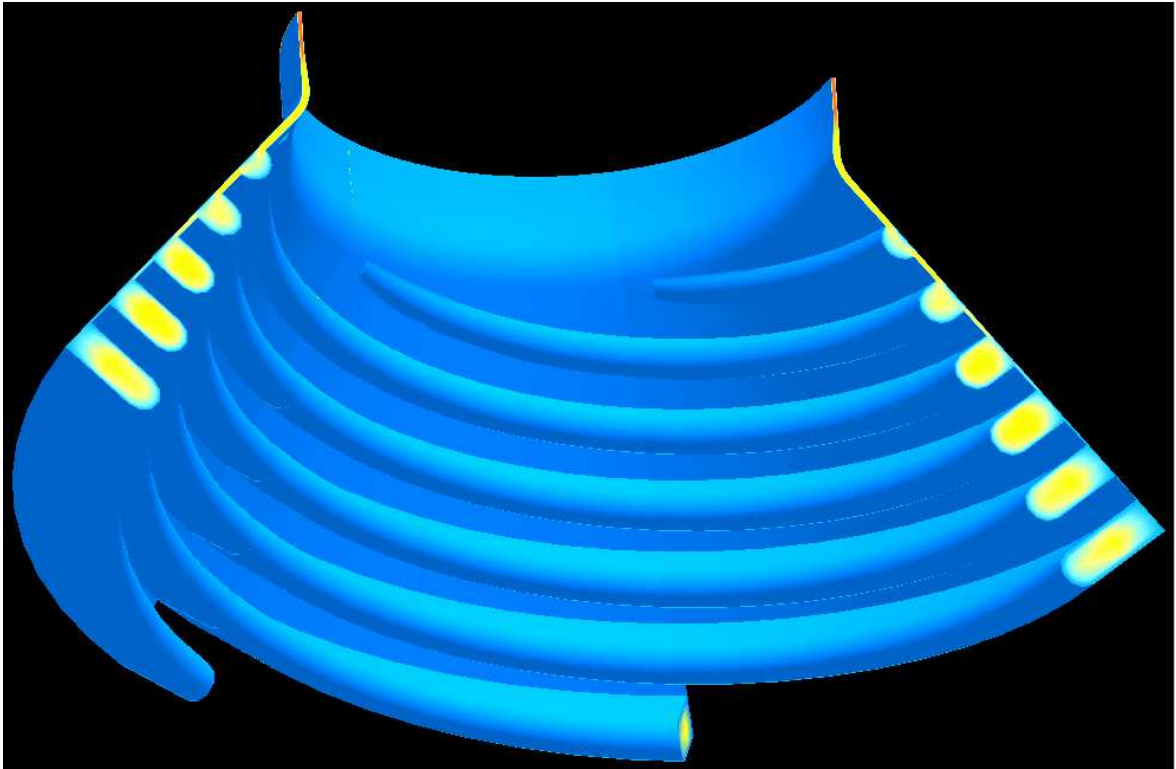
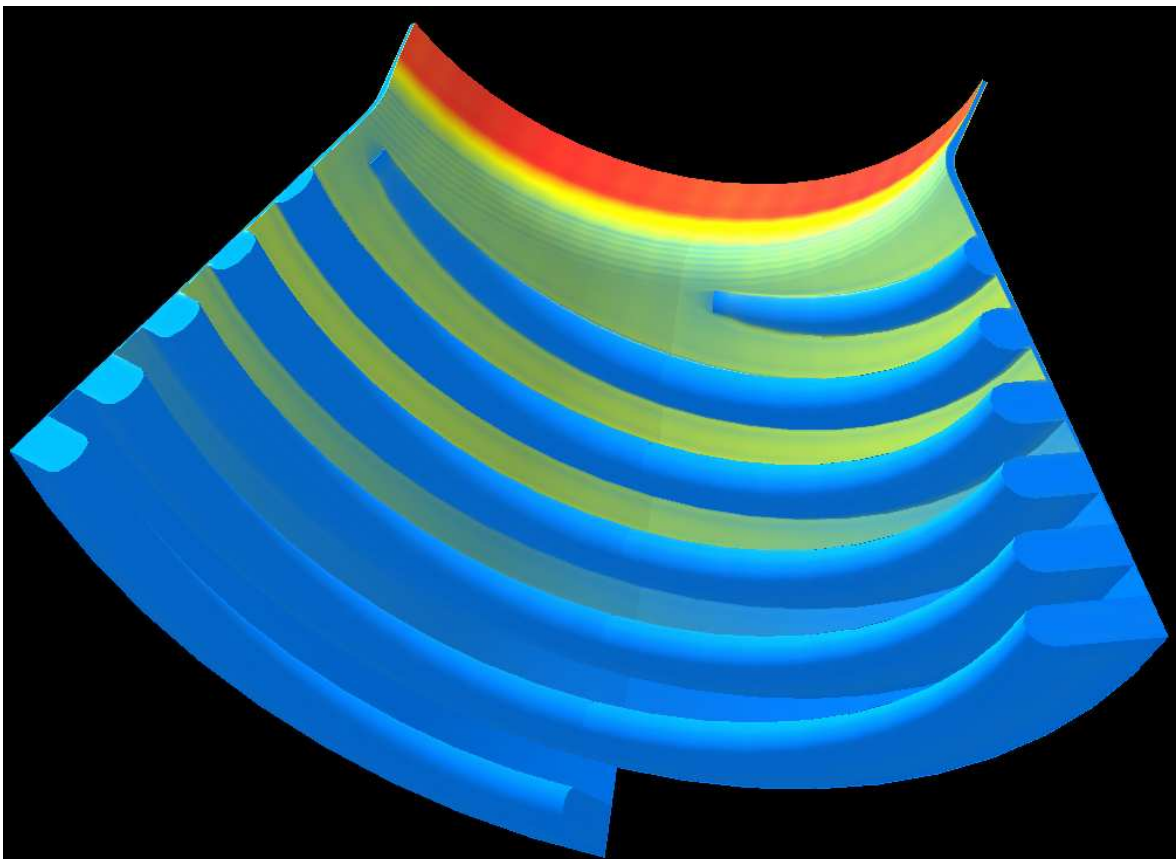


Fig. 39. Conical Die – Velocity magnitude profile



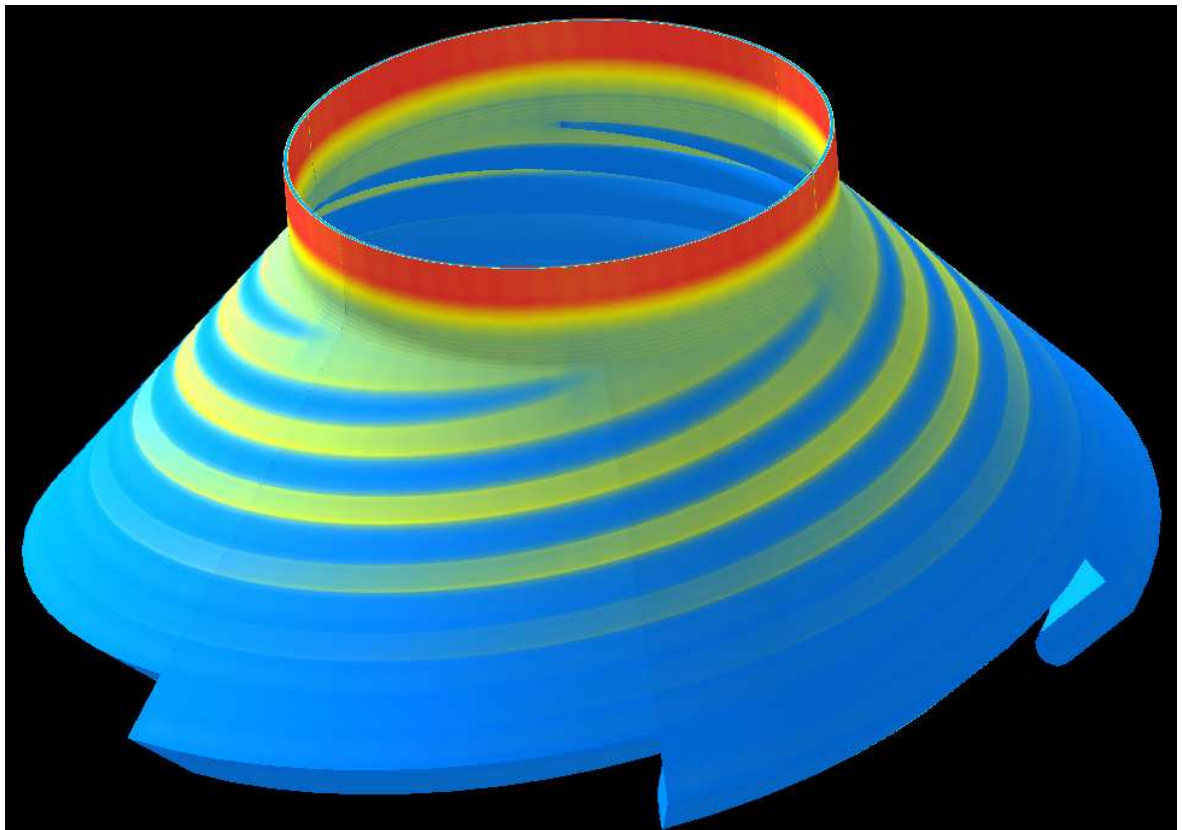
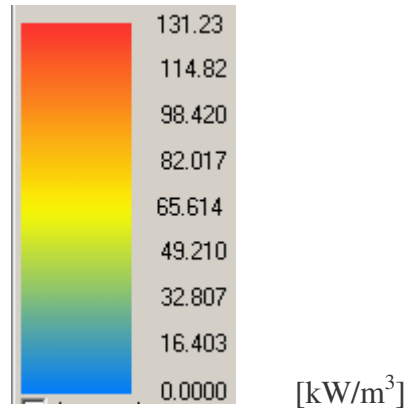
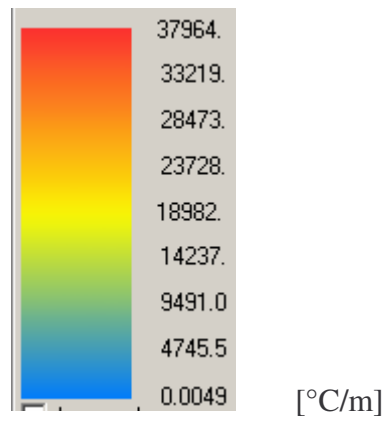


Fig. 40. Conical Die – Disipation profile



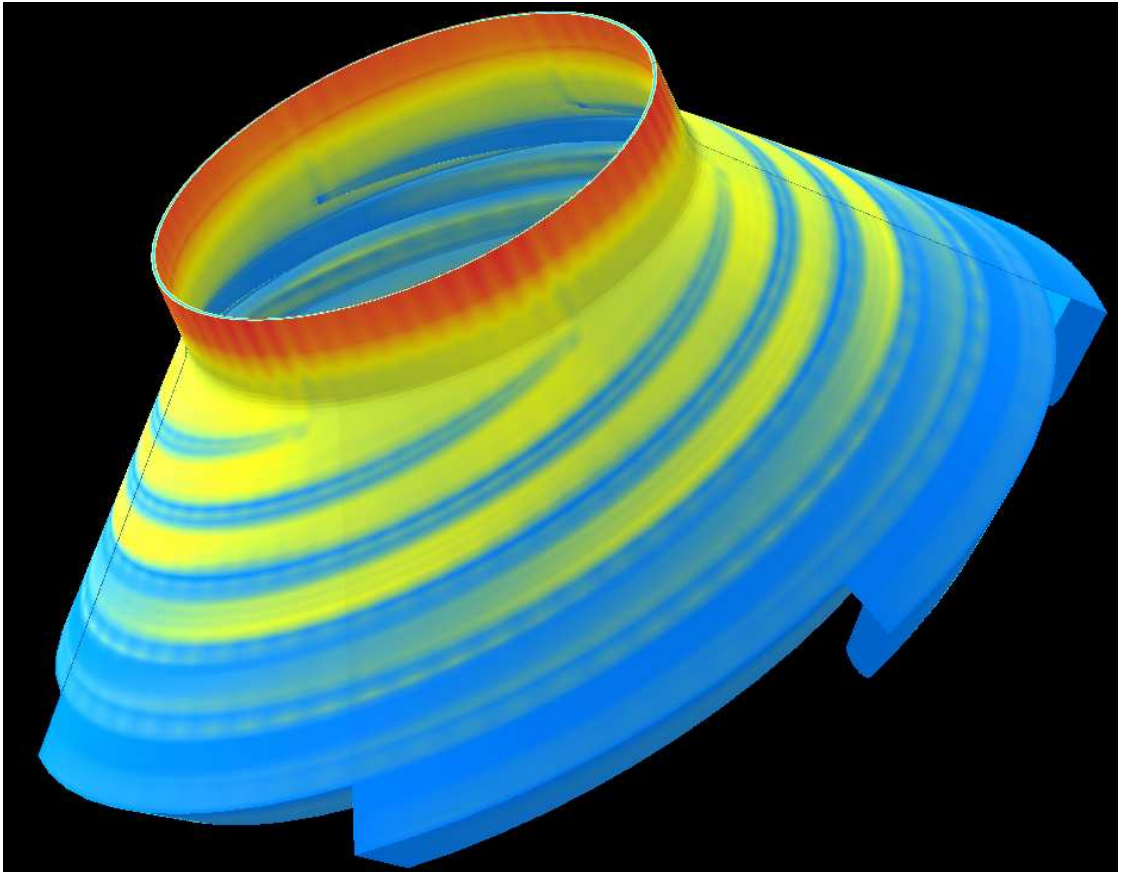
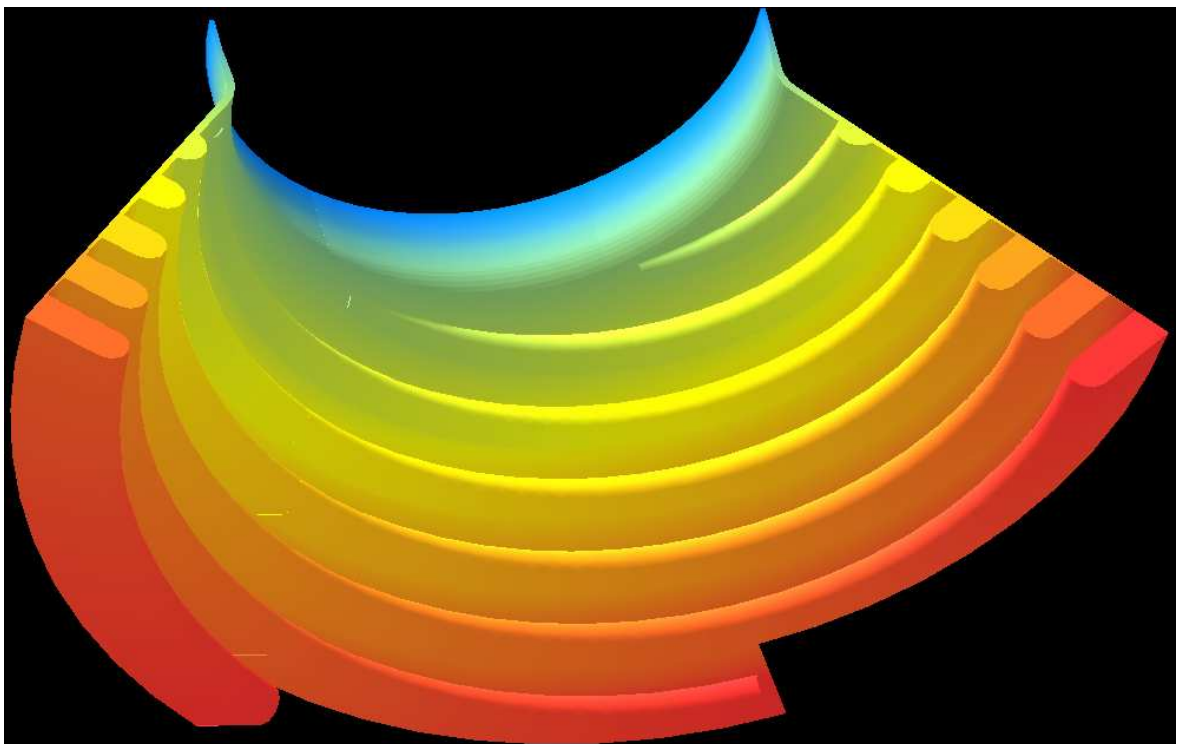


Fig. 41. Conical Die – Temperature gradient profile



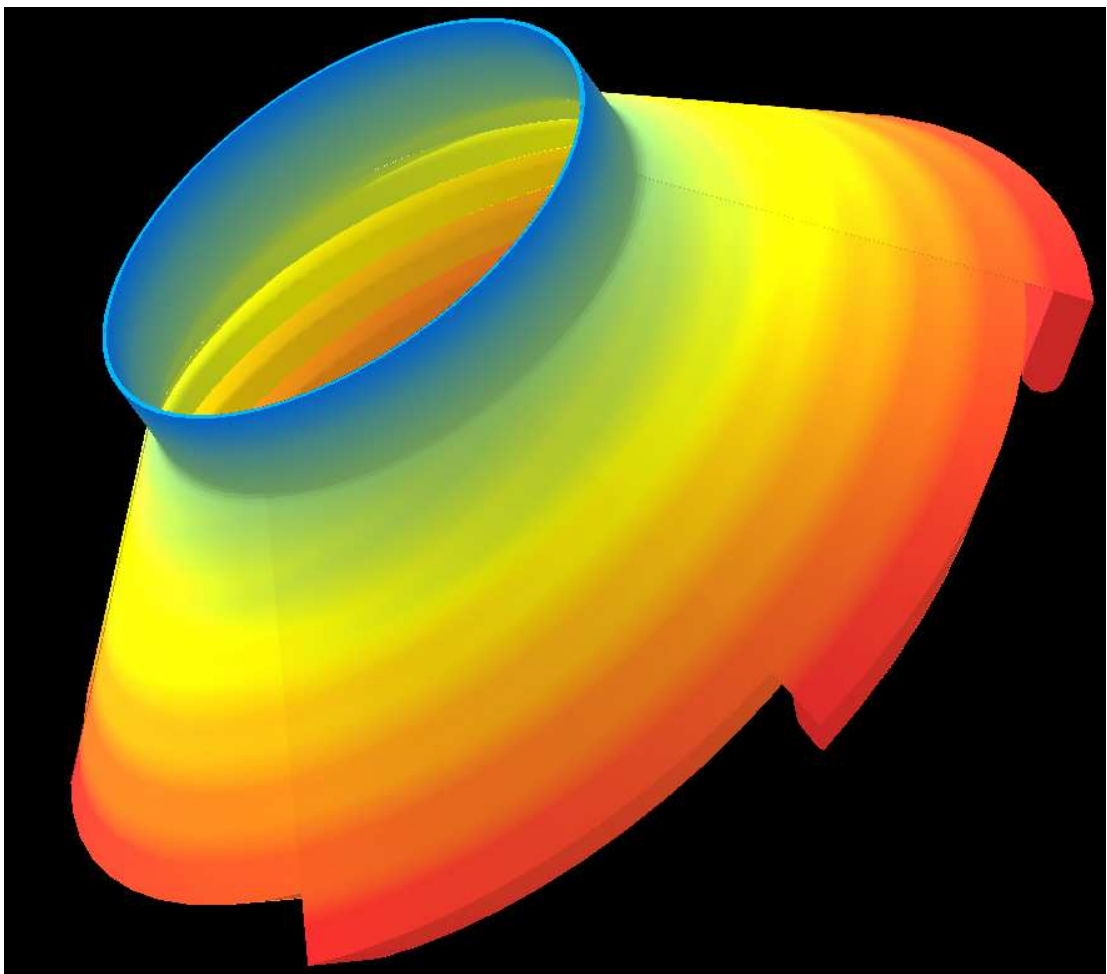
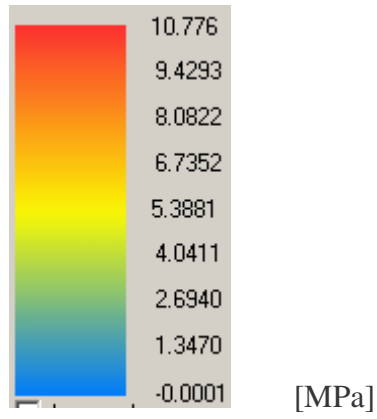


Fig. 42. Conical Die – Pressure profile

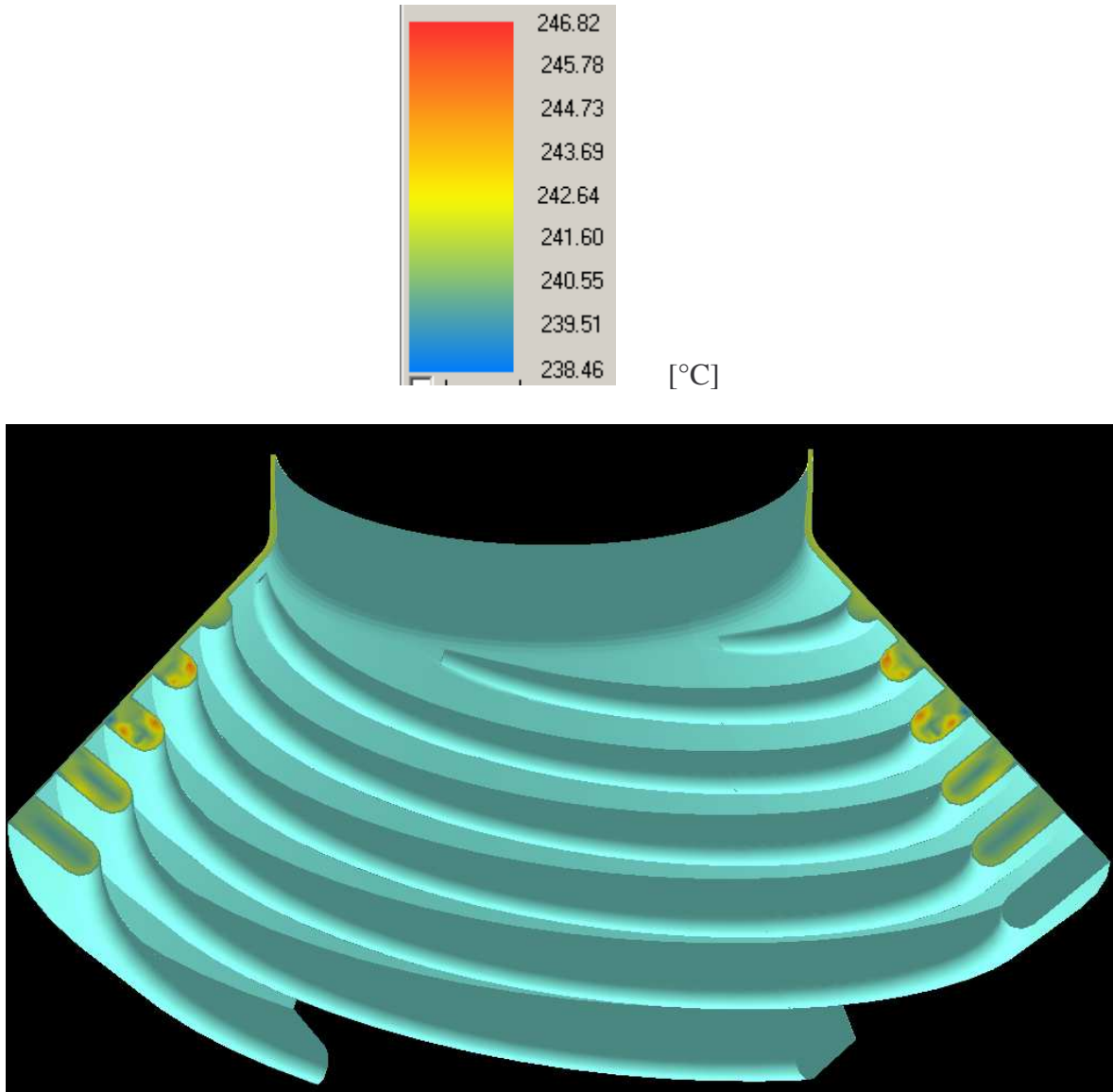
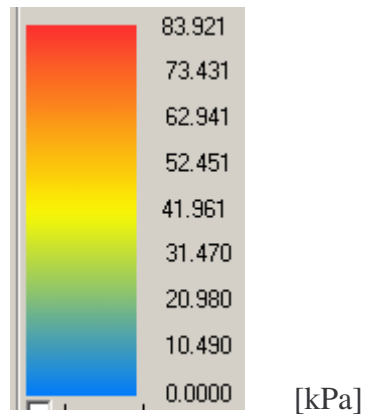


Fig. 43. Conical Die – Temperature profile



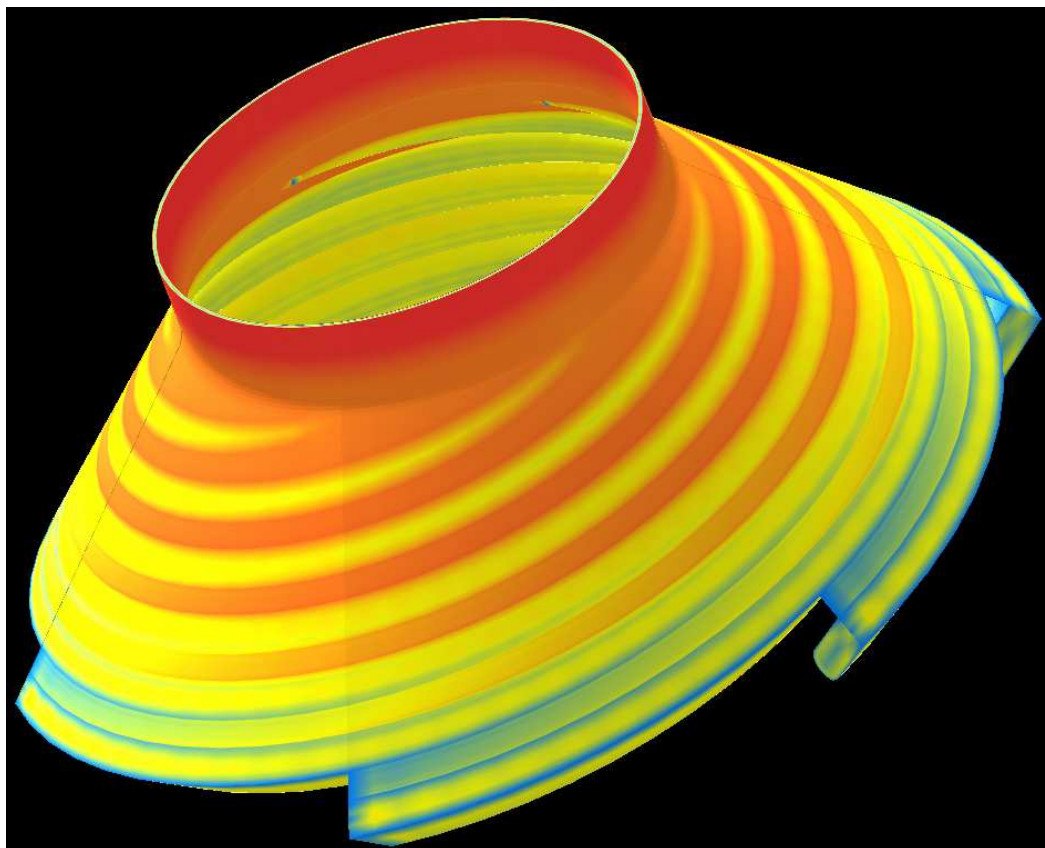
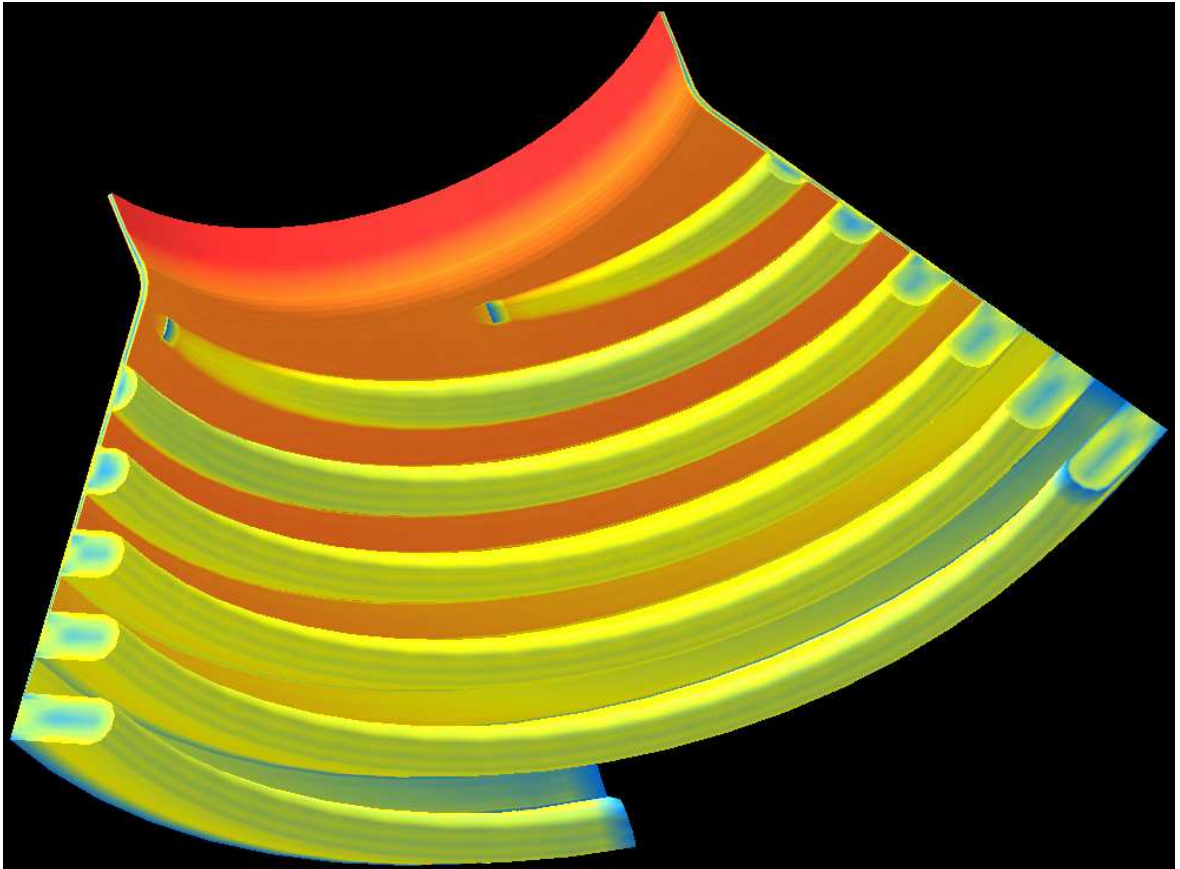


Fig. 44. Conical Die – Shear stress profile

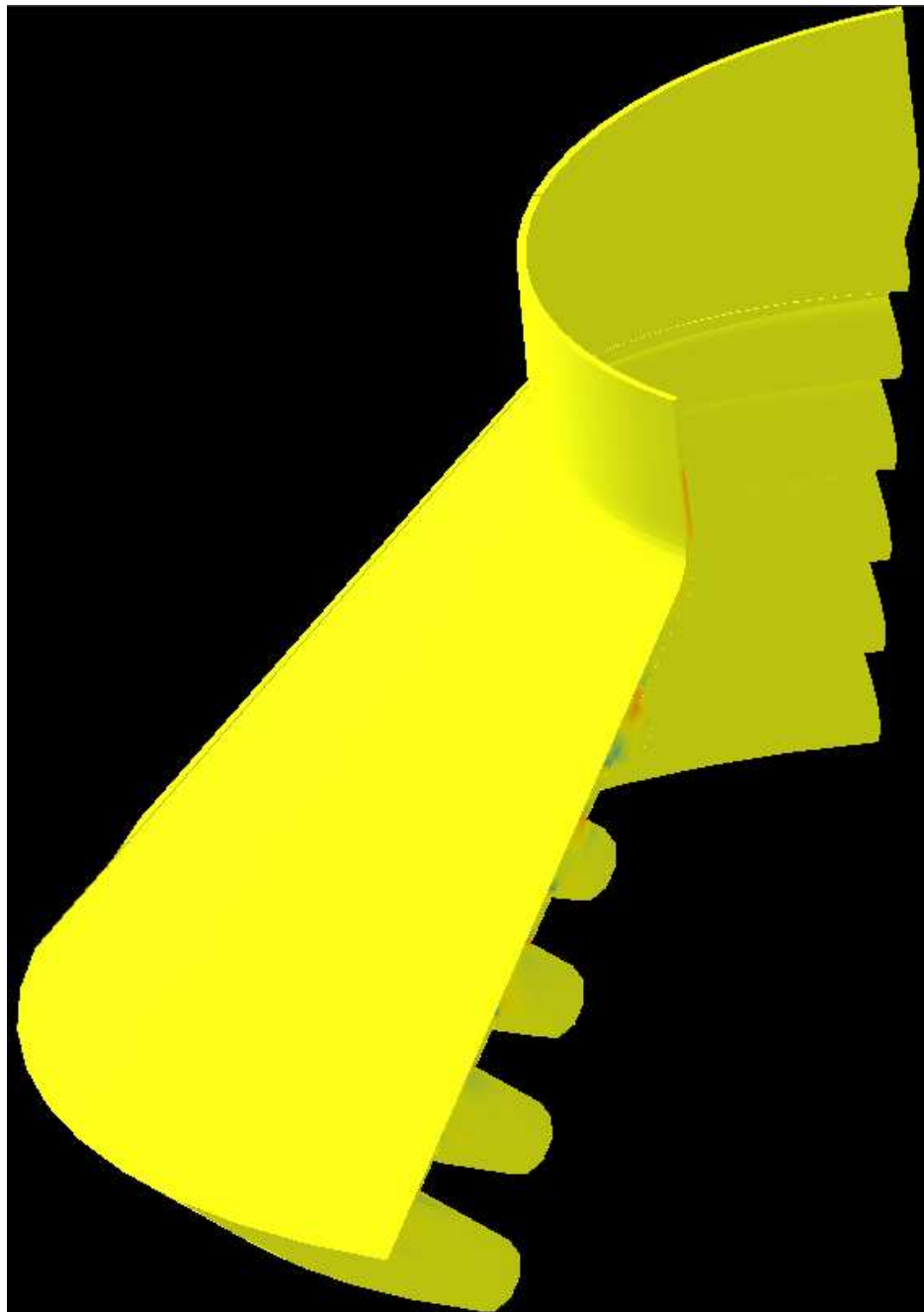
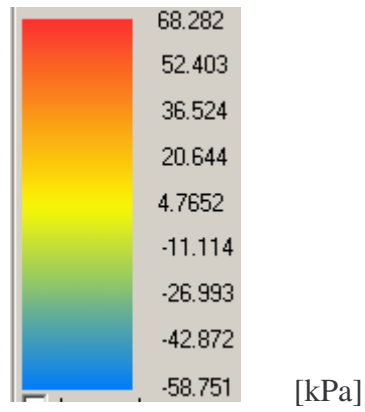


Fig. 45. Conical Die – Elongation stress profile

We can look at outlet flow rate results. It is easy to see results because we can use predefined function Flow rate axi symmetrical deviation. This function is in the main tool-bar of 3D-FEM module of VEL software in User commands/ Reports/ Studio. Measured values show tab.5. The angle value 1.5° represents the center value of interval $0-3^\circ$. This is the same for all measure dies. Microsoft Excel is used for every calculation necessary for this Master thesis.

Angle [°]	Mass flow rate [kg/h]	Volumetric flow rate [cm ³ /s]
1.500	1.796	0.631
4.500	1.805	0.634
7.500	1.815	0.638
10.500	1.826	0.642
13.500	1.837	0.646
16.500	1.846	0.649
19.500	1.854	0.652
22.500	1.860	0.654
25.500	1.864	0.656
28.500	1.866	0.656
31.500	1.866	0.656
34.500	1.863	0.655
37.500	1.859	0.654
40.500	1.851	0.651
43.500	1.840	0.647
46.500	1.826	0.642
49.500	1.812	0.637
52.500	1.799	0.633
55.500	1.792	0.630
58.500	1.791	0.630
SUM	36.666	12.893
AVERAGE	1.833	0.645
DEVIATION [%]	±1,5	±1,4

Tab. 5. Conical die - Outlet flow rate measured values

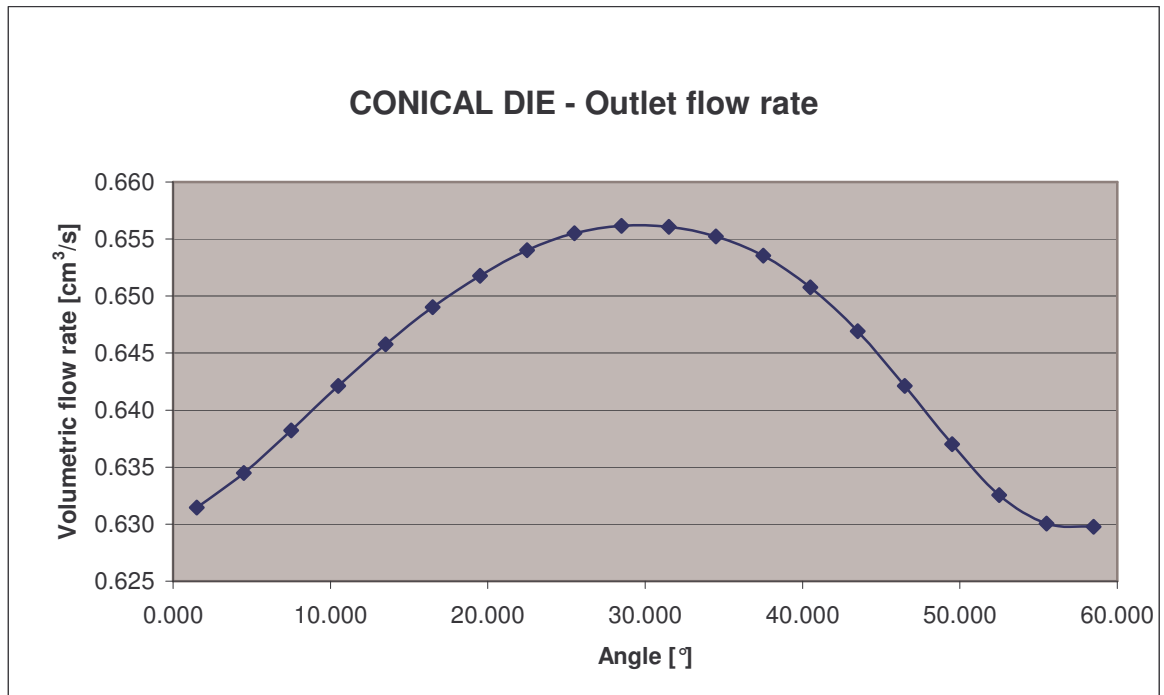


Fig. 46. Conical die – Outlet flow rate

Channel flow rate values were got harder than outlet flow rate values. We had to create a cylindric 2D cut throught the die and than use an Integral function to get channel flow rate value. Cuts were created every 12°. Measured value was Angle velocity.

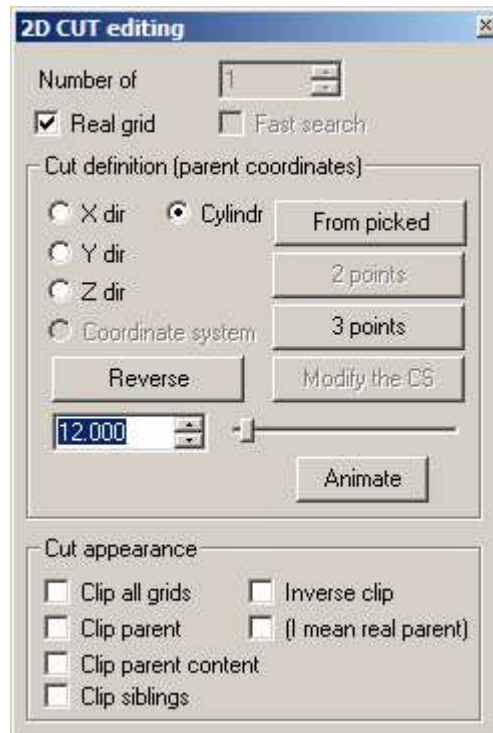


Fig. 47. 2D cut setting

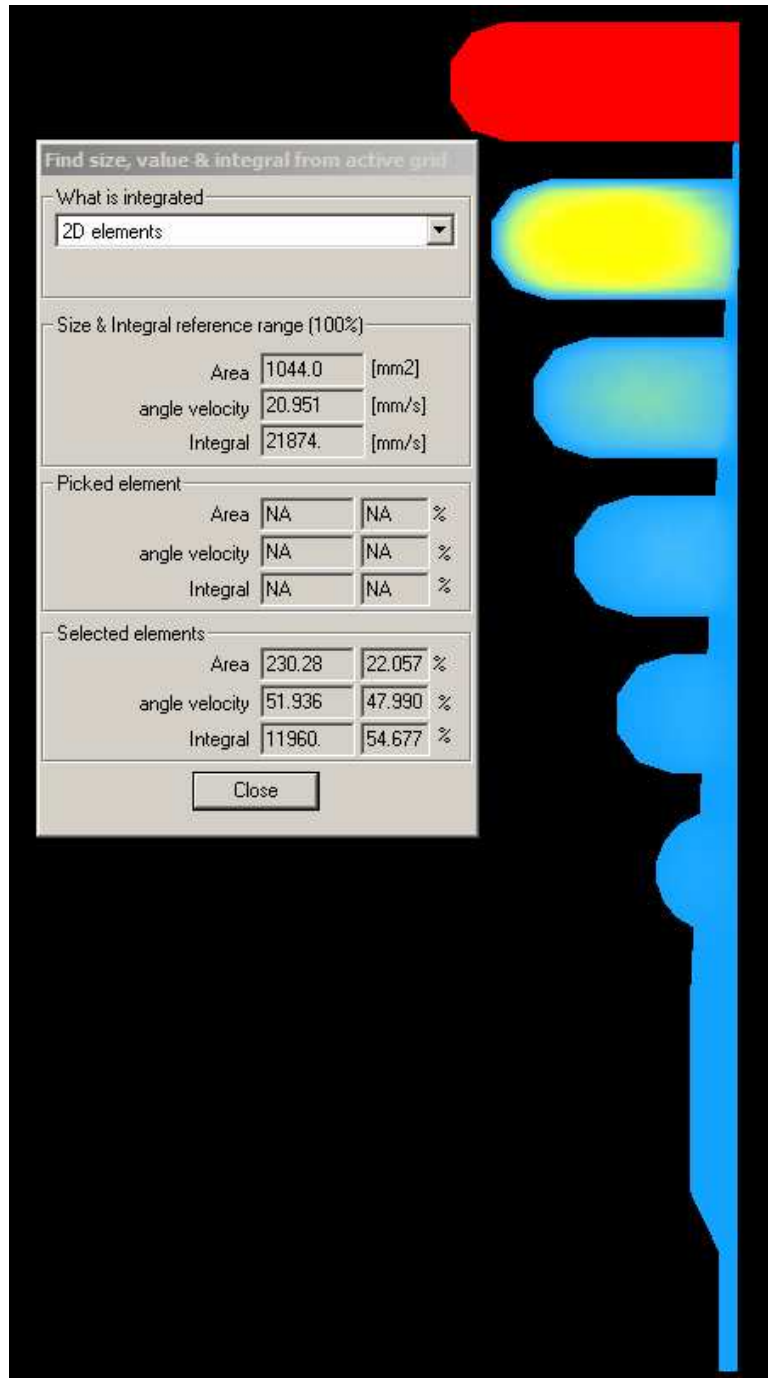


Fig. 48. Channel flow rate integration

Position [-]	Volumetric flow rate [cm ³ /s]
0.028	12.893
0.056	12.913
0.083	13.060
0.111	13.053
0.139	13.194
0.167	13.053
0.194	13.053
0.222	13.038
0.250	12.981
0.278	12.886
0.306	13.353
0.333	12.422
0.361	12.422
0.389	12.277
0.417	11.517
0.444	11.374
0.472	10.055
0.500	9.035
0.528	9.036
0.556	8.602
0.583	6.849
0.611	5.752
0.639	4.696
0.667	3.753
0.694	3.756
0.722	3.394
0.750	2.221
0.778	1.653
0.806	1.236
0.833	0.971
0.861	0.971
0.889	0.870
0.917	0.442
0.944	0.227
0.972	0.065
1.000	0.024

Tab. 6. Conical die – Channel leakage

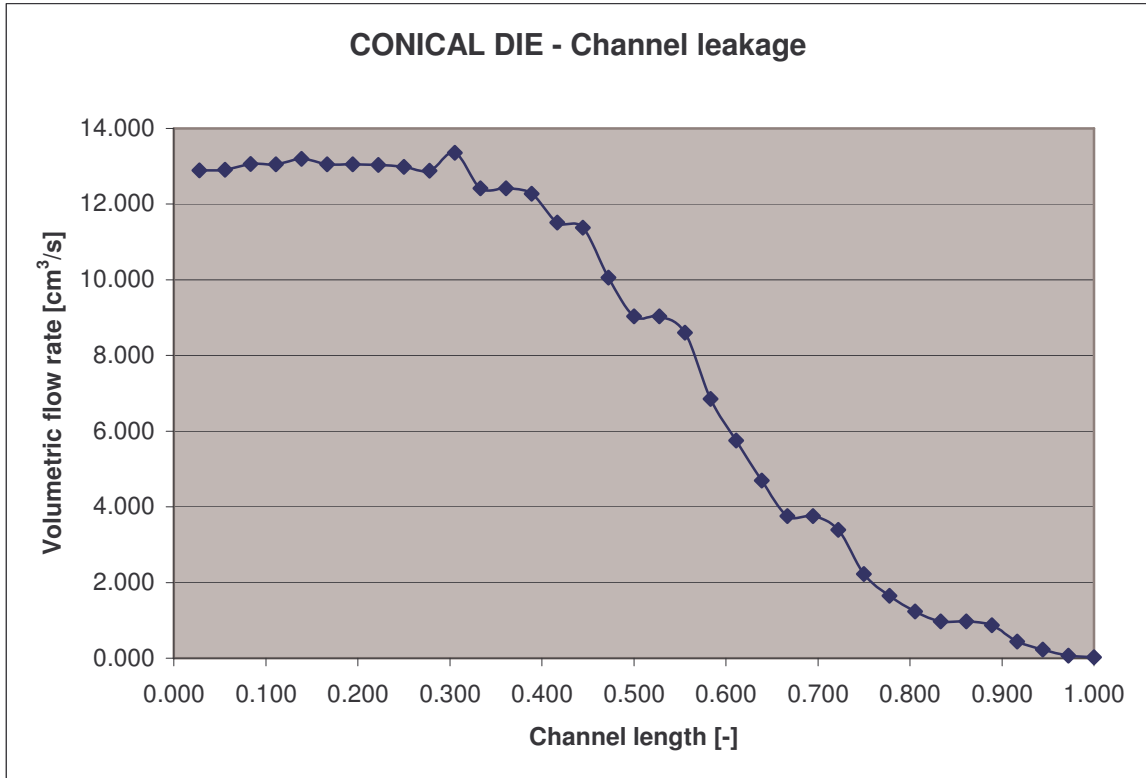


Fig. 49. Conical die – Channel leakage

8.3 Die with strong leakage – Spiral die module results

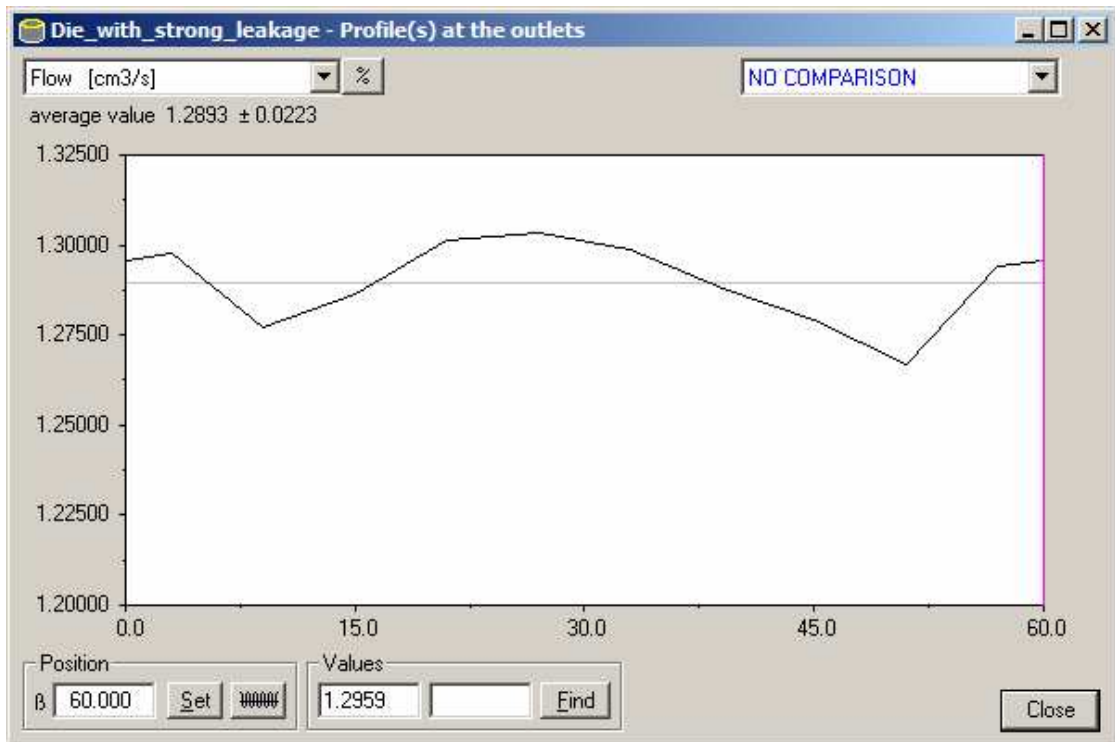


Fig. 50. Die with strong leakage – Outlet flow rate

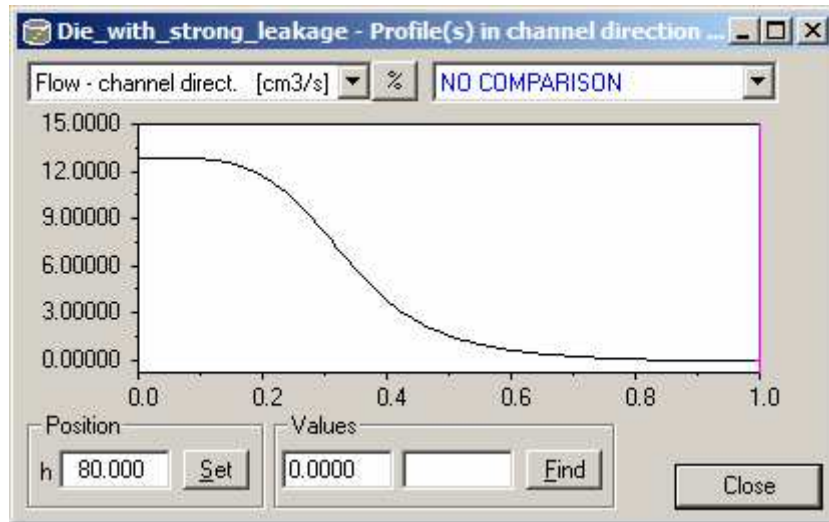


Fig. 51. Die with strong leakage – Channel flow rate

8.4 Die with strong leakage – 3D FEM module results

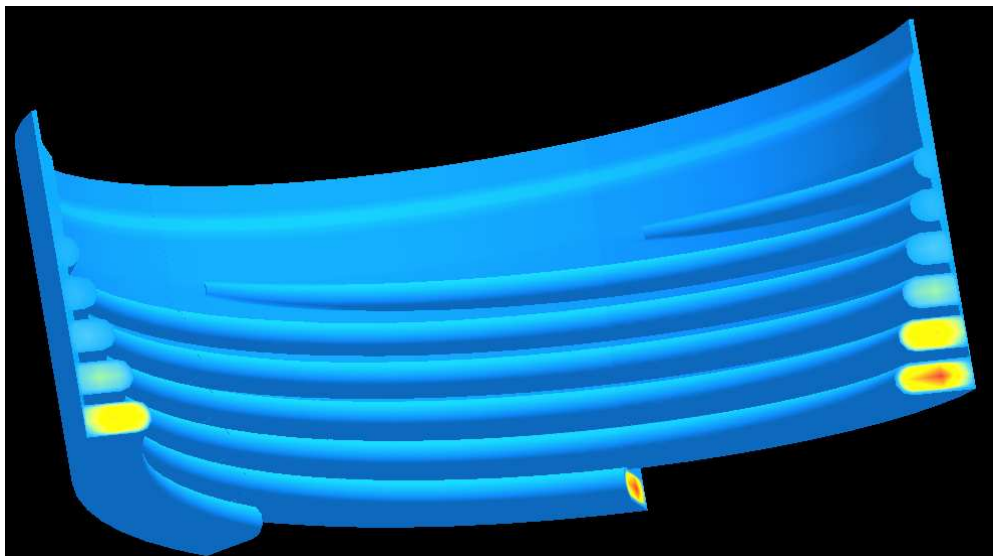
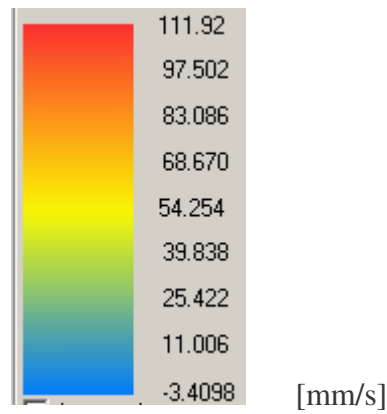


Fig. 52. Die with strong leakage – Angle velocity profile

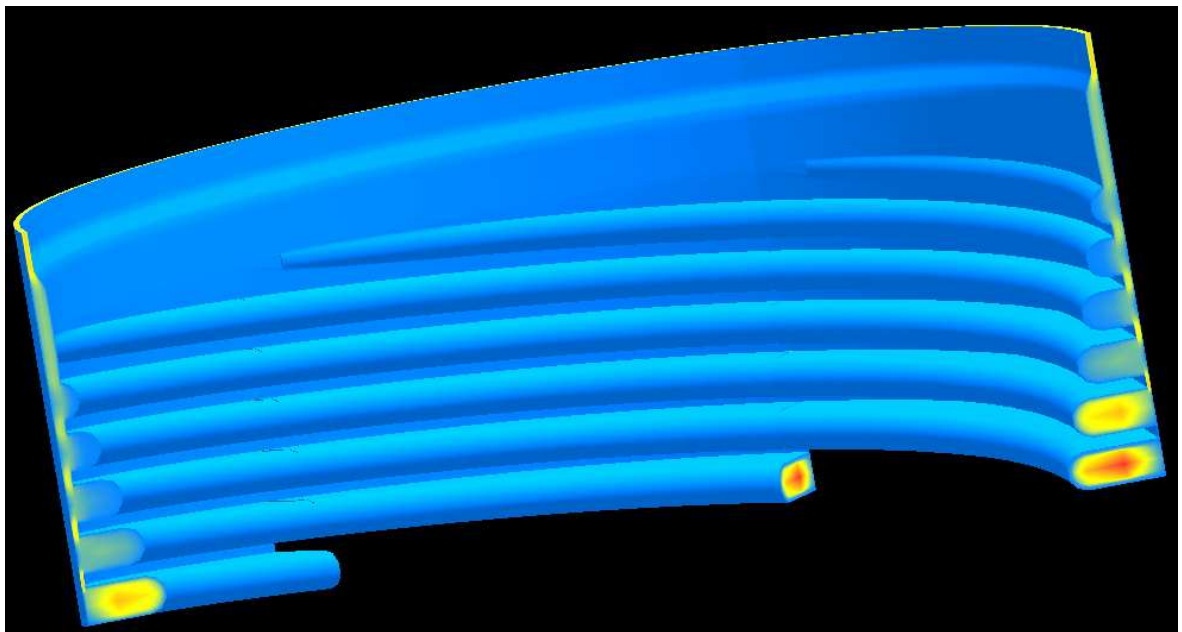
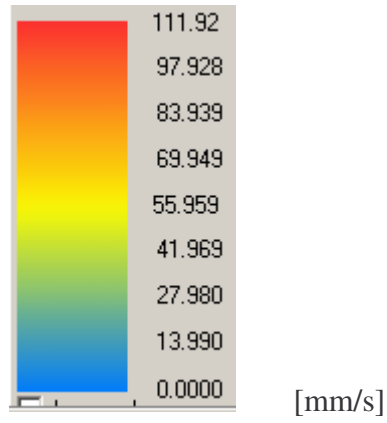
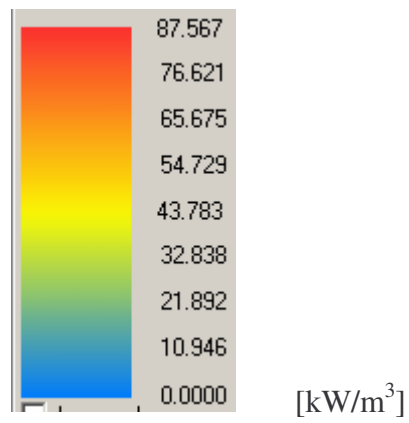


Fig. 53. Die with strong leakage – Velocity magnitude profile



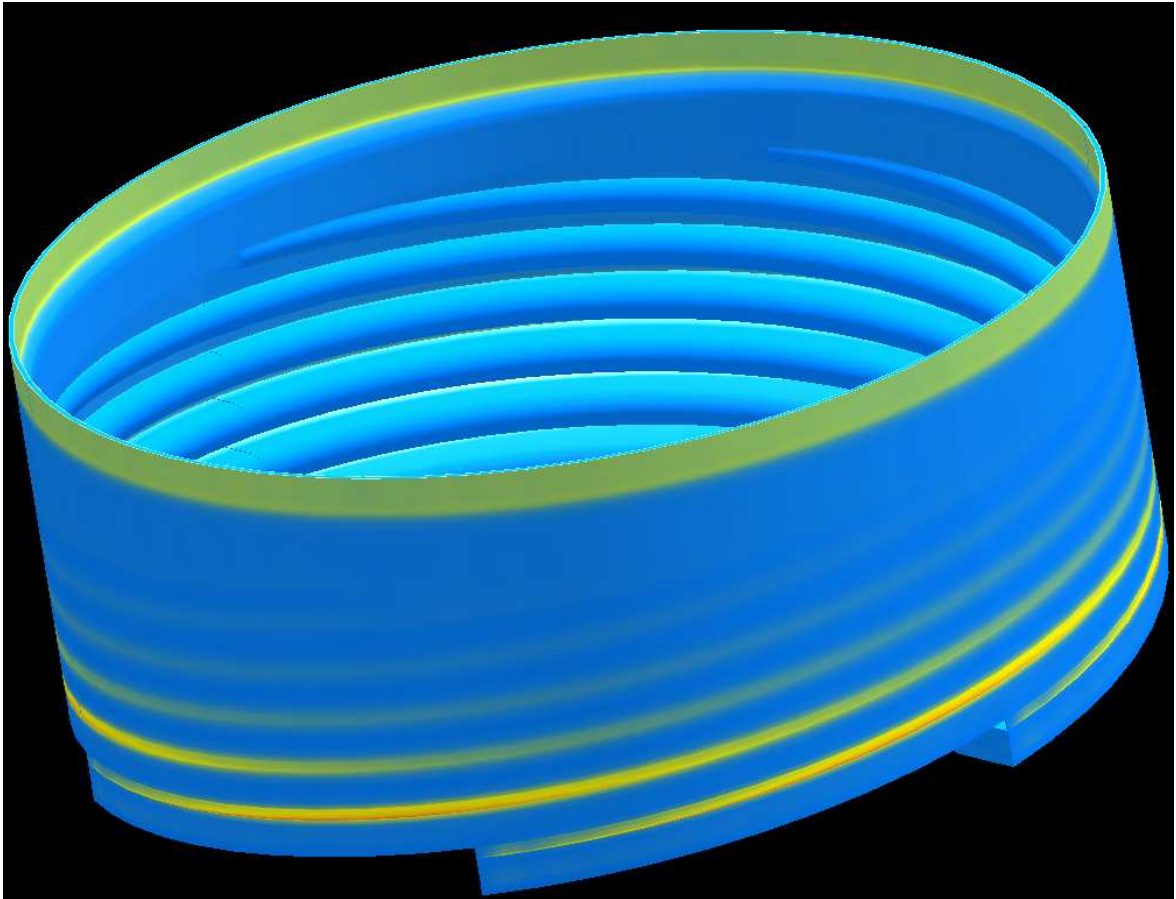
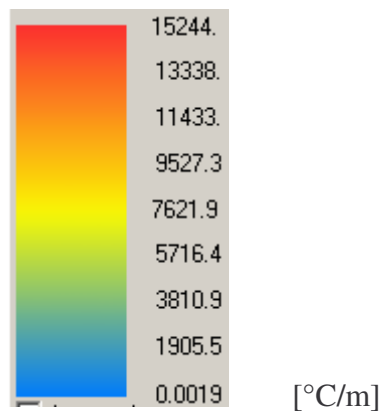


Fig. 54. Die with strong leakage – Dissipation profile



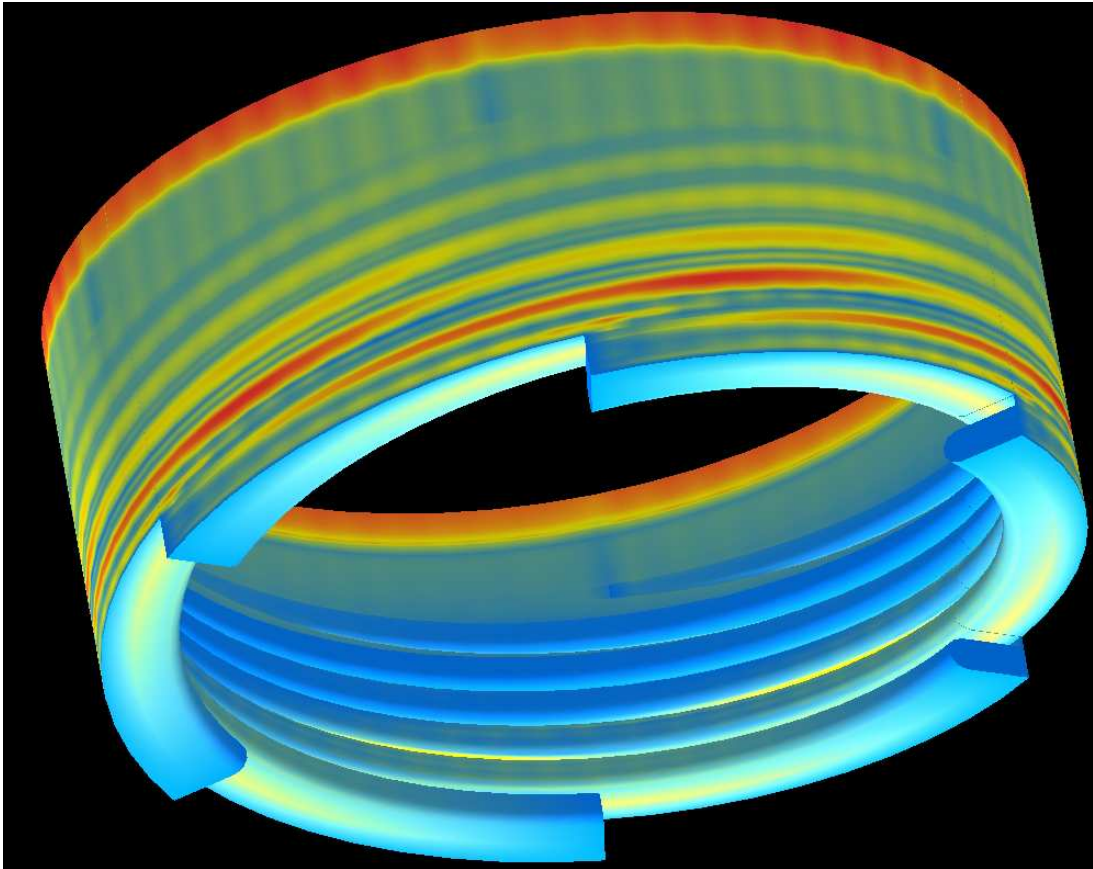


Fig. 55. Die with strong leakage – Temperature gradient profile



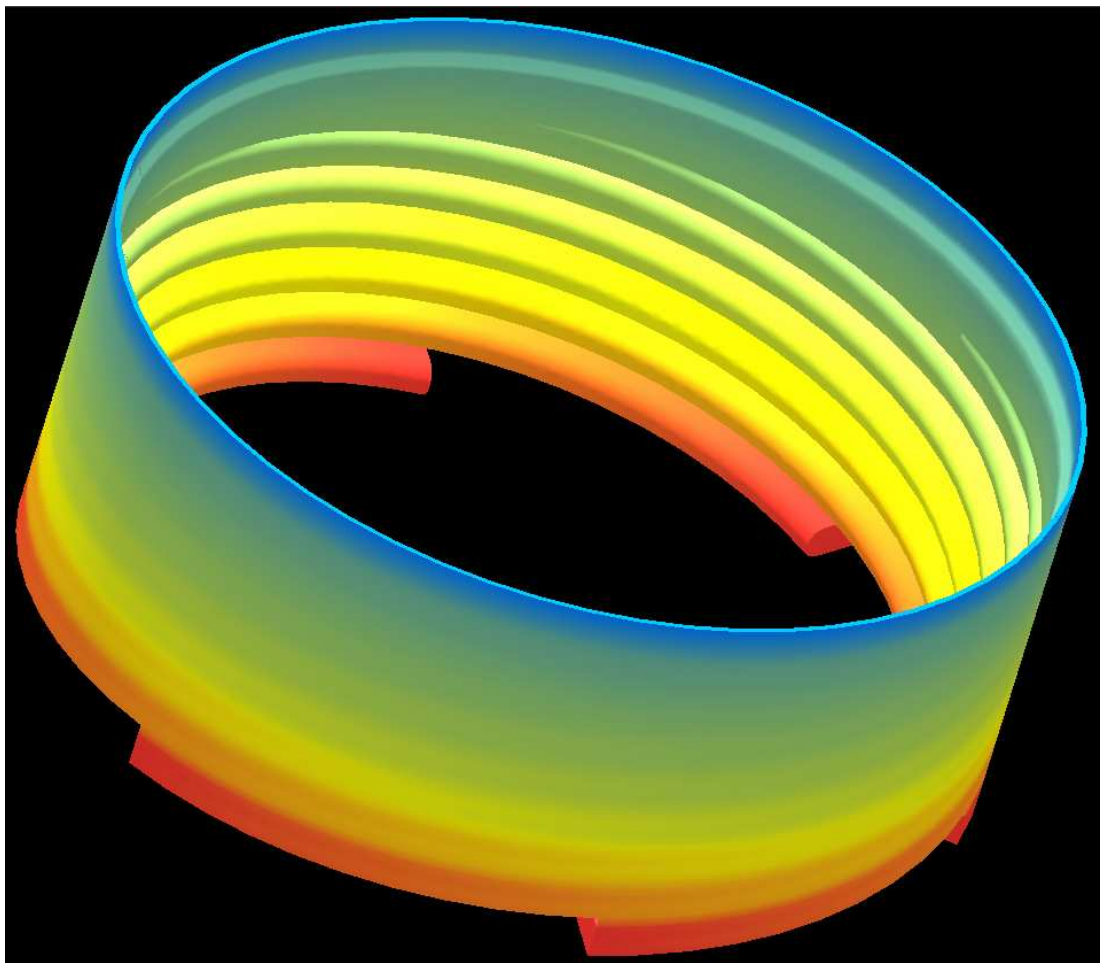
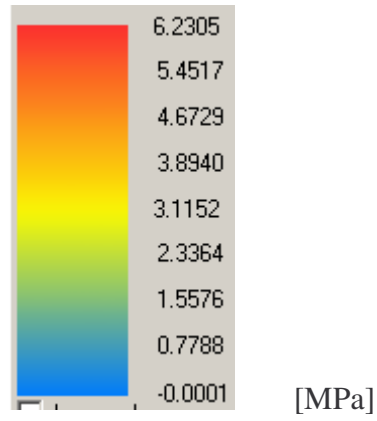


Fig. 56. Die with strong leakage – Pressure profile

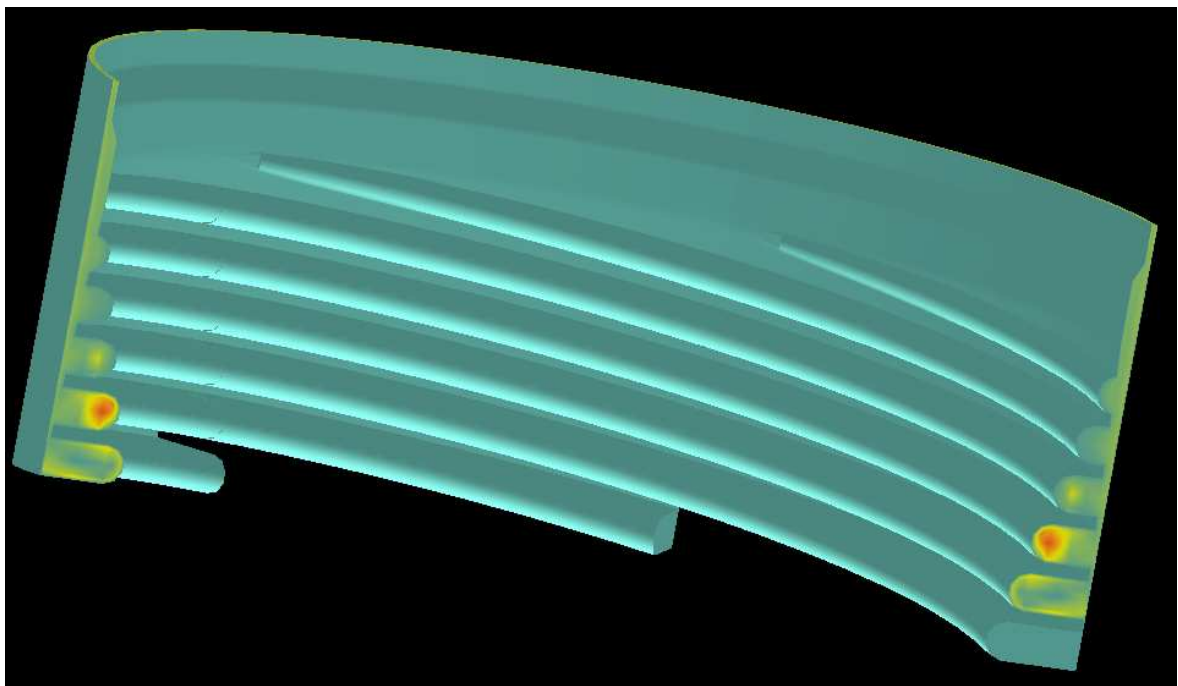
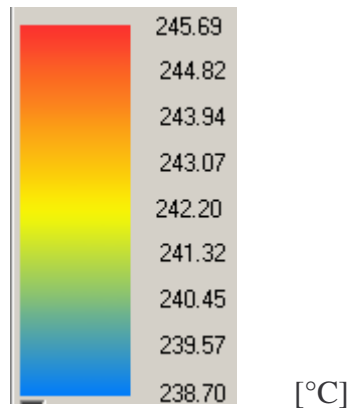
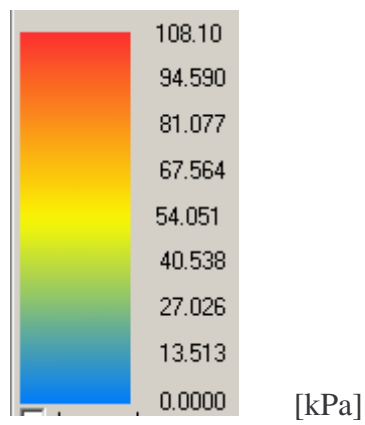


Fig. 57. Die with strong leakage – Temperature profile



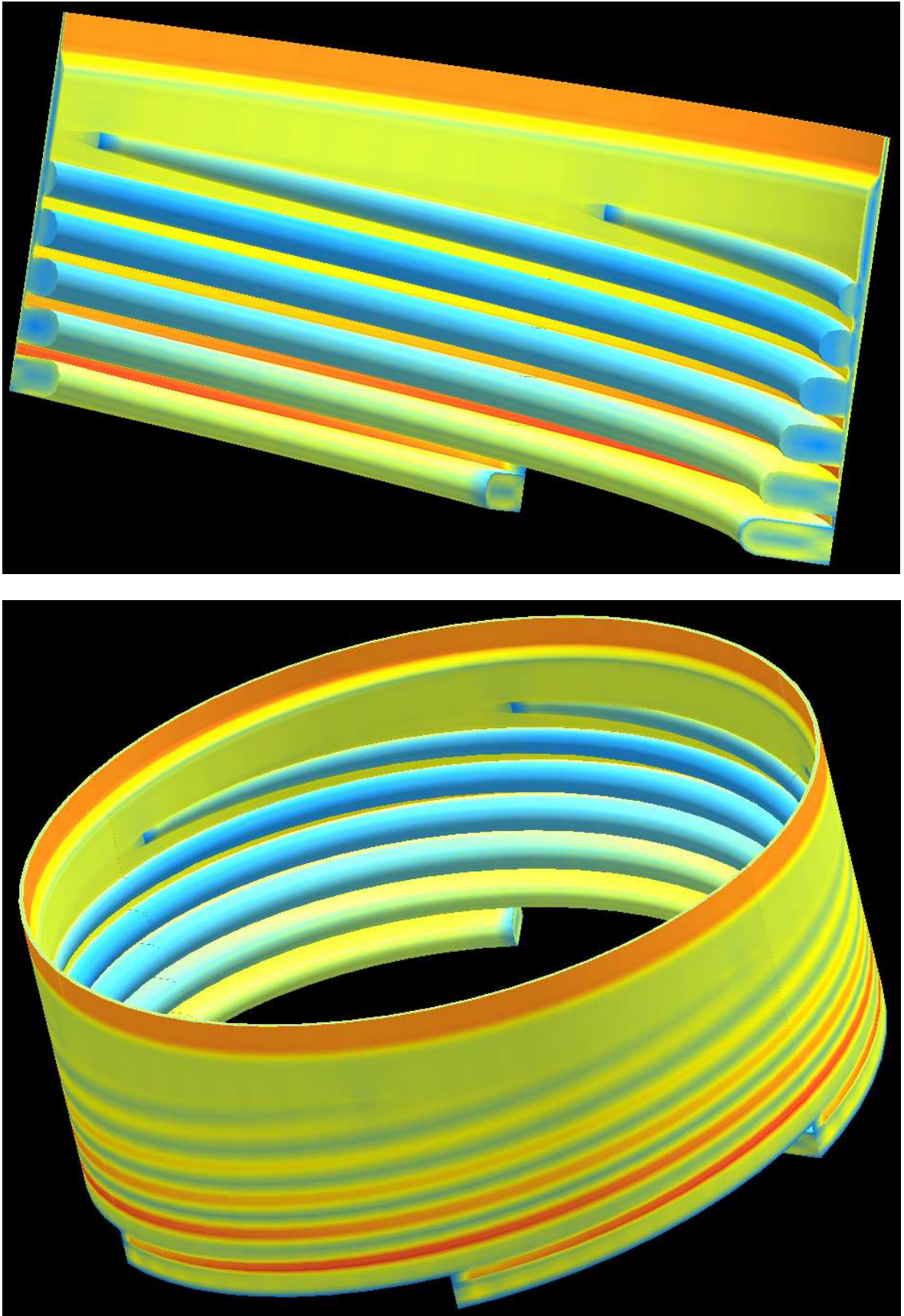


Fig. 58. Die with strong leakage – Shear stress profile

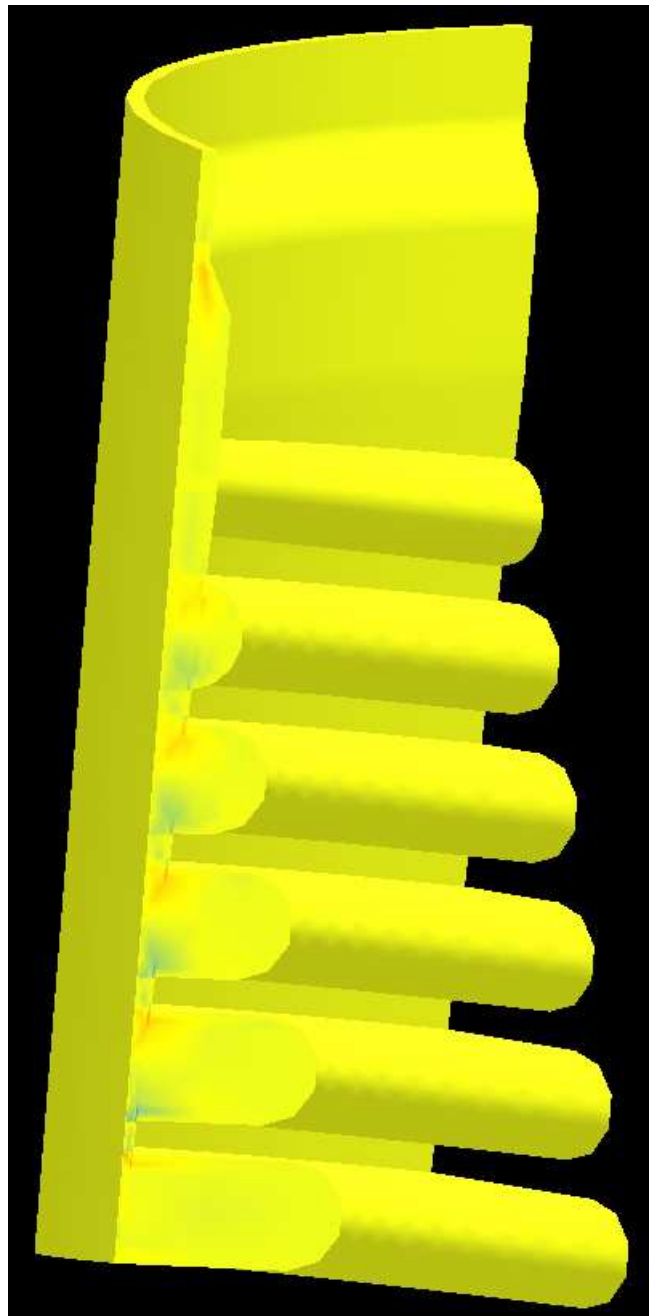
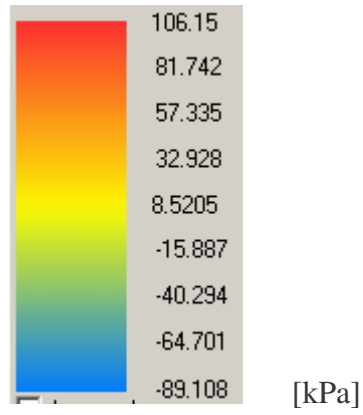


Fig. 59. Die with strong leakage – Elongation stress profile

Angle [°]	Mass flow rate [kg/h]	Volumetric flow rate [cm ³ /s]
1.500	1.815	0.638
4.500	1.829	0.643
7.500	1.838	0.646
10.500	1.842	0.648
13.500	1.845	0.649
16.500	1.848	0.650
19.500	1.851	0.651
22.500	1.852	0.651
25.500	1.854	0.652
28.500	1.854	0.652
31.500	1.855	0.652
34.500	1.855	0.652
37.500	1.854	0.652
40.500	1.852	0.651
43.500	1.843	0.648
46.500	1.826	0.642
49.500	1.805	0.635
52.500	1.780	0.626
55.500	1.773	0.624
58.500	1.794	0.631
SUM	36.666	12.892
AVERAGE	1.833	0.645
DEVIATION [%]	±1,3	±1,2

Tab. 7. Die with strong leakage – Outlet flow rate measured values

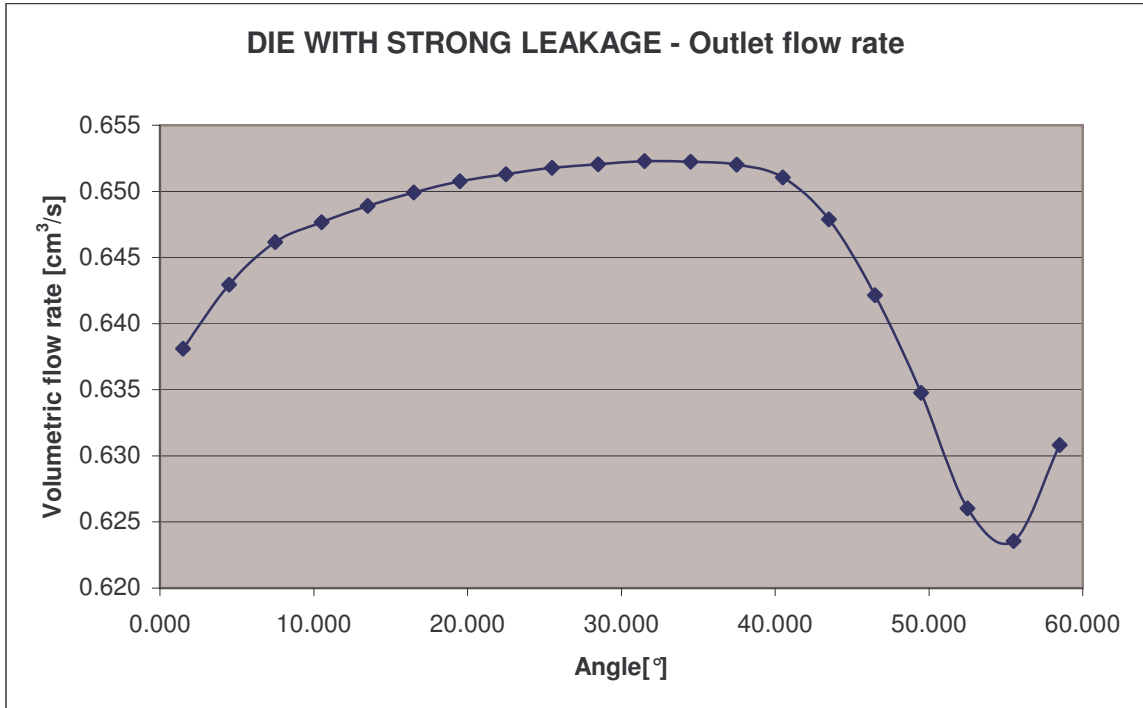


Fig. 60. Die with strong leakage – Outlet flow rate

Position [-]	Volumetric flow rate [cm ³ /s]
0.028	12.893
0.056	13.051
0.083	12.998
0.111	12.084
0.139	11.307
0.167	10.577
0.194	9.376
0.222	8.558
0.250	6.151
0.278	4.670
0.306	3.335
0.333	2.488
0.361	2.488
0.389	2.046
0.417	1.592
0.444	1.247
0.472	0.976

0.500	0.736
0.528	0.737
0.556	0.589
0.583	0.471
0.611	0.252
0.639	0.278
0.667	0.230
0.694	0.230
0.722	0.174
0.750	0.141
0.778	0.110
0.806	0.070
0.833	0.098
0.861	0.098
0.889	0.067
0.917	0.039
0.944	0.018
0.972	-0.007
1.000	-0.003

Tab. 8. Die with strong leakage – Channel leakage

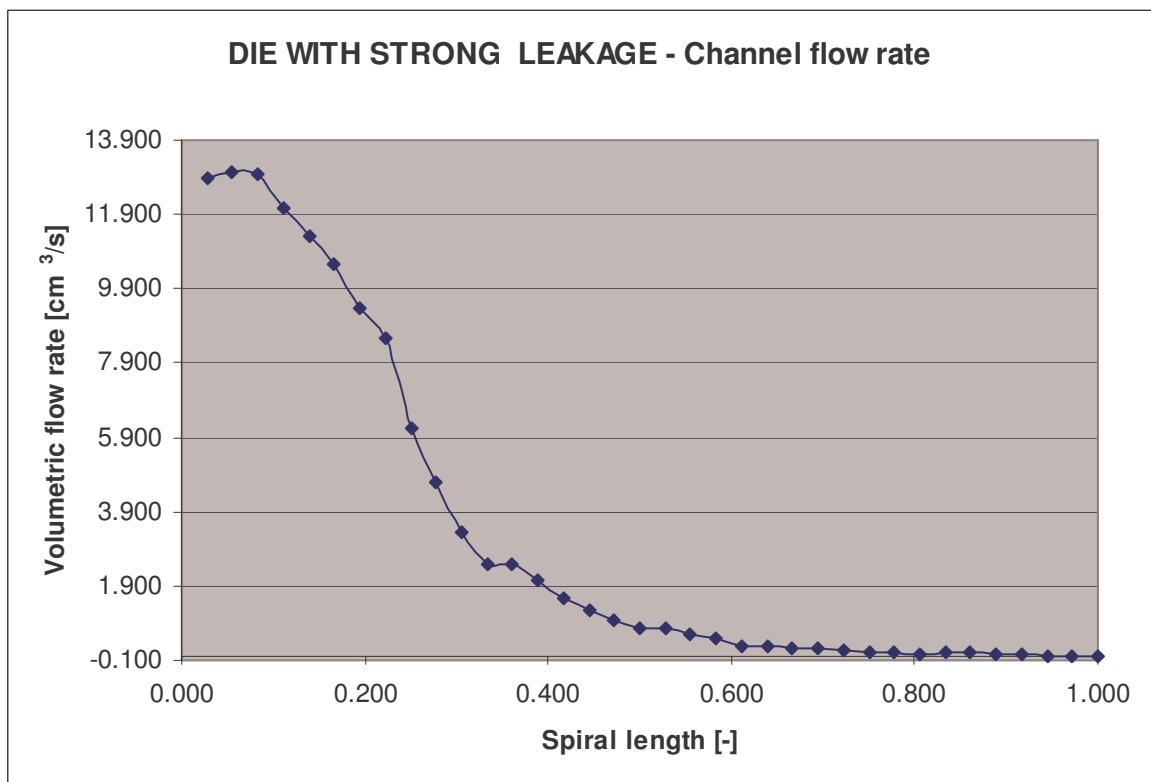


Fig. 61. Die with strong leakage – Channel flow rate

8.5 Die with strong flow in spirals – Spiral die module results

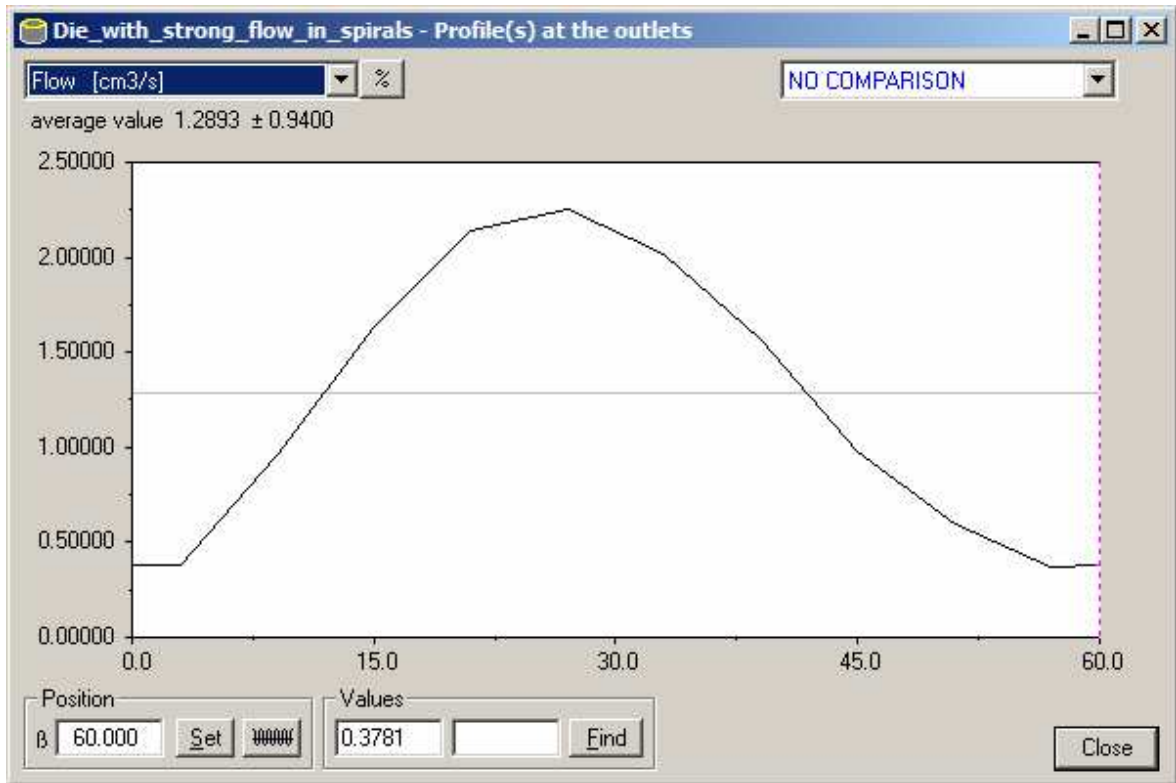


Fig. 62. Die with strong flow in spirals – Outlet flow rate

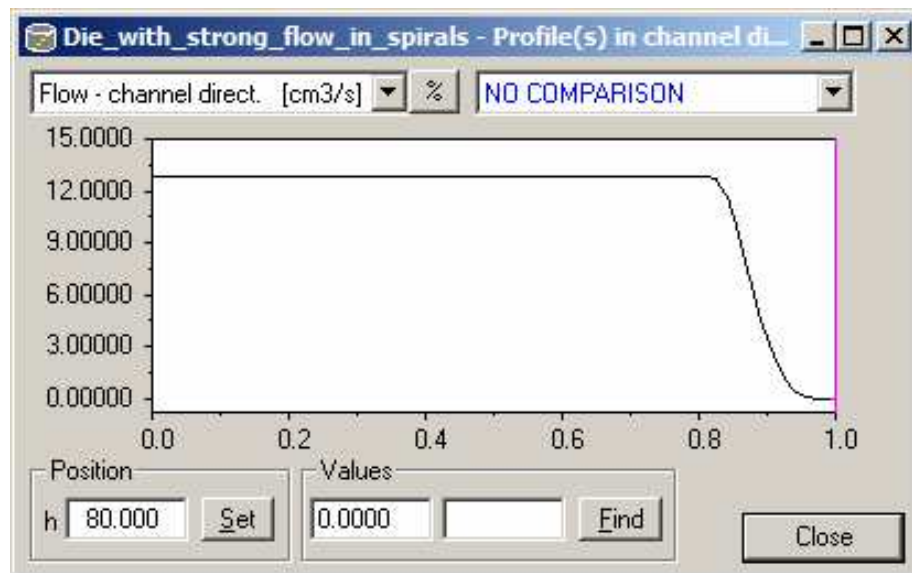


Fig. 63. Die with strong flow in spirals – Channel flow rate

8.6 Die with strong flow in spirals – 3D FEM module results

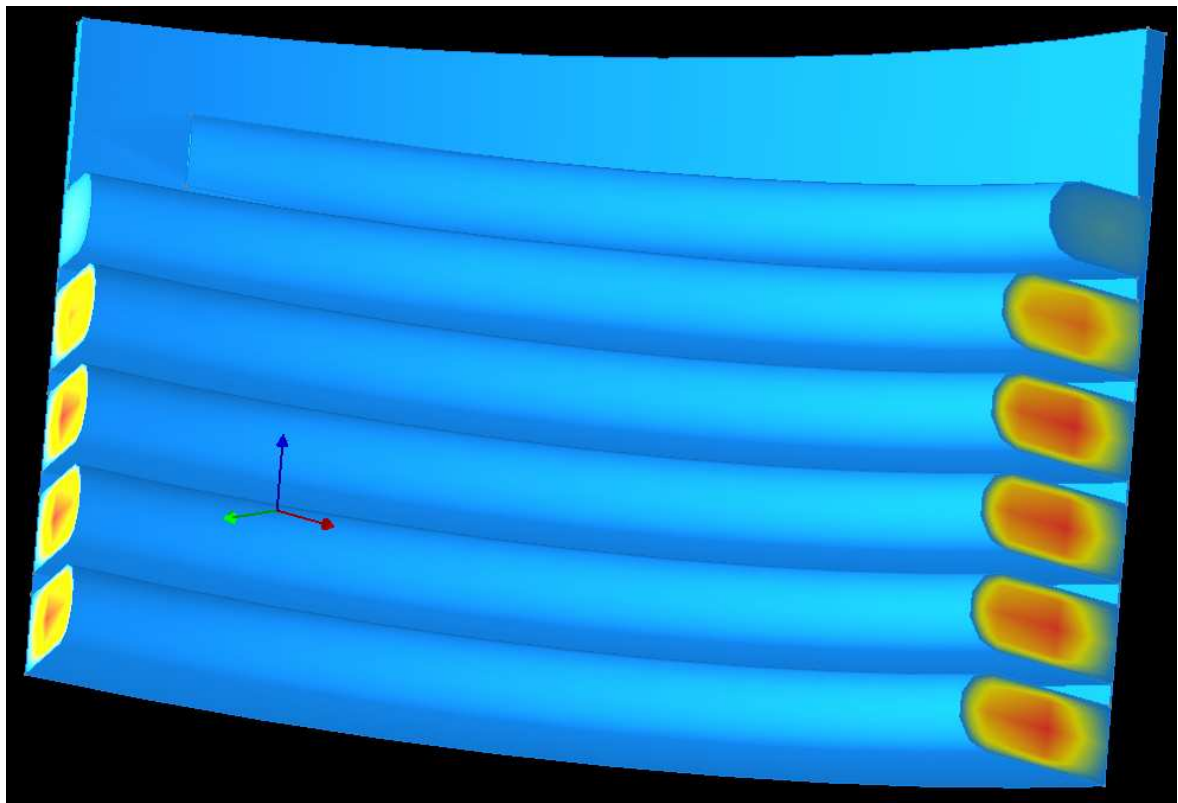
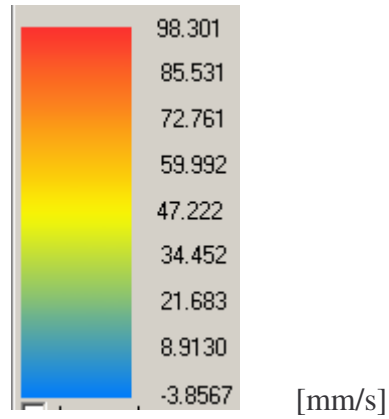
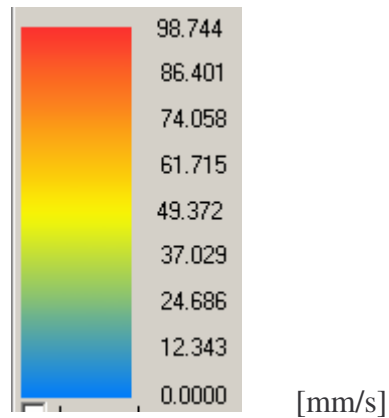


Fig. 64. Die with strong flow in spirals – Angle velocity profile



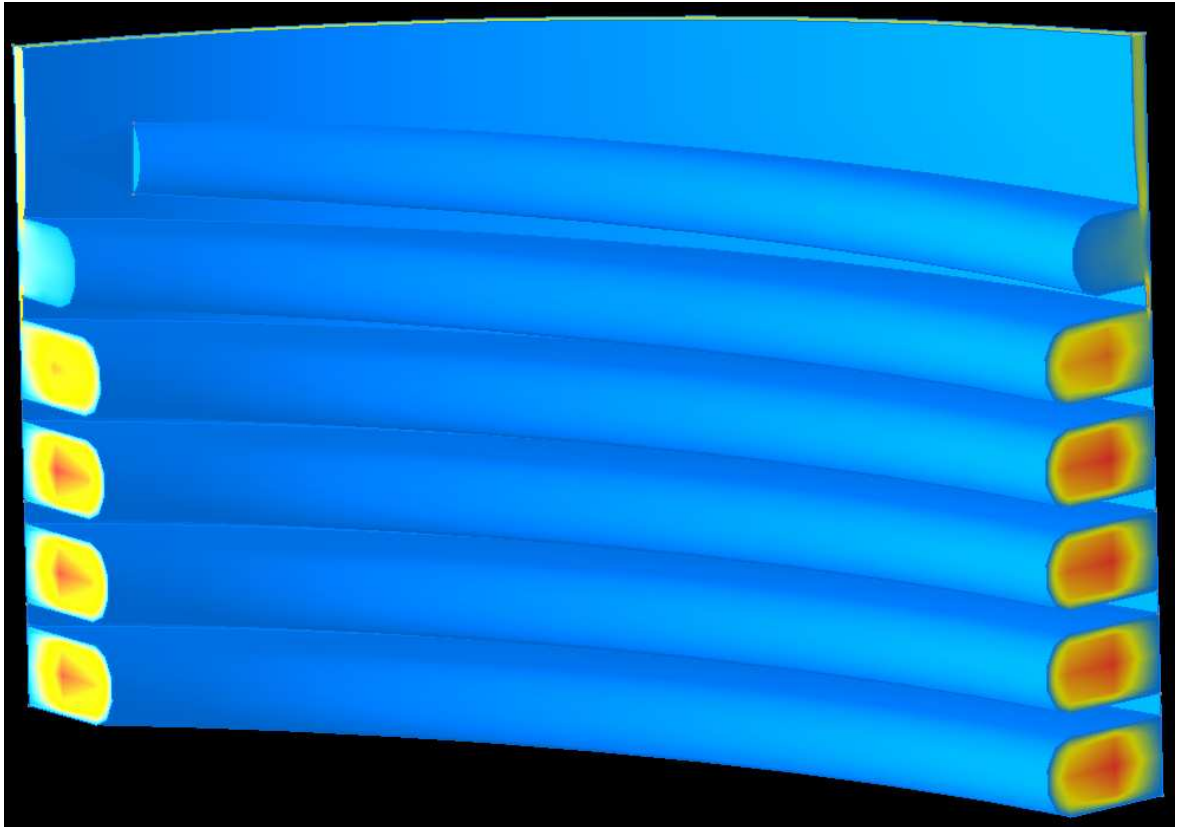
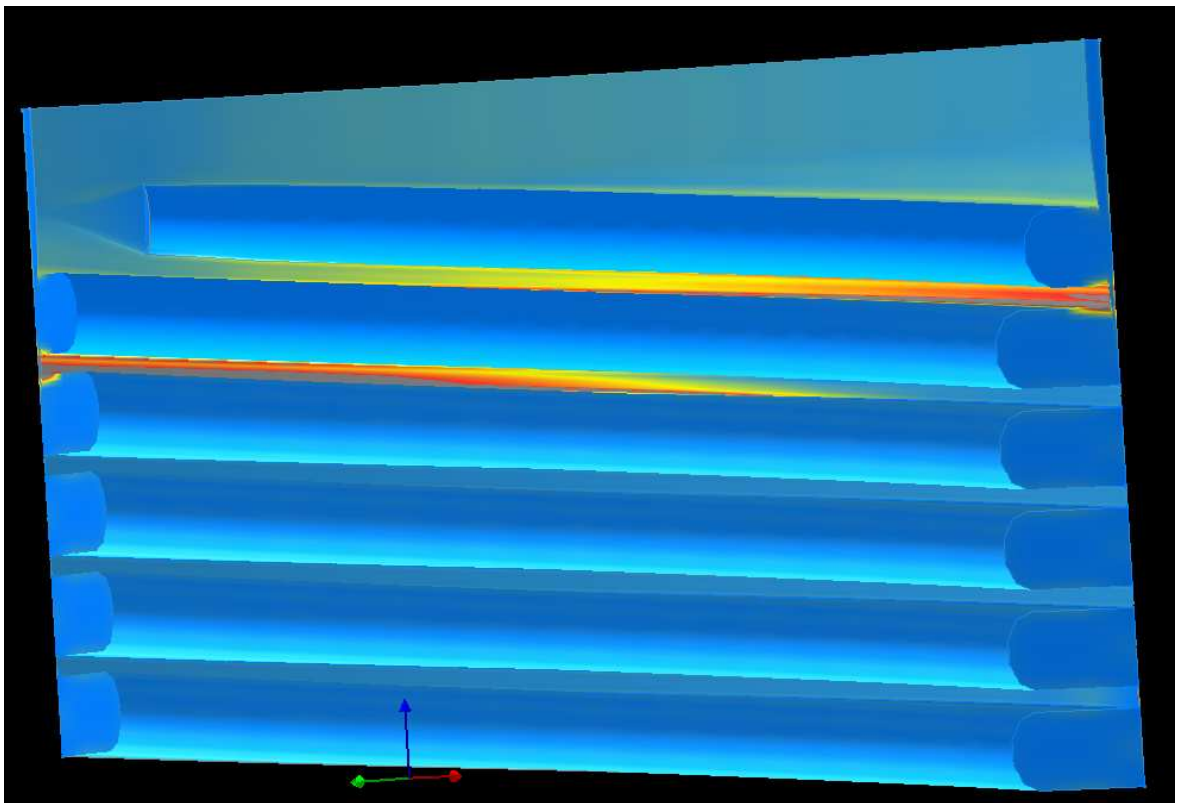


Fig. 65. Die with strong flow in spirals – Velocity magnitude profile



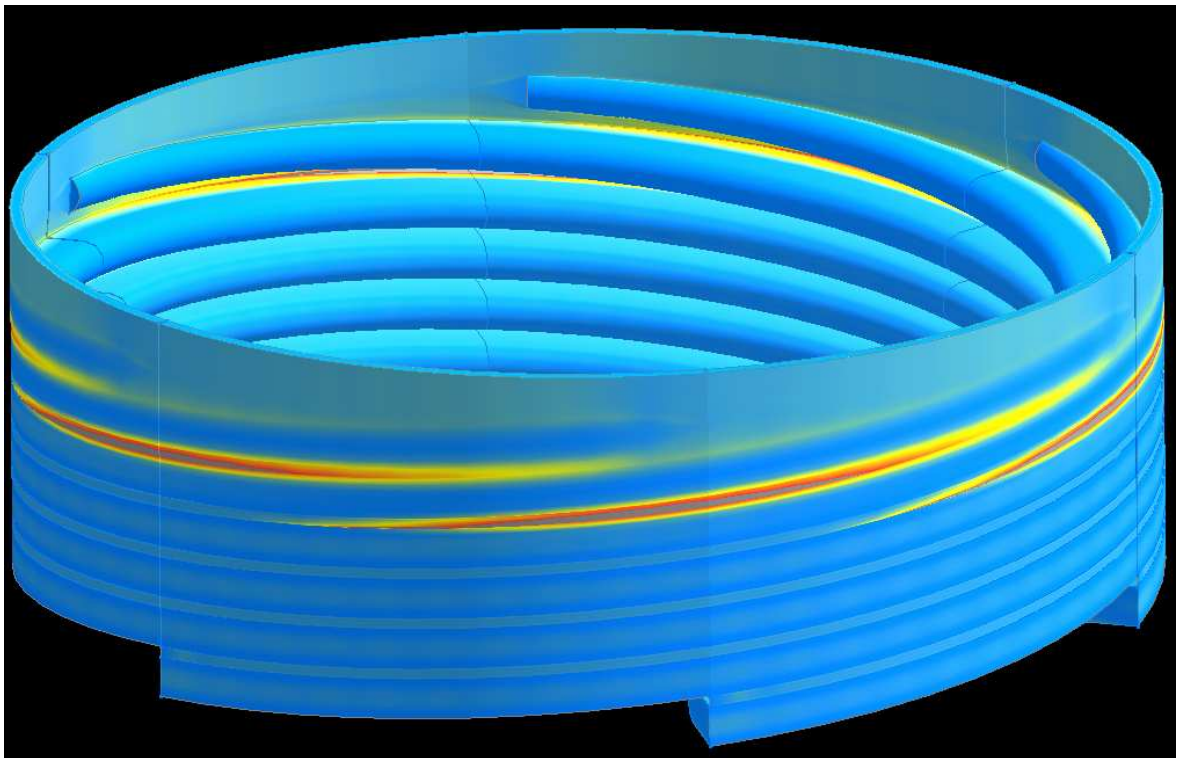
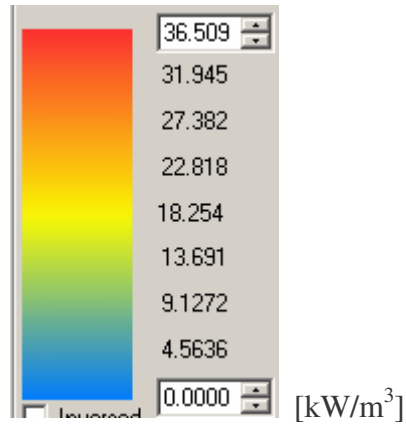
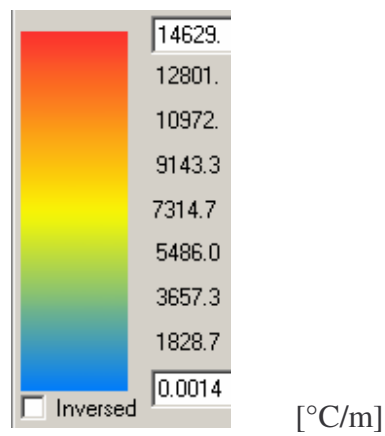


Fig. 66. Die with strong flow in spirals – Dissipation profile



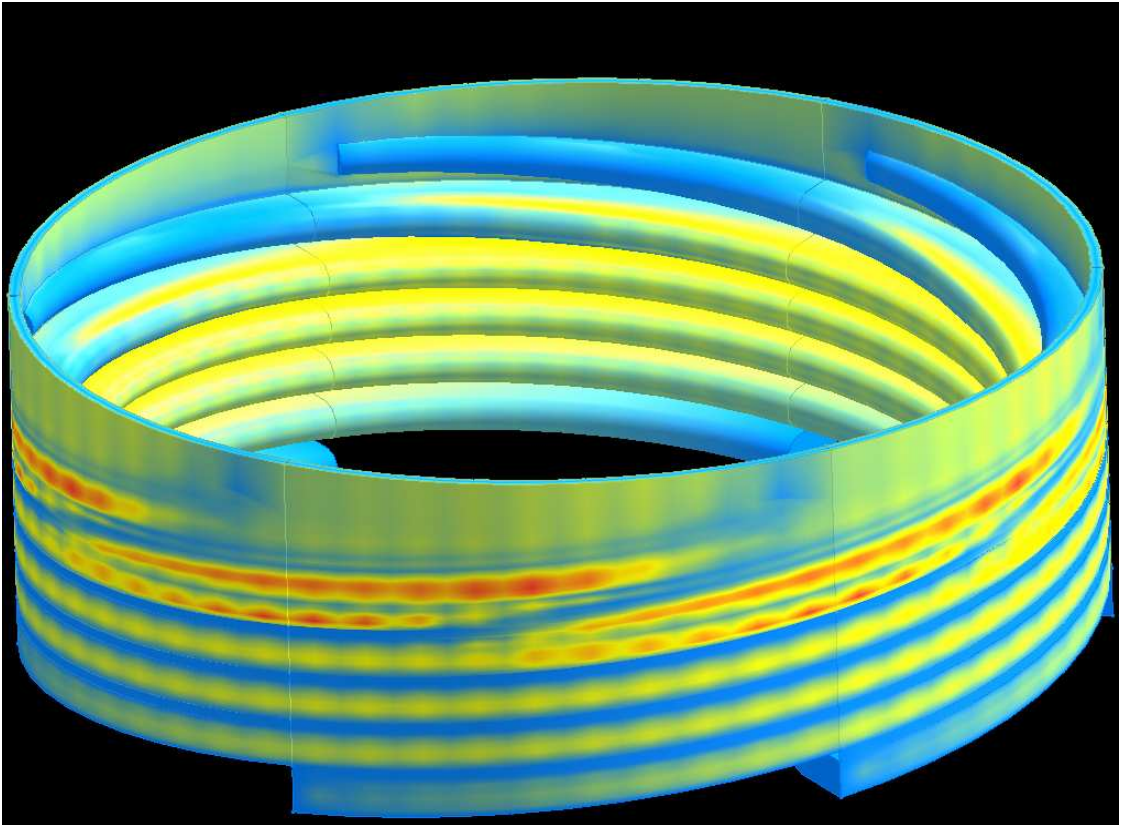
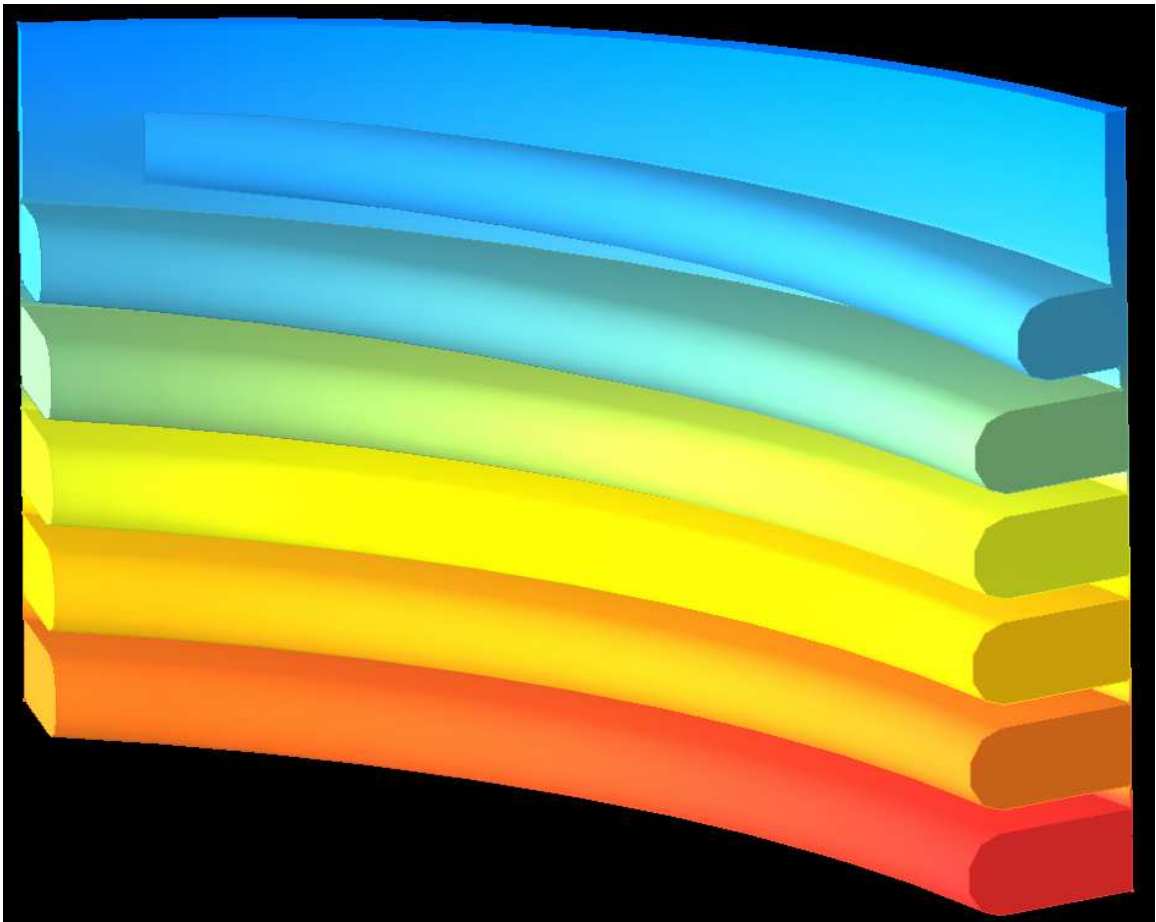


Fig. 67. Die with strong flow in spirals – Gradient profile



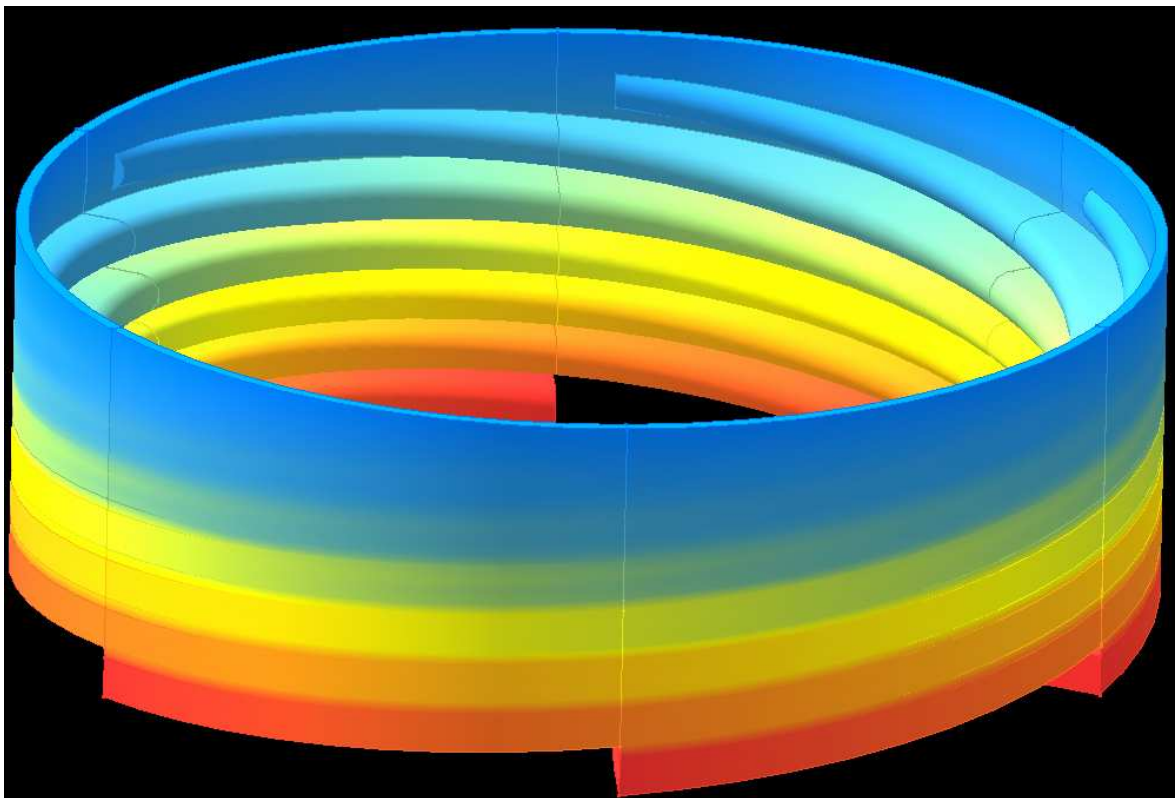
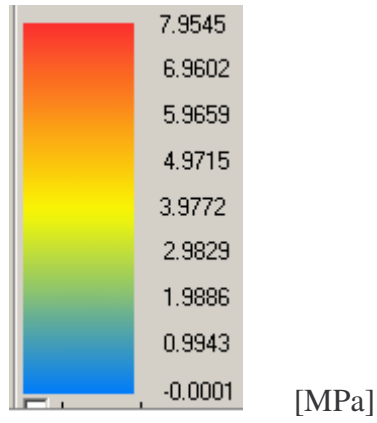
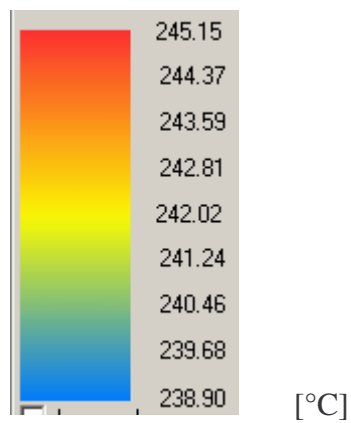


Fig. 68. Die with strong flow in spirals – Pressure profile



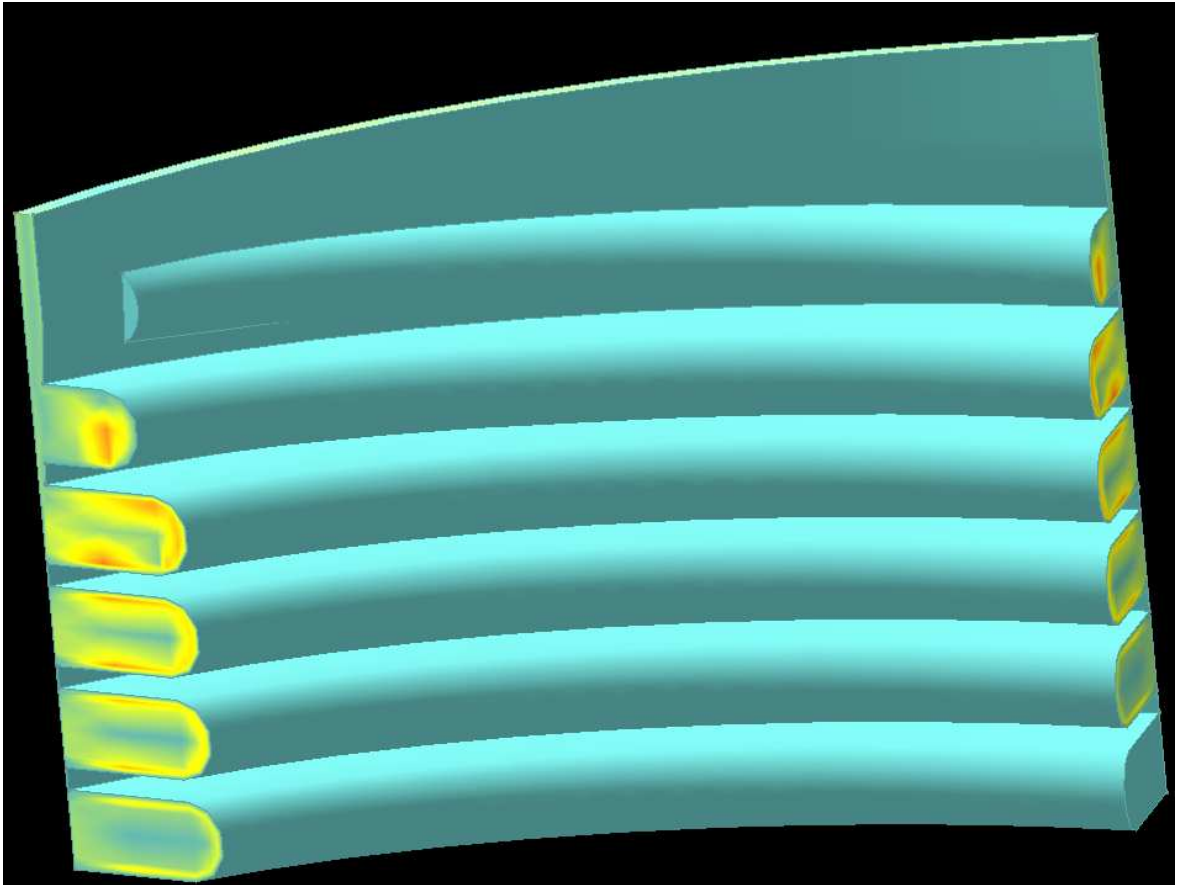
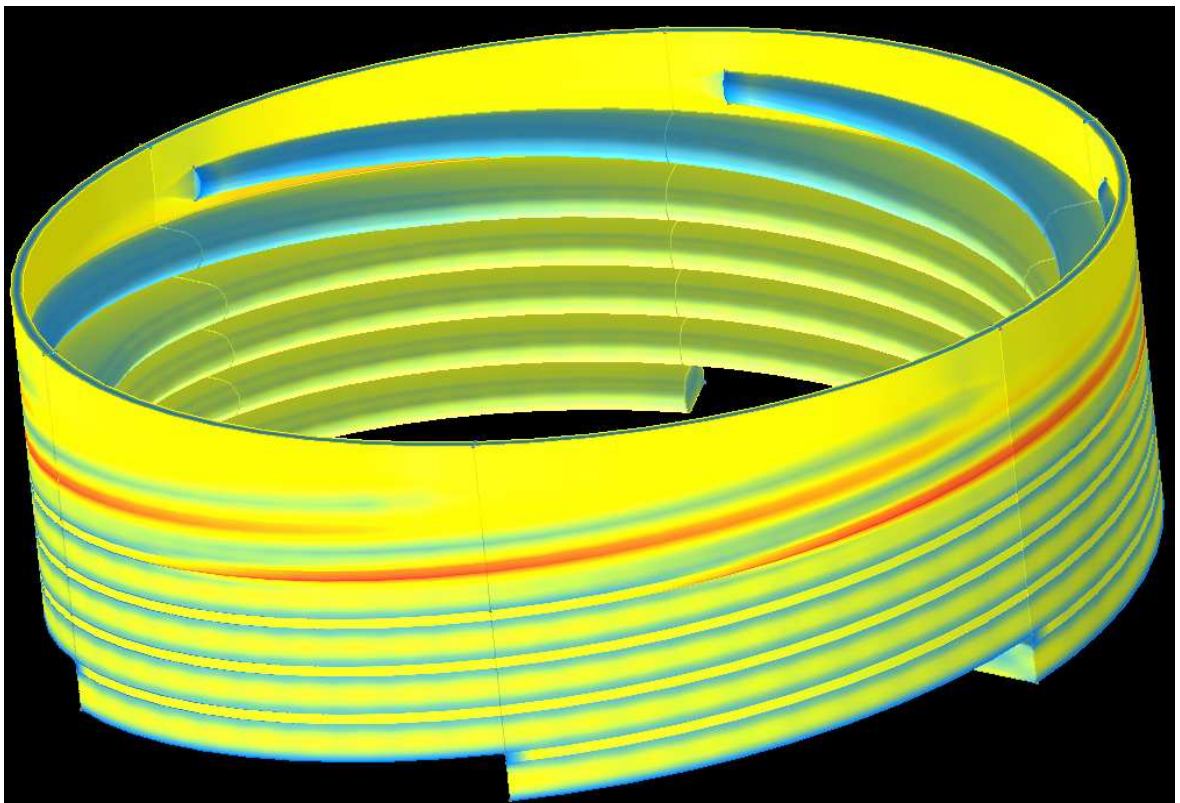


Fig. 69. Die with strong flow in spirals – Temperature profile



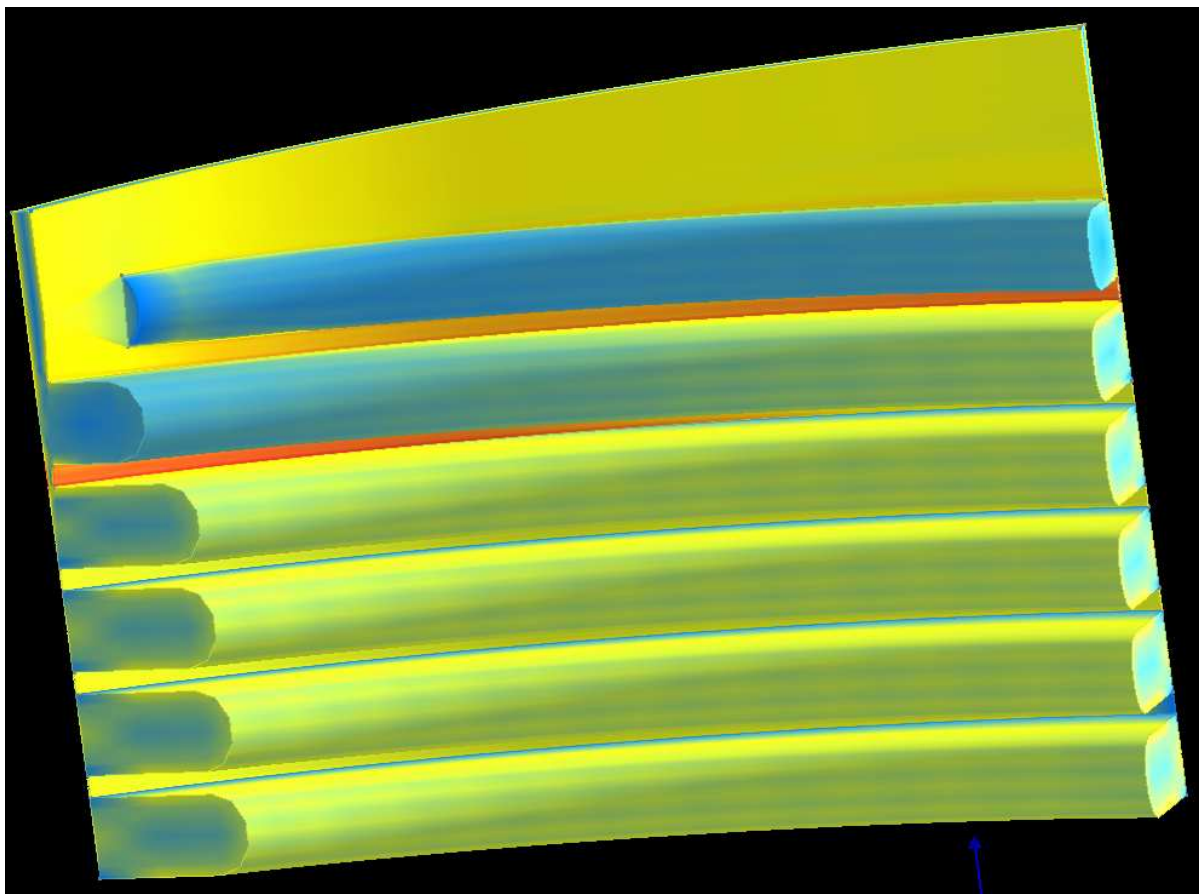
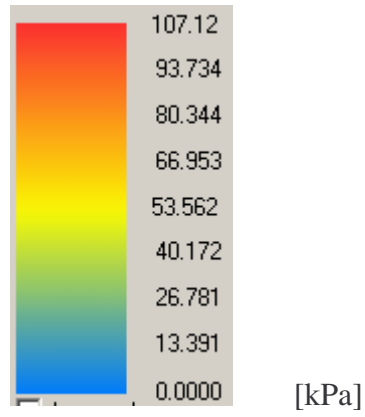
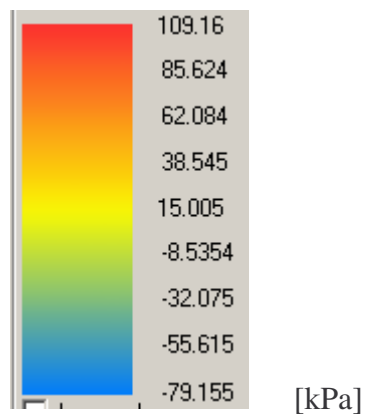


Fig. 70. Die with strong flow in spirals – Shear stress profile



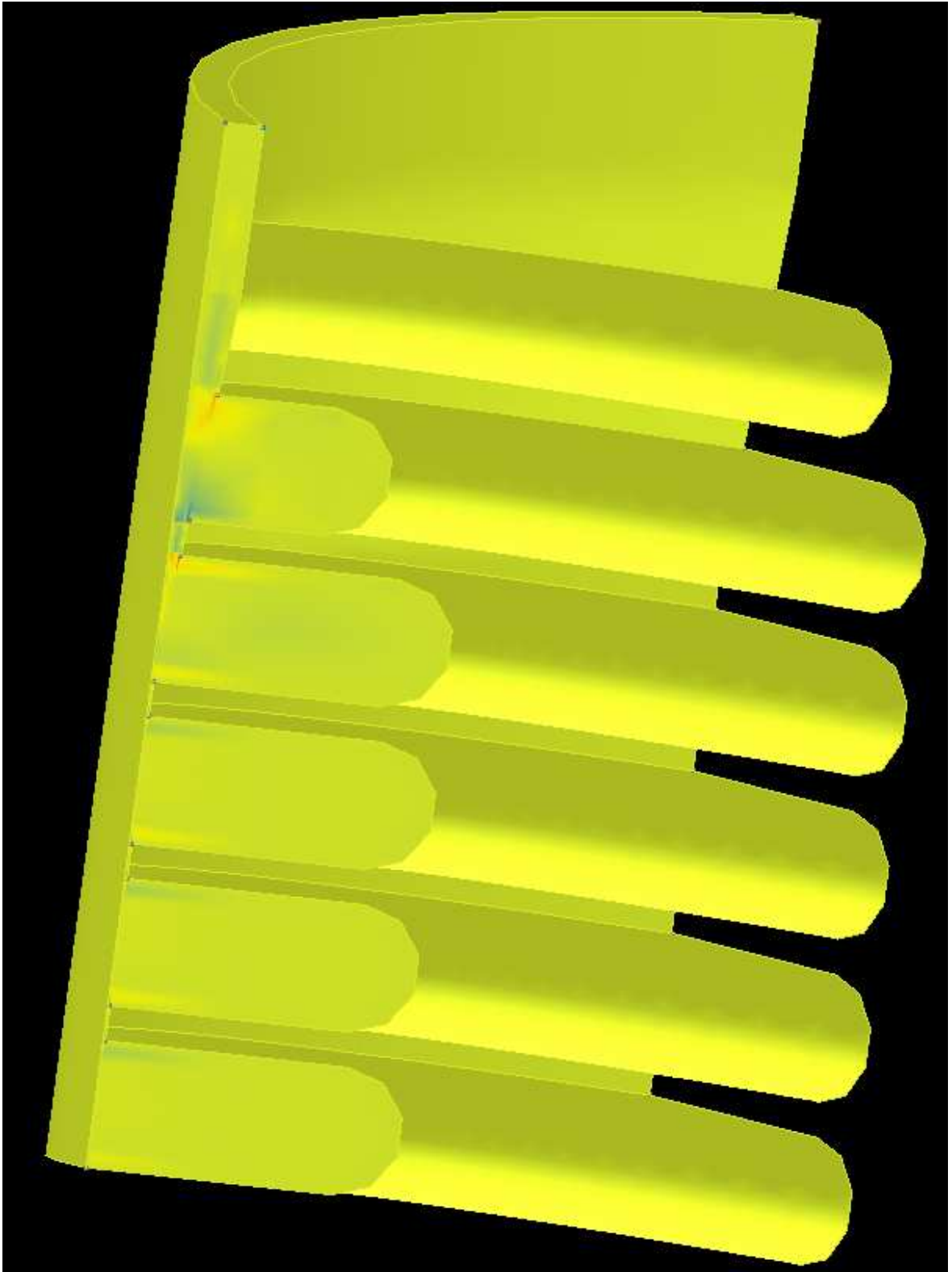


Fig. 71. Die with strong flow in spirals – Elongation stress profile

Angle [°]	Mass flow rate [kg/h]	Volumetric flow rate [cm ³ /s]
1.500	1.647	0.579
4.500	1.692	0.595
7.500	1.729	0.608
10.500	1.775	0.624
13.500	1.818	0.639
16.500	1.859	0.654
19.500	1.898	0.667
22.500	1.936	0.681
25.500	1.971	0.693
28.500	2.003	0.704
31.500	2.032	0.714
34.500	2.053	0.722
37.500	2.062	0.725
40.500	2.052	0.722
43.500	2.016	0.709
46.500	1.930	0.679
49.500	1.730	0.608
52.500	1.488	0.523
55.500	1.430	0.503
58.500	1.545	0.543
SUM	36.666	12.893
AVERAGE	1.833	0.645
DEVIATION [%]	±10,5	±10,5

Tab. 9. Die with strong flow in spirals – Outlet flow rate measured values

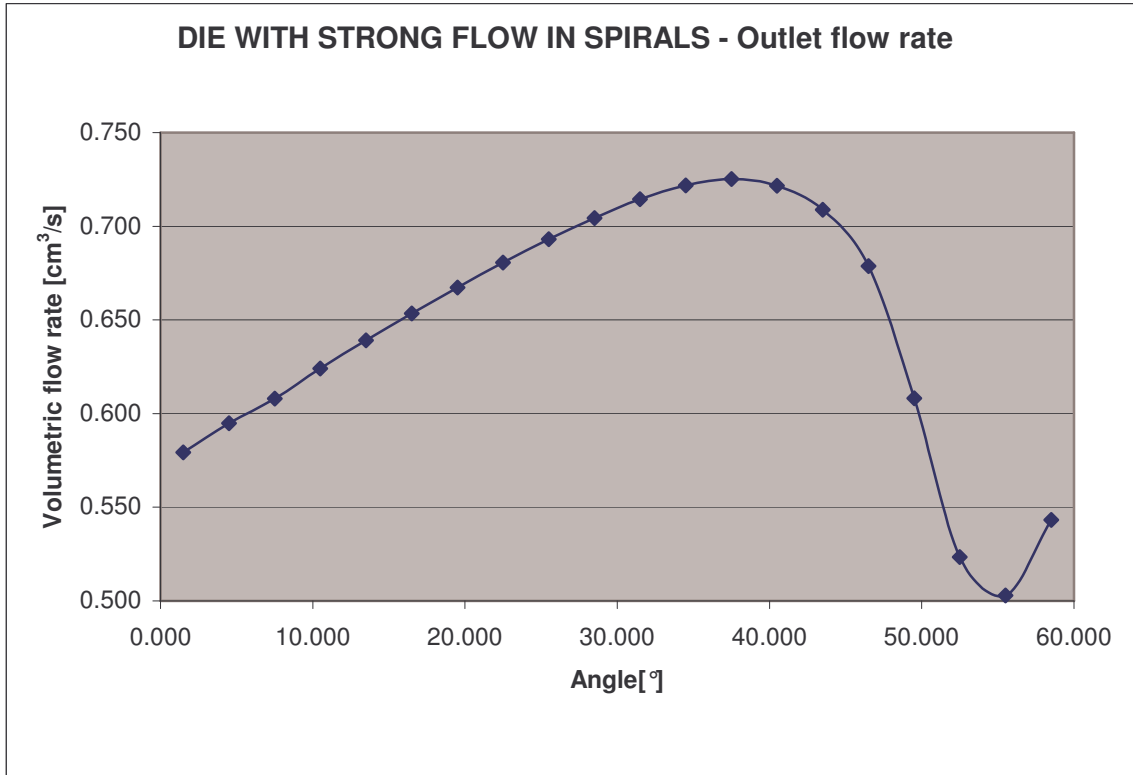


Fig. 72. Die with strong flow in spirals – Outlet flow rate

Position [-]	Volumetric flow rate [cm ³ /s]
0.028	12.893
0.056	13.232
0.083	13.140
0.111	12.991
0.139	12.971
0.167	12.969
0.194	12.969
0.222	13.520
0.250	13.208
0.278	13.289
0.306	12.971
0.333	12.976
0.361	12.976
0.389	12.976
0.417	13.309
0.444	13.259
0.472	12.979
0.500	12.984

0.528	12.985
0.556	12.982
0.583	12.967
0.611	12.753
0.639	12.336
0.667	10.627
0.694	10.624
0.722	8.646
0.750	7.085
0.778	3.840
0.806	1.895
0.833	1.062
0.861	1.062
0.889	0.679
0.917	0.447
0.944	0.225
0.972	0.039
1.000	0.028

Tab. 10. Die with strong flow in spirals – Channel leakage

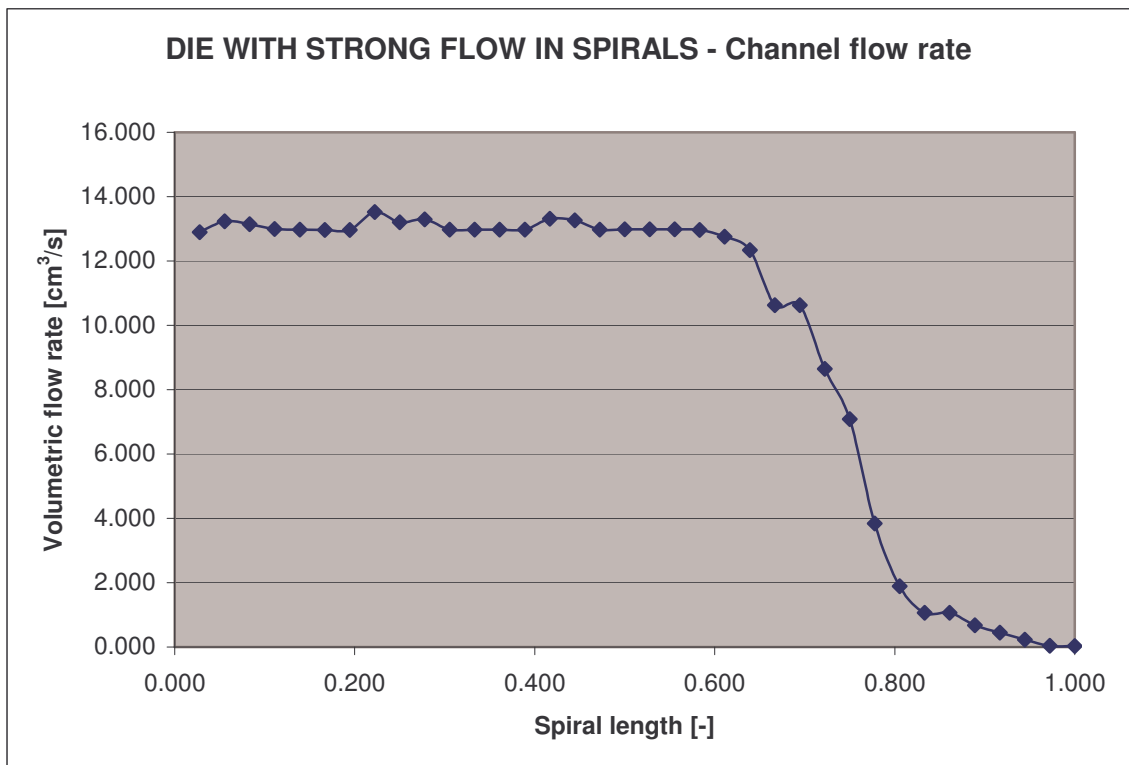


Fig. 73. Die with strong flow in spirals – Channel flow rate

8.7 Results comparison

The Fig. 74 shows a comparison of the 2D and 3D results. From the graphs it can be seen that the variation predicted by the 2D Spiral die program is higher than in the 3D case. This difference can be explained by the simplification assumptions used in the 2D method. Since it can be expected that the 3D solution is more accurate because it does not have any simplifying assumptions the practical situation is acceptable because by using the 2D approach the designer will “overdesign” the die because he will try to find the geometry with a low variation, which will be in reality even lower.

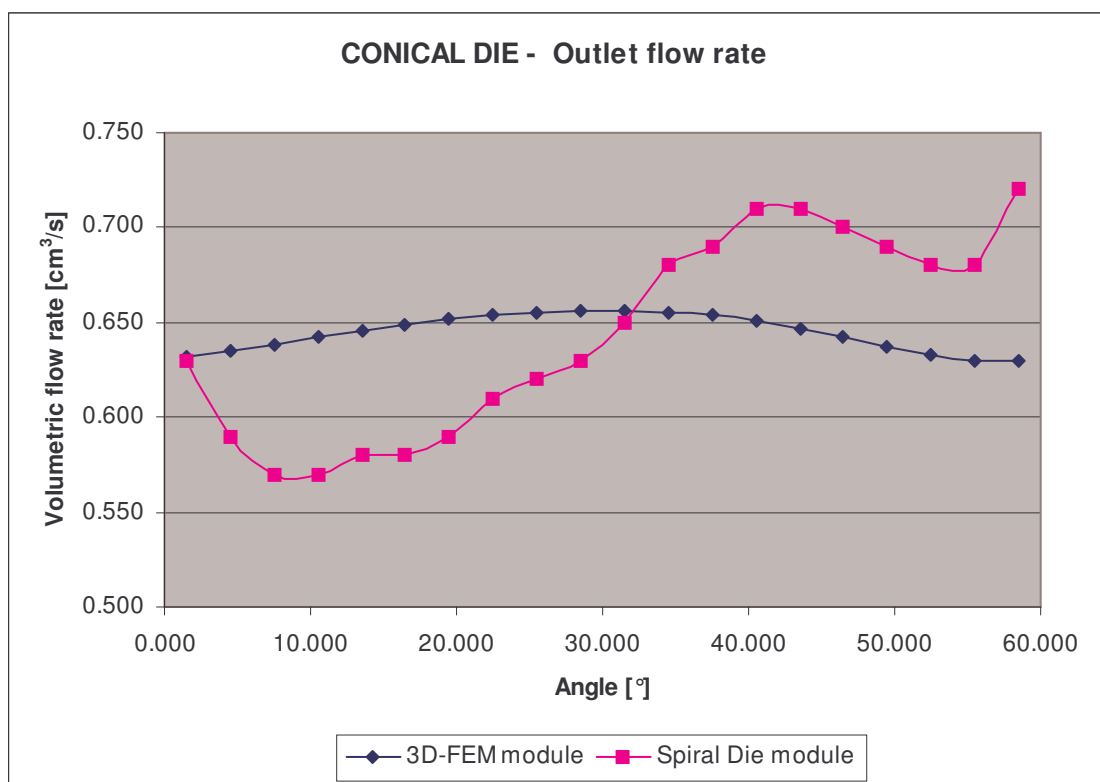


Fig. 74. Conical die - Outlet flow rate comparison

Fig. 75 shows the leakage from the spiral. It can be seen that the curves are similar and the predictions of both programs are almost identical. The fluctuation of the 3D results is caused probably by the grid roughness. To smooth out this curve the grid should be denser, which the used template did not allow. Nevertheless, the graphs 74 and 75 show that the predictions of both programs are similar, so the 2D program, which is much faster and easier to use is acceptable.

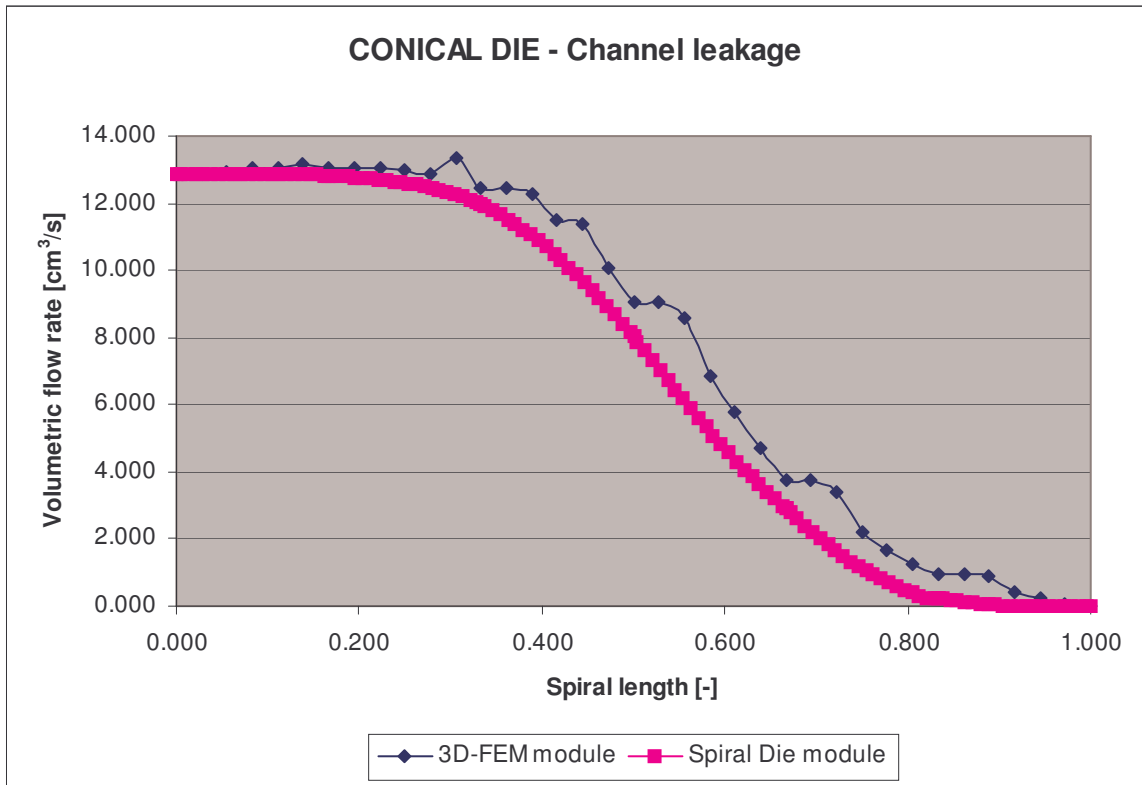


Fig. 75. Conical Die - Channel leakage comparison

Tab. 11 shows a comparison of the calculated pressure drops generated on the die. It can be seen that the Spiral die module overpredicts the pressure drop in about 30%. The reason for this may be that the Spiral die program overestimates the role of the squeezing of the flow domain. This program behavior should be further investigated.

CONICAL DIE			
SPIRAL DIE MODULE		3D-FEM MODULE	
Pressure [MPa]	13,396	Pressure [MPa]	10,776

Tab. 11. Conical die – Pressure drop

The conical die was a type of die where the material remains for a relatively long time in the spirals.

Figs. 76 and 77 show a comparison for another die where the leakage from the spiral is faster.

From Fig. 76 it can be seen that the prediction of the final distribution has similar variation and both results indicate the minimum on the right hand side. Again, from the point of view of the design the 2D program can be used because the predicted distribution is similar like for the 3D program

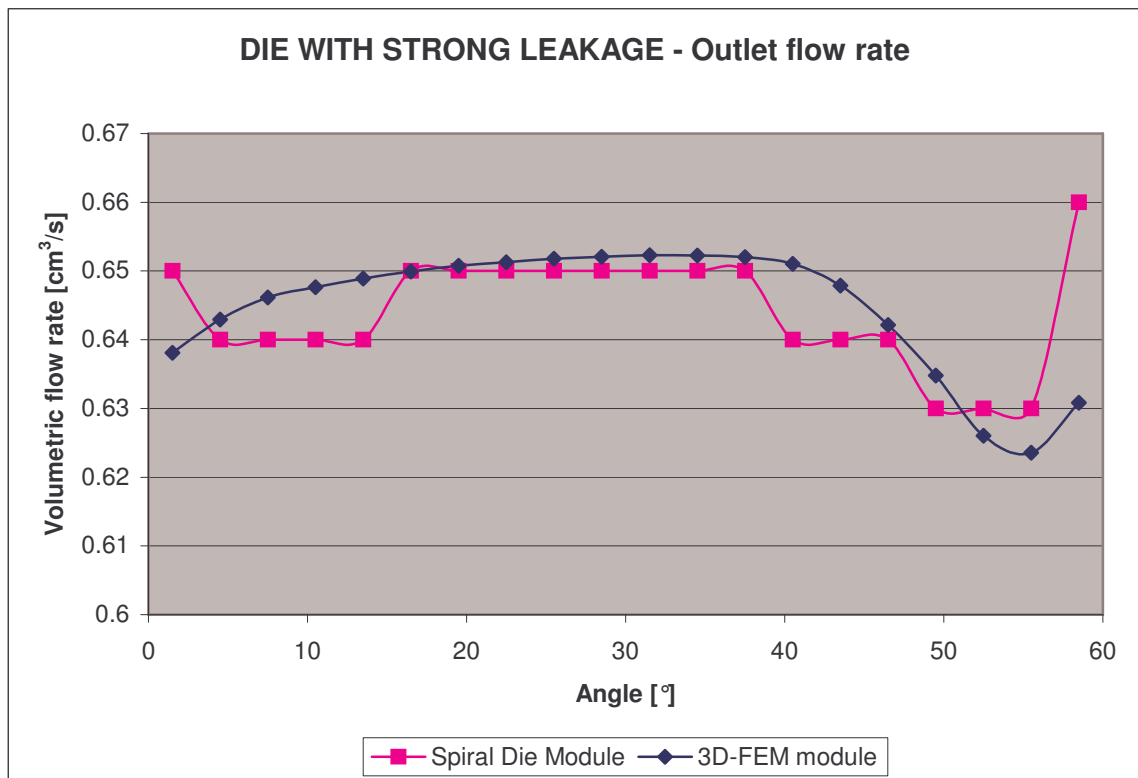


Fig. 76. Die with strong leakage – Outlet flow rate comparison

Fig. 77 indicates that the material flows for a longer time through the channel in the 2D calculation; or in other words that the leakage is faster than the 2D program predicts. This may be a problem for die purging because the amount of the material flowing through the spiral expected base on the 2D calculation is higher than in reality and therefore the expected purging will be lower. When using the 2D simulation the user should be aware of this and he should try to have the flow through the channel as far as possible. Then, even when the material leaks faster the purging will remain good.

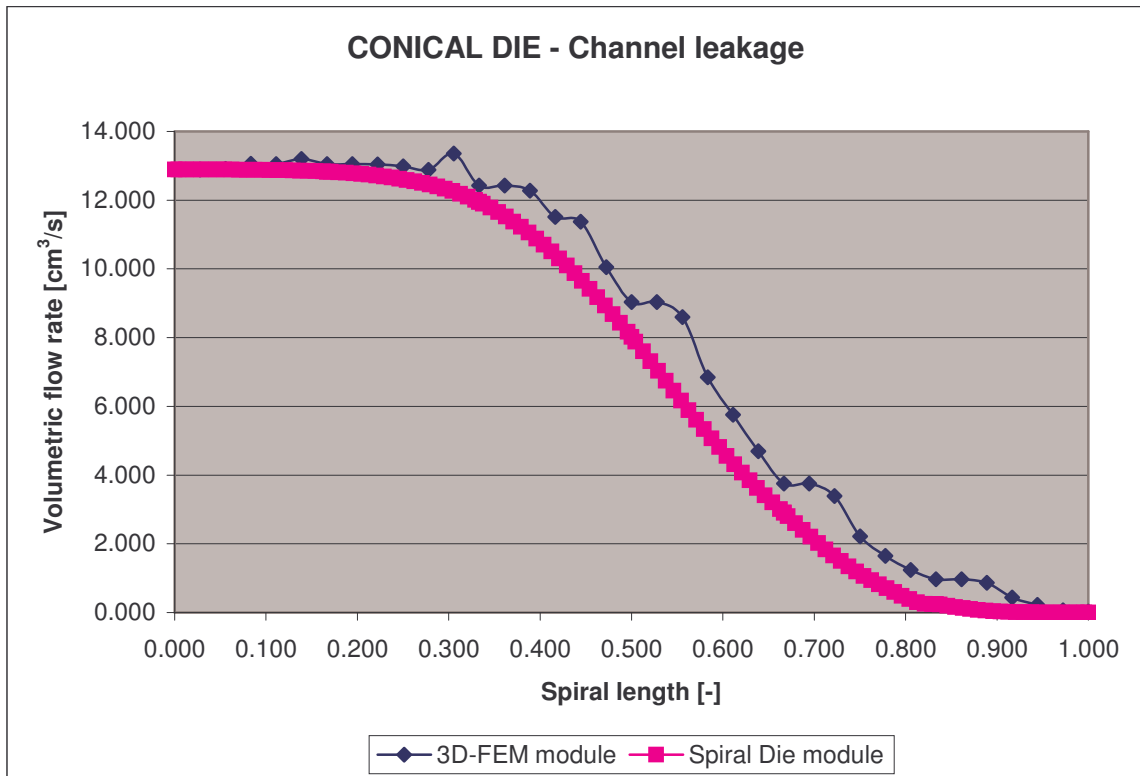


Fig. 77. Die with strong leakage – Channel leakage comparison

Tab. 12 shows the predicted pressure drops by both programs. It can be seen that the predicted values are close.

DIE WITH STRONG LEAKAGE			
SPIRAL DIE MODULE		3D-FEM MODULE	
Pressure [MPa]	6,433	Pressure [MPa]	6,231

Tab. 12. Die with strong leakage – Pressure drop

The last comparison was done for a die, which is almost not realistic just to see the program reaction. The die was designed in a way that the gap between the mandrel and the body is closed almost to the end of the spiral and the material can leak just in the last part of the die.

Fig. 78 shows the comparison of the final distributions. It can be seen that the variation predicted by the Spiral die program is much worse than the distribution calculated by the 3D program. The leakage in Fig. 79 indicates again that the 3D program predicts a faster leakage than the Spiral die program.

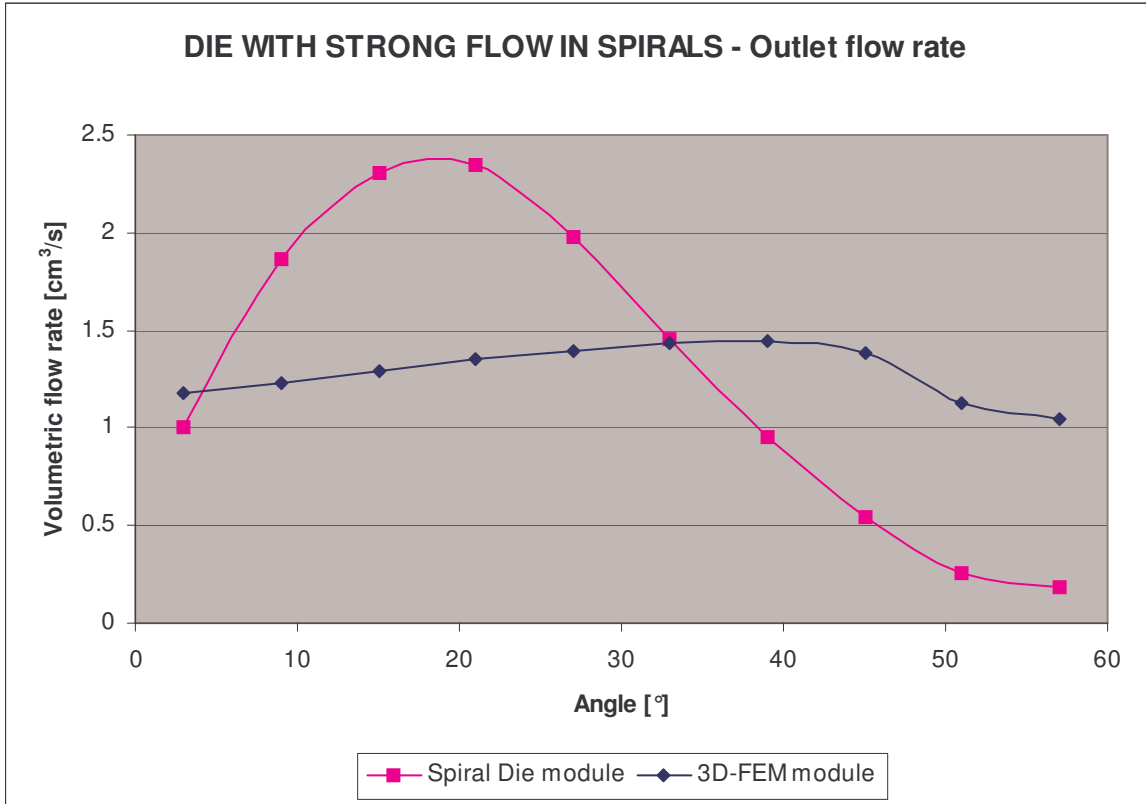


Fig. 78. Die with strong flow in spirals – Outlet flow rate comparison

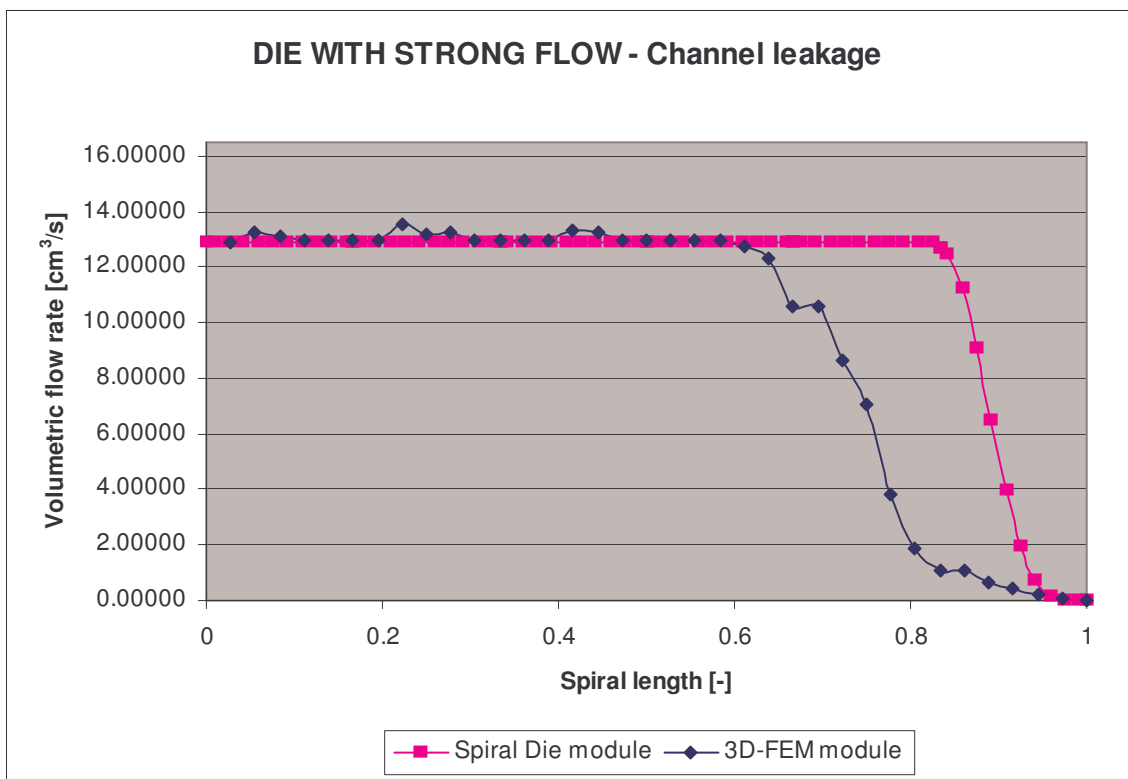


Fig. 79. Die with strong flow in spirals – Channel leakage comparison

The pressure drops calculated by both programs are compared in Tab. 13. It can be seen, that the Spiral die overpredicts the pressure drop.

DIE WITH STRONG FLOW IN SPIRALS			
SPIRAL DIE MODULE		3D-FEM MODULE	
Pressure [MPa]	9,924	Pressure [MPa]	7,955

Tab. 13. Die with strong flow in spirals – Pressure drop

RESUME

The aim of this work was to compare the behavior of two commercially available programs from the Compuplast VEL™.

If we take into account Fig. 74, Fig. 76 and Fig. 78 we can conclude that the Spiral die program overpredicts always the volumetric flow rate variation at the mandrel exit. For practical application this is good because the designer always has to “overdesign” the die with a perfect distribution. On the other hand it may lead to a lot of effort to design a proper geometry, which is in reality not needed (the last example).

The leakage predicted by the Spiral die program is weaker than from 3D. This may have a negative impact but it is probably usually compensated by the effort to keep the material as long as possible in the spiral. Even when the real leakage is faster than the predicted one it is still enough for a good purging behavior in reality.

The Spiral die program has been used for designing a lot of dies around the world and most of them were successful. The program was in the period 1995 – 2001 the most popular and very successful Compuplast program. The presented simulations explain why. The program overpredicts the generated pressure drop, this means that the die is sized for higher forces than in reality and there is no danger for material leakage. The predicted distribution is similar or worse than in reality; this also helps to have a better design.

The only weakness of the Spiral die program is the leakage but in the program manual it is stress-out several times that the design should be done in a way that the material stays in the spiral as long as possible. This may be a balancing effect for the program behavior.

From a long lasting experience with the Spiral die program and cooperation with several companies [10] it is known that the program predicts “normal” dies. This means dies when the gap opens gradually and also the channel depth is changed gradually. The calculation of the last example confirms also this experience because this die is some kind of geometry extreme when the gap opens suddenly. It can be seen that in this case the Spiral die program fails to predict reasonably the distribution.

I believe that the overall conclusion can be that the Spiral die program can be used for the die design with keeping in mind that the leakage is a little bit faster than the program predicts and the geometry should be gradually changing.

REFERENCES

- [1] KUBÍK, P. *Studium mechanického chování tenkostěnných tvarovaných plastových prvků v ohybu*. UTB ve Zlíně, 2006, p. 10-16. Bachelor Thesis
- [2] BUTLER, T. I. *Film extrusion Manual: Process, materials, properties*. Atlanta : Tappi press, 2005, 616 p, ISBN 1-59510-075-X.
- [3] MAŇAS, M., HELŠTÝN, J. *Výrobní stroje a zařízení – Gumárenské a plastikářské stroje II*. Brno : VUT Brno, 199p, ISBN 80-214-0213-X
- [4] KOLAŘÍK, R. *Modeling of the Film Blowing Process by using Variational Principles*. UTB ve Zlíně, 2006, p. 11-12. Bachelor Thesis
- [5] CANTOR, K. *Blown Film Extrusion*. Munich : Carl Hanser Verlag, 2006, 165 p, ISBN 1-56990-396-4
- [6] KANAI, T., CAMPBELL, G. A. *Film Processing*. Munich : Carl Hanser Verlag, 1999, ISBN 1-56990-252-6
- [7] MICHAELI, W. *Extrusion Dies*. Munich : Carl Hanser Verlag, 1984
- [8] WHELAN, A., DUNNING, D. J. *Developments in Plastics Technology*. London : Applied Science, 1982
- [9] PERDIKOULIAS, J. Master`s Thesis. Hamilton, Ontario, Canada : McMaster University, 1988
- [10] Courtesy of Brampton Engineering Inc. Brampton, Ontario, Canada
- [11] BRYDSON, J. A. *Flow Properties of Polymer Melts* : Geoge Godwin, 1981
- [12] O`BRIEN, K. T. *Applications of CAE in Extrusion and Other Continuous Processes*. Munich : Carl Hanser Verlag, 1992
- [13] HAN, C. D., *Multiphase Flow in Polymer Processing*. New York : Academic Press, 1981
- [14] PROCTOR, B. *SPE Journal*, 1972, no. 28, p. 34-41
- [15] VLCEK, J., KRAL, V., KOUBA, K. *Plast. Rubber Proc. Appl.*, 1984, no. 4, p. 309-315
- [16] MENGES, G., MAYER, A., BARTILLA, T., WORTHBERG, J. *Adv. Polym. Proc.*, 1988, no. 2, p. 174-181

- [17] RAUWENDAAL, C. *Proc. SPE ANTEC Tech. Papers*, 1986, p. 917-923
- [18] VLCEK, J., PERDIKOULIAS, J., VLACHOPOULOS, J. *Int. Polym. Proc.*, 1988, no. 2, p. 174-181
- [19] BENKHOUCHA, K., SEBASTIAN, D.H. *SPE ANTEC.*, May 1984, p. 1774-1778
- [20] PERDIKOULIAS, J., VLCEK, J., VLACHOPOULOS, J. *Adv. Polym. Technol.*, 1987, no. 7, p. 333-341
- [21] PERDIKOULIAS, J., VLCEK, J., VLACHOPOULOS, J. *Pro. SPE ANTEC.*, 1988, p. 179-182
- [22] PERDIKOULIAS, J., VLCEK, J., VLACHOPOULOS, J. *Adv. Polym. Technol.*, 1990, no. 10, p. 111-123
- [23] PERDIKOULIAS, J., TZOGANAKIS, C., VLACHOPOULOS, J. *Plast. Rubber Proc. Appl.*, 1989, no. 11, p. 156-161
- [24] WORTBERG, J., SCHMITZ, K.P. *Kunststoffe*, 1982, no. 72, p. 198-205
- [25] PARNABY, J., HASSAN, G.A., HELMY, A.A., Ali, A. *Plast. Rubber Proc. Appl.*, 1981, no. 1, p. 305-315
- [26] COYLE, D.J., PERDIKOULIAS, J. *Proc SPE ANTEC*. Montreal, Quebec, Canada, May 1991, p. 2445-2447
- [27] COYLE, D.J., PERDIKOULIAS, J. *Paper presented at 7th annual meeting of the Polymer Processing Society*. Hamilton, Ontario, Canada, April 1991
- [28] KURZBUCH, W. *Plast. Eng.*, August 1974, p. 43-46
- [29] CHENG, C.Y. *Polym. Plast. Technol. Eng.*, 1981, no.17, p. 45-58
- [30] SAILLARD, P., AGASSANT, J.F. *Polym. Proc. Eng.*, 1984, no. 2, p. 37-52
- [31] FAHY, E.J., GILMOUR, P.W. *Int. J. Numer. Methods Eng.*, 1986, no. 23, p.1-11
- [32] *SPIRALCAD: Spiral Mandrel Die Simulation Software*. Hamilton, Ontario, Canada : Polydynamics Inc., Zlín, Czech Republic : Compuplast International

- [33] *LAYERCAD: Coextrusion Flow Simulation Software*. Hamilton, Ontario, Canada : Polydynamics Inc., Zlín, Czech Republic : Compuplast International
- [34] HELMY, H. A. A., WORTH, R. A. *Rheology*, 1981, no. 3
- [35] ASTARIA, G., MARRUCCI, G. T., NICOLAIS, L. 8th International Congress on Rheology. Naples, Italy, Sept. 1-5 1981, p. 69-75
- [36] ŠVÁBÍK, J. *Numerical Modeling in Extrusion*. VUT Brno, 1996, p. 20-30. Master Thesis
- [37] BEDROSIAN, G. *Shape Functions and Integration Formulas for Three Dimensional Finite Element Method Analysis*. Int. J. for Num. Meth. in Eng., 1992, no. 35, p. 95-108
- [38] *Compuplast Tutorial for Spiral Die Module*. Zlín, Czech Republic : Compuplast International, 2007
- [39] *Compuplast Tutorial for 3D FEM Module*. Zlín, Czech Republic : Compuplast International, 2007

LIST OF SYMBOLS

BUR	Blow-up ratio	1
R_1	Bubble radius at the freeze line height FLH	m
R_0	Bubble radius at the die exit	m
DDR	Draw down ratio	1
v_F	Film velocity at the freeze line height	$\text{m}\cdot\text{s}^{-1}$
v_D	Film velocity at the die exit	$\text{m}\cdot\text{s}^{-1}$
p	Pressure	Pa
f, g	Flow resistance functions	
m	Consistency index	
n	Power-Law index	
γ	Shear rate	s^{-1}
Q	Volumetric flow rate	$\text{m}^3\cdot\text{s}^{-1}$
D_1	Subelement length	m
D_2	Subelement width	m
S	Subelement thickness	m
τ	Deviatorics extra stress tensor	
v	Velocity vector	$\text{m}\cdot\text{s}^{-1}$
ρ	Density	$\text{kg}\cdot\text{m}^{-3}$
C_p	Heat capacity	$\text{J}\cdot\text{kg}^{-1}\cdot\text{K}^{-1}$
T	Temperature	K
∇	Gradient	
k	Thermal conductivity	$\text{W}\cdot\text{m}^{-1}\cdot\text{K}^{-1}$
R	Residual	
\bar{v}	Approximate velocity	$\text{m}\cdot\text{s}^{-1}$

N	Quadratic shape function vector	
M	Linear shape function vector	
u	Unknown variables [v, P,T]	
B	Matrix used to simplify notation of equations	
η	Viscosity	Pa·s
I_2	Invariant of the strain rate tensor	
p	Pressure	Pa
J	Jacobian matrix	
Ω	3D flow domain	
$ J $	Determinant of the Jacobian matrix	
ξ, η, ζ	Local coordinates in parent element	m
w	Gauss integration weight vector	

LIST OF FIGURES

Fig. 1. Polystyrene structure	12
Fig. 2. Melt extrusion.....	14
Fig. 3. Coextrusion feeding process	16
Fig. 4. Film blowing line	17
Fig. 5. Types of die constructions.....	18
Fig. 6. Basic mandrel support systems	19
Fig. 7. Weld lines orientation	19
Fig. 8. Spiral mandrel die flow distribution.....	20
Fig. 9. Typical spider mandrel die construction	21
Fig. 10. Three-layer spider mandrel die.....	21
Fig. 11. Relaxation chambers and final gap.....	23
Fig. 12. Basic correction of flow variation	24
Fig. 13. Cross-section view of the spiral mandrel die	25
fig. 14. Geometry comparison	26
Fig. 15. Perspective view of flow space	27
Fig. 16. Subdivision of control volume	27
Fig. 17. Typical subelement for the model	28
Fig. 18. Model prediction versus experimentally measured data	30
Fig. 19. Body dimensions	38
Fig. 20. Mandrel dimensions	38
Fig. 21. Channel dimensions.....	39
Fig. 22. Section above the spiral part	39
Fig. 23. Pipe system dimensions.....	40
Fig. 24. Mandrel design	40
Fig. 25. Reference diameters editation	41
Fig. 26. Body dimensions editation	42
Fig. 27. Mandrel dimensions editation	43
Fig. 28. Channel dimensions editation	44
Fig. 29. Channel radius and end angle.....	45
Fig. 30. Round section calculated values.....	46
Fig. 31. Transition channel calculated values.....	47
Fig. 32. Output lips caculated values.....	48

Fig. 33. Pipes feeding system	49
Fig. 34. Iteration setup	51
Fig. 35. Relaxation values	52
Fig. 36. Conical die - Outlet flow rate	53
Fig. 37. Conical die – Channel flow rate	53
Fig. 38. Conical Die - Angle velocity profile	54
Fig. 39. Conical Die – Velocity magnitude profile	55
Fig. 40. Conical Die – Disipation profile	56
Fig. 41. Conical Die – Temperature gradient profile.....	57
Fig. 42. Conical Die – Pressure profile.....	58
Fig. 43. Conical Die – Temperature profile.....	59
Fig. 44. Conical Die – Shear stress profile	60
Fig. 45. Conical Die – Elongation stress profile.....	61
Fig. 46. Conical die – Outlet flow rate	63
Fig. 47. 2D cut setting.....	63
Fig. 48. Channel flow rate integration	64
Fig. 49. Conical die – Channel leakage	66
Fig. 50. Die with strong leakage – Outlet flow rate.....	66
Fig. 51. Die with strong leakage – Channel flow rate	67
Fig. 52. Die with strong leakage – Angle velocity profile.....	67
Fig. 53. Die with strong leakage – Velocity magnitude profile.....	68
Fig. 54. Die with strong leakage – Dissipation profile	69
Fig. 55. Die with strong leakage – Temperature gradient profile.....	70
Fig. 56. Die with strong leakage – Pressure profile.....	71
Fig. 57. Die with strong leakage – Temperature profile.....	72
Fig. 58. Die with strong leakage – Shear stress profile	73
Fig. 59. Die with strong leakage – Elongation stress profile.....	74
Fig. 60. Die with strong leakage – Outlet flow rate.....	76
Fig. 61. Die with strong leakage – Channel flow rate	77
Fig. 62. Die with strong flow in spirals – Outlet flow rate	78
Fig. 63. Die with strong flow in spirals – Channel flow rate.....	78
Fig. 64. Die with strong flow in spirals – Angle velocity profile.....	79
Fig. 65. Die with strong flow in spirals – Velocity magnitude profile.....	80

Fig. 66. Die with strong flow in spirals – Dissipation profile	81
Fig. 67. Die with strong flow in spirals – Gradient profile.....	82
Fig. 68. Die with strong flow in spirals – Pressure profile	83
Fig. 69. Die with strong flow in spirals – Temperature profile	84
Fig. 70. Die with strong flow in spirals – Shear stress profile.....	85
Fig. 71. Die with strong flow in spirals – Elongation stress profile	86
Fig. 72. Die with strong flow in spirals – Outlet flow rate	88
Fig. 73. Die with strong flow in spirals – Channel flow rate.....	89
Fig. 74. Conical die - Outlet flow rate comparison	90
Fig. 75. Conical Die - Channel leakage comparison	91
Fig. 76. Die with strong leakage – Outlet flow rate comparison.....	92
Fig. 77. Die with strong leakage – Channel leakage comparison.....	93
Fig. 78. Die with strong flow in spirals – Outlet flow rate comparison	94
Fig. 79. Die with strong flow in spirals – Channel leakage comparison	94

LIST OF TABLES

Tab. 1. Material properties.....	37
Tab. 2. Transition channel values	46
Tab. 3. Output lips values	47
Tab. 4. Project definition data.....	50
Tab. 5. Conical die - Outlet flow rate measured values.....	62
Tab. 6. Conical die – Channel leakage	65
Tab. 7. Die with strong leakage – Outlet flow rate measured values	75
Tab. 8. Die with strong leakage – Channel leakage	77
Tab. 9. Die with strong flow in spirals – Outlet flow rate measured values	87
Tab. 10. Die with strong flow in spirals – Channel leakage.....	89
Tab. 11. Conical die – Pressure drop	91
Tab. 12. Die with strong leakage – Pressure drop	93

LIST OF APPENDICES

APPENDIX A 1: CD-ROM